Calhoun: The NPS Institutional Archive

DSpace Repository

Theses and Dissertations | 1. Thesis and Dissertation Collection, all items

1995-09

Evaluation of the NASA-Ames panel method (PMARC) for aerodynamic missile design

Lambert, Mark A.

Monterey, California. Naval Postgraduate School

http://hdl.handle.net/10945/7573

This publication is a work of the U.S. Government as defined in Title 17, United States Code, Section 101. Copyright protection is not available for this work in the United States.

Downloaded from NPS Archive: Calhoun

Calhoun is the Naval Postgraduate School's public access digital repository for research materials and institutional publications created by the NPS community. Calhoun is named for Professor of Mathematics Guy K. Calhoun, NPS's first appointed -- and published -- scholarly author.

Dudley Knox Library / Naval Postgraduate School
411 Dyer Road / 1 University Circle
Monterey, California USA 93943

http://www.nps.edu/library

NAVAL POSTGRADUATE SCHOOL
Monterey, California

THESIS

EVALUATION OF THE NASA-AMES PANEL METHOD (PMARC) FOR AERODYNAMIC MISSILE DESIGN

by

Mark A. Lambert

September, 1995

Thesis Advisor: Max F. Platzer

Thesis
L25155

Approved for public release; distribution is unlimited

REPORT DOCUMENTATION PAGE	Form Approved OMB No. 0704-0188

Public reporting burden for this collection of information is estimated to average 1 hour per response, including the time for reviewing instruction, searching existing data sources, gathering and maintaining the data needed, and completing and reviewing the collection of information. Send comments regarding this burden estimate or any other aspect of this collection of information, including suggestions for reducing this burden, to Washington Headquarters Services, Directorate for Information Operations and Reports, 1215 Jefferson Davis Highway, Suite 1204, Arlington, VA 22202-4302, and to the Office of Management and Budget, Paperwork Reduction Project (0704-0188) Washington DC 20503.

1. AGENCY USE ONLY (Leave blank)	2. REPORT DATE September 1995	3. REPORT TYPE AND DATES COVERED Engineer's Thesis

4. TITLE AND SUBTITLE EVALUATION OF THE NASA-AMES PANEL METHOD (PMARC) FOR AERODYNAMIC MISSILE DESIGN	5. FUNDING NUMBERS
6. AUTHOR(S) Mark A. Lambert	
7. PERFORMING ORGANIZATION NAME(S) AND ADDRESS(ES) Naval Postgraduate School Monterey CA 93943-5000	8. PERFORMING ORGANIZATION REPORT NUMBER
9. SPONSORING/MONITORING AGENCY NAME(S) AND ADDRESS(ES)	10. SPONSORING/MONITORING AGENCY REPORT NUMBER

11. SUPPLEMENTARY NOTES The views expressed in this thesis are those of the author and do not reflect the official policy or position of the Department of Defense or the U.S. Government.

12a. DISTRIBUTION/AVAILABILITY STATEMENT Approved for public release; distribution is unlimited.	12b. DISTRIBUTION CODE

13. ABSTRACT (maximum 200 words)

The NASA Ames Research Center developed panel code (PMARC) is investigated to explore its suitability for aerodynamic missile design. To this end, PMARC is first assessed by applying it to several problems for which other solutions and experimental data are available, i.e., steady flow past a wing-body configuration, delta wings, biplane wings, wings in ground effect, and unsteady flow of pitching and impulsively started wings. Good agreement is found in all cases. PMARC is then applied to two missile configurations. Again, encouraging agreement with available experimental data is found provided the wake shedding from the missile body is modeled properly.

14. SUBJECT TERMS PMARC, Panel Methods, Aerodynamic Coefficients, Potential Flow, Missile Aerodynamic Design	15. NUMBER OF PAGES 16. PRICE CODE

17. SECURITY CLASSIFICATION OF REPORT	18. SECURITY CLASSIFICATION OF THIS PAGE	19. SECURITY CLASSIFICATION OF ABSTRACT	20. LIMITATION OF ABSTRACT
Unclassified	Unclassified	Unclassified	UL

NSN 7540-01-280-5500

Standard Form 298 (Rev. 2-89)
Prescribed by ANSI Std. 239-18 298-102

Approved for public release; distribution is unlimited.

EVALUATION OF THE NASA-AMES PANEL METHOD (PMARC) FOR AERODYNAMIC MISSILE DESIGN

Mark A. Lambert
Civilian, United States Navy
B. S., University of New Mexico, 1987

Submitted in partial fulfillment of the
requirements for the degree of

AERONAUTICAL ENGINEER

from the

NAVAL POSTGRADUATE SCHOOL
September 1995

Author: [redacted]
Mark A. Lambert

Approved by: [redacted]
Max F. Platzer, Thesis Advisor

[redacted]
Kevin Jones, Second Reader

[redacted]
Daniel J. Collins, Chairman
Department of Aeronautics and Astronautics

Thesis
L25155
c.2

ABSTRACT

The NASA Ames Research Center developed panel code (PMARC) is investigated to explore its suitability for aerodynamic missile design purposes. To this end, PMARC is first assessed by applying it to several problems for which other solutions and experimental data are available, i.e., steady flow past a wing-body configuration, delta wings, biplane wings, wings in ground effect, and unsteady flow of pitching and impulsively started wings. Good agreement is found in all cases. PMARC is then applied to two missile configurations. Again, encouraging agreement with available experimental data is found provided the wake shedding from the missile body is modeled properly.

TABLE OF CONTENTS

I. INTRODUCTION 1

II. OVERVIEW OF PMARC CODE 3

A. GENERAL PMARC USAGE 4
1. Running PMARC with an Existing Executable 4
2. Creating a PMARC Executable 5

B. GEOMETRY MODELING IN PMARC 7

C. GRAPHICS VISUALIZATION 8
1. The General Visualization System (GVS) 8
2. GVS Operation 8
a. Loading a PMARC Output File 9
3. Flow Phenomena Animation 9
4. Plotting from GVS 10

III. DATA EXTRACTION 11

IV. VERIFICATION OF THE PMARC CODE 15

A. STEADY STATE COMPARISONS 15
1. Wing-Body Configuration 15
2. Delta Wings 15
3. Biplane Wings 16
4. Wings in Ground Plane Effect 20

B. UNSTEADY FLOW COMPARISONS 21
1. Pitching Wing Comparisons 21
2. Impulsively Started Wings 22
3. Wings in Tandem 25

V. RESULTS OF MISSILE MODELING 29

A. MISSILE AIRFRAME DISCUSSION 29

B. AERODYNAMIC COEFFICIENTS 29
1. Pressure Coefficient (Cp) 32
a. Nose Geometry 32
b. First Order Slender Body Theory 33
c. Second Order Slender Body Theory 34
d. Experimental Data Comparison 35
2. Normal Force Coefficient (C_N) from Initial Wake Model 37

C. WAKE MODELING 40
1. Vortex Sheet Separation Line for the Meyer Body-Alone 41
2. Vortex Sheet Separation Line for the Smith Canard-Controlled Missile 44

VI. SUMMARY AND CONCLUSIONS 47
APPENDIX A. NACA 4418 DATA5 INPUT FILE 49
APPENDIX B. NACA 65-412 DATA5 INPUT FILE 51
APPENDIX C. CRUCIFORM WING-BODY DATA5 INPUT FILE 53
APPENDIX D. CANARD CRUCIFORM MISSILE DATA5 INPUT FILE 57
APPENDIX E. TANGENT-OGIVE NOSE BODY DATA5 INPUT FILE 63
APPENDIX F. SAMPLE PARAM.DAT FILE 65
APPENDIX G. SAMPLE COMMON.F FILE 67
LIST OF REFERENCES 69
INITIAL DISTRIBUTION LIST 73

I. INTRODUCTION

Typical air-to-air missile aerodynamic design work is done primarily using semi-empirical chart or computer tools. These tools are limited to previously investigated missile configurations and flight regimes. Another method to be used for initial design tasks may be the use of a relatively "inexpensive" code like the NASA-developed Panel Method-Ames Research Center (PMARC) software. This code allows for any arbitrary configuration to be modeled within the limitations of inviscid, incompressible aerodynamics.

The purpose of this work is to determine if the PMARC computer code provides a viable tool for initial design tasks of tactical missile airframes. All of this work is conducted on the Naval Postgraduate School's (NPS) computer systems. The majority of the work is completed on the Department of Aeronautics and Astronautics Silicon Graphics Incorporated (SGI) workstations while much of the unsteady computations and other large jobs are run on the NPS Computer Center's Y-MP EL98 Cray computer. The analysis of oscillating wings requires a large amount of memory and processor time. This part of the study is done exclusively on the Cray computer.

The scope of this analysis is to understand the design capabilities of the PMARC code in terms of initial missile aerodynamic design tasks. The approach is to validate PMARC against existing data. Steady as well as unsteady flows are modeled by PMARC. Comparisons are made for each type of flow. The ability to provide design data is examined to validate the usefulness of PMARC as a missile design tool.

Initial work is done to verify previous results using PMARC, and comparisons are made to existing experimental and theoretical data. The primary focus of the remaining work is to evaluate PMARC for the analysis of missile configurations. To this end, two missile configurations are investigated.

II. OVERVIEW OF PMARC CODE

The PMARC code is used to computationally predict inviscid, incompressible flow fields around arbitrarily shaped three-dimensional configurations. All solutions presented in this study are produced using version 12.21 of the PMARC code. The principal limitation of the PMARC code is that it is based on potential flow modeled by the Laplace equation [Ref. 1].

$$\nabla^2 \Phi = 0 \tag{2.1}$$

The lack of viscous modeling inhibits the computation of drag due to viscosity, but the induced drag due to lift (C_{Di}) may be calculated. As an example, for a symmetric wing at zero angle-of-attack (AOA) in uniform flow, PMARC calculates zero drag force which reproduces the classical d'Alembert's paradox.

PMARC also provides some capability to model internal three-dimensional and jet flows [Ref. 2]. The modeling of a complex three-dimensional body in PMARC requires extensive experience and understanding of the PMARC construction process. An excellent supplementary introduction on the general use of PMARC is shown in a NPS prepared manual [Ref. 4]. Reference [4] is limited primarily to the discussion of using PMARC to analyze wing shapes and does not provide specific information on wing-body configurations.

PMARC is written in FORTRAN with an open architecture to allow easy user modification to the code. Also, provided the user has access to the source code, PMARC can be resized (i.e., the maximum number of panels can be changed) in a matter of minutes to optimize the code for the model size being run. This type of utility is discussed in more detail later.

The body representation of the flow potential is modeled by constant strength source and doublet distributions over each panel. The use of constant source distributions indicates that PMARC is a low-order method. The code uses an internal Dirichlet boundary condition at each discretized point on the surface in order to solve the velocity potential at that point. Therefore, the sources are explicitly determined based on the external normal velocities which is zero for a configuration with no jet flow (i.e., no flow through the surface) and the known onset velocity vector [Ref. 1]. The doublet strengths are determined using an integral equation which prescribes the condition on the inner potential. The inner potential defines the velocity field on

and around the body. The shed vortex sheets are generated by wake doublet panels, and the vortex strength is calculated by applying the Kutta condition at the trailing edge for lifting wings [Refs. 2, 5]. For lifting bodies, such as missiles, the doublet strength of the wake panels being shed from along the body length is calculated by differencing the doublet strength of the neighboring panels whose common edges define the wake separation line [Refs. 1, 2].

PMARC employs a time-stepping wake model routine that allows the user to specify a prescribed motion for the paneled configuration. This provides analysis of modeled bodies executing maneuvers or oscillating motions. The time-stepping routines permit the solution of either steady or unsteady flows to be solved as well as investigating indicial aerodynamics. The wakes from the modeled geometry are developed over a series of time steps and show the development of the flow and wake trajectory [Ref. 1].

A. GENERAL PMARC USAGE

The use of the PMARC code consists of generating an input file necessarily named DATA5 which contains the information defining the geometry of the model as well as the flow conditions and any boundary conditions imposed. This process in PMARC is similar, albeit much simpler, to the meshing process needed in a full Computational Fluid Dynamics (CFD) analysis.

A DATA5 input file for a wing-body configuration is shown in the PMARC manual [Ref. 1]. Sample DATA5 input files are included in the appendices for a similar wing-body configuration [Ref. 23] and also for a more complicated canard-tail-body missile model [Ref. 21, 22]. Additional input files for basic wing models are shown in Ref. [4] and in the appendices. For the beginning PMARC user understanding the analysis of a basic wing model is the best place to start.

1. Running PMARC with an Existing Executable

Assuming a PMARC executable file (e.g., pmarc12) has already been placed in a user executable directory (e.g., /usr/local/bin), the only other necessary item needed to produce a set of PMARC output is the input file named DATA5. Several sample input files can be copied into a user directory from the /usr/local/PMARC_Models directory. Typically, a user subdirectory (e.g., /d4/smith/pmarc) is created and used to store the data files. The following is an example of

a command which can be issued at the UNIX prompt to copy a file into the current user directory:

cp /usr/local/PMARC_Models/planform1 DATA5

This copies a PMARC input file named "planform1" into the current directory and changes its name to DATA5. This file contains the information to model a NACA 4-digit wing. There are other input files located in this PMARC model directory that can be copied into the user directory. To execute PMARC, the following command is entered at the UNIX prompt:

pmarc12

At the end of a successful run, two other files (DATA6 and DATA22) are generated in this directory. These are the only two output files left at the end of the run as the several other "fort" files appearing during PMARC execution are temporary files and they are deleted automatically.

The DATA6 output file contains all the information generated by PMARC in ASCII form including the aerodynamic coefficients and the geometric data. The DATA22 output file contains the information used in the post-processor visualization program. This code is discussed later.

Two corrections are noted from material presented in the Subsonic Load Analysis Manual [Ref. 4]. First, it states that only the DATA5 input file can exist in the current directory when executing PMARC. Actually, any number of files can exist in the directory with DATA5 as long as they are not named the same as any of the PMARC output files (i.e., DATA6, DATA7, DATA22, fort.16, fort.18, fort.19, fort.20, and fort.21). Second, the wing model for the NACA 6-digit input file included in the manual shows data points defining the airfoil section starting at the wing leading edge. PMARC handles wing analysis best when the wing is constructed from the trailing edge and wraps continuously around the underside to the leading edge and back to the trailing edge. This allows the slope discontinuity in the wing patch to occur at the trailing edge where the wake is forced to separate. Otherwise, erroneous results may occur when calculating the aerodynamic coefficients for the wing.

2. Creating a PMARC Executable

A situation might exist where only the PMARC source code is available, and it has not been compiled. Similarly, a new executable might be needed if the existing PMARC executable is compiled with certain arrays (e.g., the number of allowable surface or wake panels) set too low

for the current model. For example, if the PMARC executable available on the system is compiled with a maximum allowable number of surface panels set at 2000, and the user model requires 5000 panels then a new executable should be compiled with a larger number of allowable panels indicated.

Three files are needed for compiling the PMARC code: the PMARC source code (i.e., pmarc12.f), PARAM.DAT, and COMMON.F. The COMMON.F file deals with the FORTRAN common blocks inside the PMARC source code. It is unlikely a user would need to modify this file unless modifications are made to the source code itself. A typical item to change in PARAM.DAT is the NSPDIM parameter which sets the limit on the number of surface panels allowed on the current model. It is important to note that the number of specified surface panels needs to be only as large as necessary to run the current model. If this parameter is set unnecessarily large, it drives up the memory requirements for running PMARC which can slow down the execution of the code especially if operating on the Cray computer. Reference [1] discusses the memory requirements based on the user specified size of the input arrays.

To update a PMARC executable to reflect the current values of the parameters in PARAM.DAT, the source code must be recompiled. Changing the values in PARAM.DAT without recompiling the source code will have no effect on the current executable being used.

If a user is operating with his own copy of the source code, it is recommended that the PMARC executable be placed in a "bin-type" subdirectory which is searched from all locations of the user's account. This allows the user to execute PMARC from any subdirectory. The path must be set in the user's .login file to alert the system that it should search this bin directory for executables. The path should be set to the user's particular disk and user name. A line like the following should be placed in the .login file:

set path = (/d4/smith/bin $path)

While inside the bin subdirectory that contains the pmarc12.f, PARAM.DAT, and COMMON.F files, the following command is issued on a SGI workstation to create a PMARC executable called "pmarc12_2":

f77 -o pmarc12_2 pmarc12.f

A different name should be assigned to the new executable other than the one residing on the system to avoid confusion (e.g., pmarc12_2 instead of pmarc12). This different name can be any

chosen by the user to help identify the PARAM.DAT parameters set for that given executable. If compiling on the Cray computer the same process is followed except the command is:

cf77 -o pmarc12_2 pmarc12.f

There are also different options for compiling on the Cray to take advantage of vectorized and parallel processing capabilities. The above Cray command shows a process that will generate a functional executable without any optimization.

After the above steps are taken, typing the command **pmarc12_2** at the UNIX prompt in a subdirectory containing a valid DATA5 input file should properly execute the PMARC code and generate the DATA6 and DATA22 output files.

B. GEOMETRY MODELING IN PMARC

As in any mesh generation for CFD or Finite Element Analysis (FEA) knowledge of the tools available and their limitations is based on experience and training. The true "art" of such analysis is being able to determine what makes a viable grid and what does not. The accuracy from any type of computational analysis is limited by the assumptions and capability of the computer code being used. The best way to start modeling in PMARC is to modify an existing file that is similar to the model of current interest. Several sample input files currently exist on the Department of Aeronautics and Astronautics SGI workstation network.

When dealing with a NACA 4-digit airfoil, like a NACA 2412 for example, PMARC offers an automatic airfoil generation option. This process is well outlined in Ref. [4]. The user has options in specifying the number of spanwise and chordwise panels as well as the desired aspect ratio. For more complicated cross-sections like a NACA 6-digit airfoil, a set of actual discretized panel points must be inputted to the DATA5 file as shown for the NACA 65-412 airfoil in Ref. [4].

The generation of a wing-body geometry is a more complicated process. Now the wing must be modeled as before plus the body must be coupled with the wing. Reference [1] and several appendices show sample DATA5 input files for several wing-body configurations. What must be understood is that the wing and body panel points must be aligned so that there are no holes in the interface between the surfaces. This requires an effort in defining the geometry precisely and accounting for each and every panel corner point location. As seen in any of the wing-body input files the panel spacing on the body must correspond to the chordwise panel

spacing on the wing. Unfortunately, since each panel intersection point along the fuselage must be manually placed to match the wing points, changing the number of chordwise wing panels at a later time becomes very arduous. Hence, it is beneficial to initially know the best panel configuration, but obviously this is not always possible.

C. GRAPHICS VISUALIZATION

1. The General Visualization System (GVS)

Another code to be used in addition to PMARC is the NASA GVS software [Ref. 3]. This is a post-processor software which takes the graphical DATA22 output file from PMARC and provides visualization of the geometry and flow parameters. The documentation for the GVS Version 3.1.00 used here is very limited [Ref. 3]. Fortunately, the GVS software is mouse driven, fairly intuitive and easy to use for most general cases. A supplementary explanation of the GVS software is made in Ref. [4].

The GVS software is useful when initially constructing a geometric model. PMARC has the option of running the model for the geometry only. This allows the user to quickly visualize the geometry and check it for errors. This is beneficial because PMARC is unforgiving when syntax errors exist or any required terms are omitted in the DATA5 input file. PMARC does not contain any internal diagnostic type programming. At best, when an input error is made in DATA5, the user can expect a cryptic FORTRAN error message which does not provide much help.

2. GVS Operation

This section provides a general overview of the GVS setup and operation and is included for the sake of completeness. The basic process to set up an user account for GVS use is as follows. First a user subdirectory called GVSDIR is created. Second, the directories and files from /usr/local/GVSDIR_INSTALL are copied into the GVSDIR subdirectory. When this is completed the GVSDIR directory should have two subdirectories: /TMP, and /LOCAL. Now the GVS code can be run by making sure the current directory is GVSDIR and entering the command **gvs** at the UNIX prompt. Several windows will appear after a few seconds.

a. Loading a PMARC Output File

To load a DATA22 file the proceeding process must be adhered to. One GVS requirement is that the DATA22 file must be changed to any name not exceeding eight characters with the extension of .fmt (e.g., wingout.fmt). In the File-Access box click the mouse on the Mod-File-List button. Click on the Null button and it changes to PMIPS. Click on the File-Name button, and type in the path to the PMARC output file in the highlighted space (e.g., /sirius/d1/smith/pmarc/wingout.fmt). Now click on the Add-Name button, and then click on the Close button. The path and file just entered should appear in the File-Access box. Click on the new File-Path button to highlight it, and then click on the Acquire button. GVS should indicate that it has started to load the selected file. The PMARC model geometry should appear in the Graphics Window after GVS has finished loading the selected file. This process to read a graphics input file into GVS is outlined in more detail in Ref. [4].

3. Flow Phenomena Animation

A useful option while visualizing wake time steps is in the Keyframe-Control box in GVS. Inside the Keyframe-Control box is the PMARC-Enabled box The use of this option can be illustrated in the following example. If the Cp distribution on an oscillating wing is selected, and the shed wakes are animated, then what is seen on the wing is the color contour Cp distribution for the first time step. By default, this Cp contour does not change with each time step. When the PMARC-Enabled box is clicked on, it changes to PMARC-Phenomena-Always-On. This option allows the Cp distribution to be updated with each time step along with each shed wake. This shows the user how the pressure is changing over the object at each subsequent time step. By activating this option, the animation process can be slowed significantly since the computer is updating the Cp color contour for each time step. For steady state problems, updating the Cp color contour is not as much an issue, but the option can still be used to visualize the developing flow field. This process can be used to update any of the flow phenomena calculated in PMARC (e.g., velocity magnitude, doublet strength, Mach number, etc.).

4. Plotting from GVS

Another option which is mainly used when generating hardcopy outputs from GVS is changing the background color of the geometry window. The default background of the graphics window is black, and the object is white. This provides a rather poor color combination for producing plots. By selecting the Color-Set box an option for selecting background color is provided. Selecting the background color to white and the object lines to color will allow a better plot to be created.

The built-in output generation capability of GVS is found to be insufficient. The SGI "snapshot" function produces a better plot. The snapshot function saves a user selected window area as a RGB file. Options to convert this RGB file into a plottable postscript file are either to use the SGI "tops" function or to read the RGB file into the "xview" program (e.g., xv filename.rgb), and then save it as a postscript file (e.g., filename.ps). Now this file can be sent to a postscript printer.

III. DATA EXTRACTION

The DATA6 output file from PMARC can contain a large amount of data generated during program execution. There are different user-selected options in the DATA5 input file to control how much data is written to the DATA6 output file depending on the needs of the user. This section is a brief overview of how a user might use the UNIX environment to extract certain pieces of data automatically from the PMARC output file. Two sample UNIX script codes are included for reference.

Often only one or two particular coefficients are of interest for a given run. For a steady state solution, it is a fairly easy task to edit DATA6 and extract the data of interest. It is, however, inefficient to edit the DATA6 file to extract the data for each time step for an unsteady case. As an example for the oscillating wing cases that are discussed later, there could be a few hundred time steps and the C_l value at, say the mid-chord, is of primary interest. Obviously, manually extracting these values at each time step from DATA6 requires a large amount of time. The following information presents options on extracting such data in a semi-autonomous method.

Shown here is the use of the UNIX Awk language to extract the desired data for a few general cases. The use of the Awk and Grep commands directs the computer to filter through a file for a particular phrase or character grouping and then extract the selected field or number. This proves to be a useful tool in the data manipulation of PMARC output data. A "script code" in UNIX is simply a list of input commands placed in a file and then executed. These commands can be individually executed by the user at the UNIX prompt, but by placing them in an executable script file an efficient method to do repeated data extraction is created. The extracted data is piped into a file in ASCII format which is read into any plotting routine or a program like MATLAB and then shown graphically.

The script code in Figure 2.1 is used to extract the C_l and C_m values at the mid-chord of an oscillating wing at every time step for a given run. The script code in Figure 2.2 is used to extract the total coefficients for the body-fixed reference frame for a missile model at each time step.

```
#!/bin/tcsh
echo
echo  Process to extract cl and cm from DATA6 PMARC output file
echo
echo  \<Please stand by\: Processing DATA6 information\>
grep  WIND DATA6 > out1
awk  'prev=="AXES" {print} {prev=$2}' out1 > out2
awk  '{print $2,$5}' out2 > clcm
rm    out1 out2
echo
echo  The output file name is \"clcm\"
echo
echo  Then this can be read into Matlab or some other graphics routine
echo  Each line is a time step \(determined from PMARC input\) starting
echo  at time step \#1. To get time step \#0 you\'ll have to manually
echo  load that from DATA6 into clcm since the awk command skips
echo  over that particular line of data
```

Figure 2.1 Sample Data Extraction File.

```
#!/bin/sh
#  AWK Script to extract values from the PMARC output DATA6 file.
#  Finds "BODY AXES" and skips 59 lines then picks first field ($1)
#  which is the total CN value and second field ($2) which is CA
#  and fourth field ($4) which is the C_m value
echo
echo  Reads in DATA6 file and
echo  CN, CA, C_m  data is put in file aimout
awk '
      /BODY AXES/  {
                NL = 59
                for(i=0;i<NL;++i)
                getline                 # Gets 59 line after BODY AXES term
                print $1, $2, $4        # Gets fields
                      }
      '  DATA6 > aimout
```

Figure 2.2 Sample Data Extraction File.

For a steady case problem, such as is examined for the missile models, the time step information is not as important. What this allows the user to easily see is how quickly the code converges to the steady state solution by examining the change in the coefficient values over the range of time steps specified. This might indicate that more time steps are needed to properly reach some convergence criteria.

For proper use of the codes, these script codes must be made executable in the UNIX environment. This is accomplished by using the following command at the UNIX prompt:

chmod +x scriptname

Where the "scriptname" in this case is whatever user-defined filename is given to the script file. These codes can be modified to fit many different data extraction needs. By changing the term to be searched for, the number of skipped lines, and the character fields to be extracted many different possibilities on data manipulation are evident. For further information on using the Awk and Grep commands, see Refs. [6, 7].

IV. VERIFICATION OF THE PMARC CODE

It is felt that to properly understand the important aspects of the PMARC code and to establish confidence in the numerical results that a series of comparisons between the PMARC results and published results is needed. Therefore, comparisons are made of steady state flows, oscillating wing cases, indicial aerodynamic responses, and wake interference results.

A. STEADY STATE COMPARISONS

1. Wing-Body Configuration

In the PMARC instruction manual [Ref. 1] a case for a slender body with wings is presented for a comparison of pressure coefficient (Cp) values over the upper and lower surfaces [Ref. 8]. Shown in Figure 3.1 is the wing-body geometry, and in Figure 3.2 is the Cp distribution from experimental data and from the PMARC output. Within the resolution of the presented data, the Cp comparison appears fairly close. A lift coefficient (C_L) comparison is made between a PMARC model and published results from Rom [Ref. 9]. The configuration is similar to that of Figure 3.1, but it has a blunt tail as seen in Figure 3.3. The comparison shown in Figure 3.4 indicates a reasonable agreement between Rom's data and the PMARC data.

2. Delta Wings

A comparison is made between PMARC and published experimental C_L results of delta wings with two different aspect ratios from Bertin and Smith [Ref. 10]. The comparisons in Figure 3.5 show good agreement in the low AOA regions and then an increasing deviation as the AOA exceeds 10° to 15°. This type of behavior is expected since the PMARC code is linear in AOA.

The delta wing with aspect ratio of 0.83 demonstrates an increased experimental C_L above the linear PMARC result at higher AOA due to the generation of vortex lift caused by the wing configuration. By using a simple trailing edge shed wake model in the PMARC analysis, no attempt to model the vortex lift is made. The additional lift from the vortex formation is seen to diminish as the AOA approaches 40° due to the vortices bursting soon after formation. A delta wing with an aspect ratio of 0.83 has a long chord to span ratio which enhances the vortex lift effects.

The delta wing with the aspect ratio of 3.97 shows a linear relationship of the experimental data until lift is reduced at around an AOA of 20°. This delta wing has a longer span to chord ratio which reduces the effect of any additional vortex lift. The developing vortices simply cannot affect a wing of this shape as much as in the case of the 0.83 aspect ratio delta wing. Therefore, for the aspect ratio 3.97 delta wing no significant additional vortex lift is generated. However, the lift curve slope, $dC_L/d\alpha$, becomes progressively smaller as the aspect ratio decreases [Ref. 10]. This is seen in the comparisons made in Figure 3.5.

3. Biplane Wings

An analysis is done by Milne-Thomson [Ref. 11] on the effects of two-dimensional airfoils flying in close proximity to one another in a biplane configuration. This analysis indicates the top airfoil has higher lift than the lower. This result is confirmed by PMARC for an aspect ratio 20 wing at an AOA of 10° as shown in Figure 3.6. Although not shown here, Milne-Thomson also shows that the lower airfoil would have less drag than the top airfoil. These effects are seen to decrease as the distance between the airfoils increased. As shown in Figure 3.6 the pair of two-dimensional wings provides a higher C_L than the aspect ratio 20 wings.

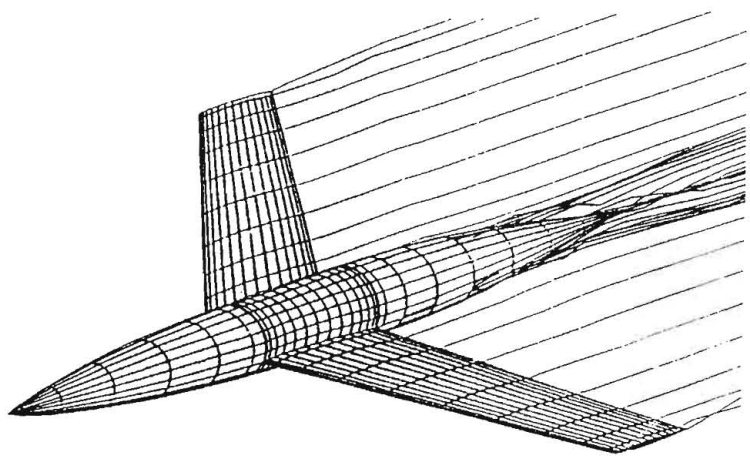

Figure 3.1 PMARC Wing-Body Panel Geometry, From Ref. [1].

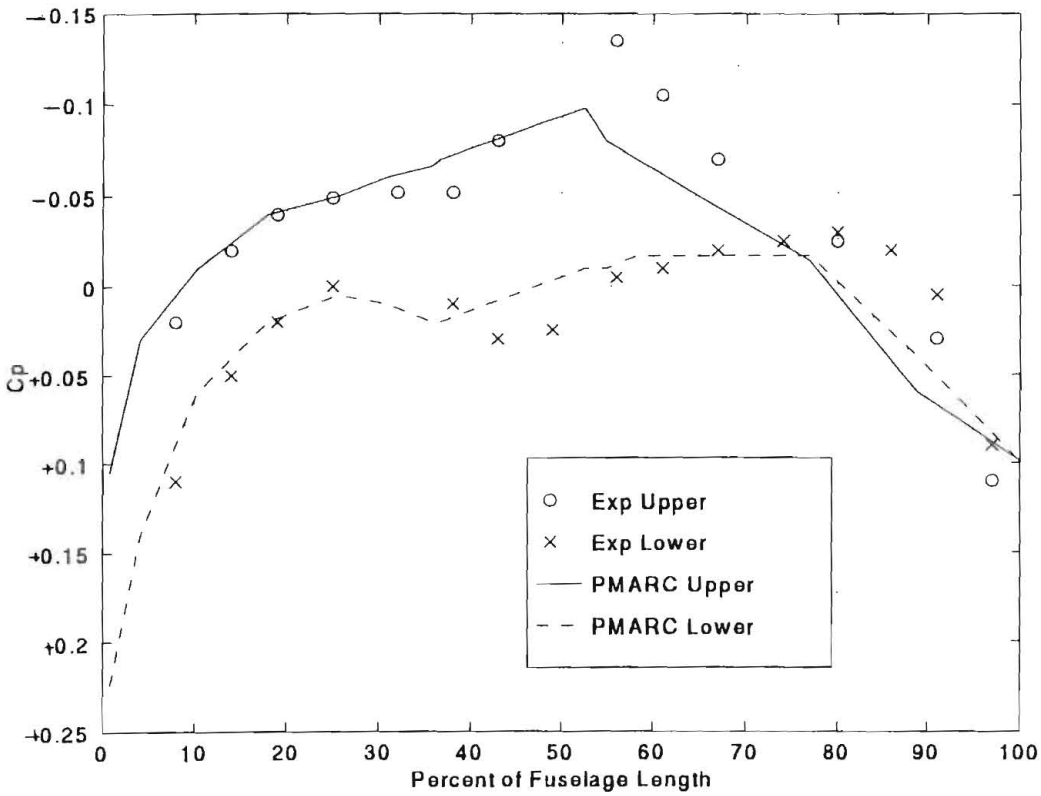

Figure 3.2 Comparison of Cp Data Along Fuselage Centerline (AOA=4°), After Ref. [8].

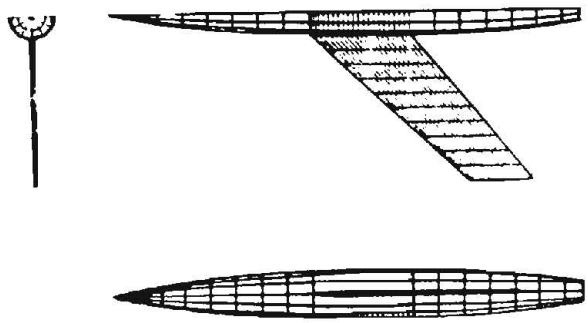

Figure 3.3 Wing-Body Panel Geometry, From Ref. [9].

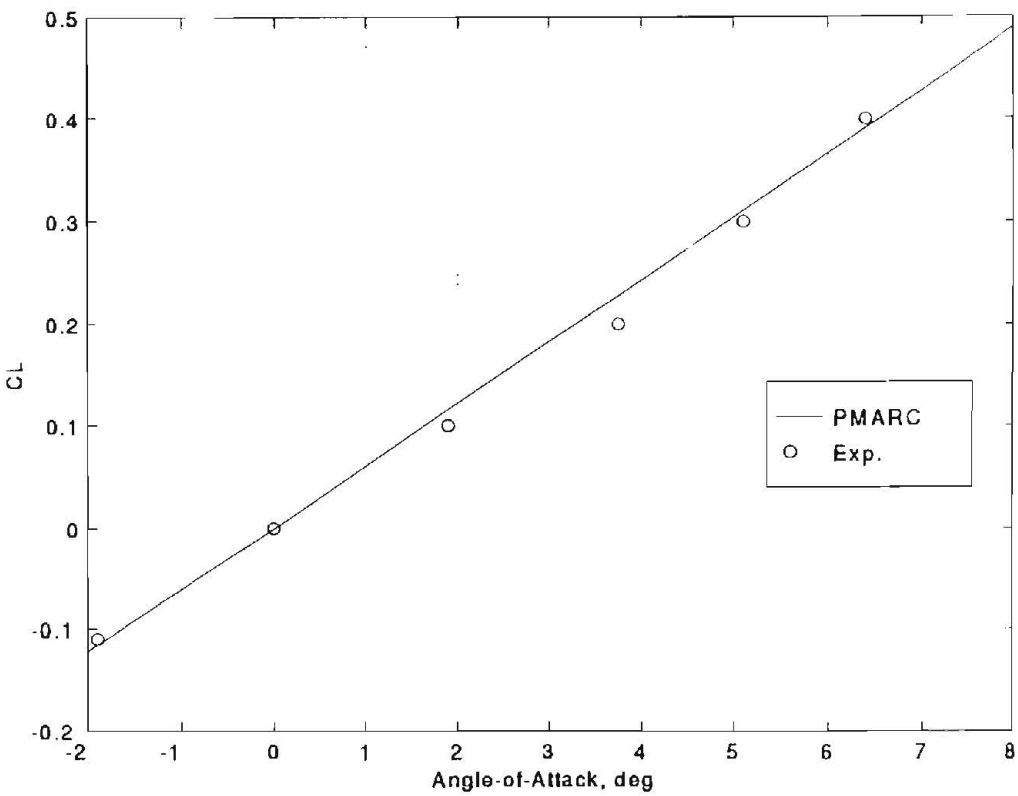

Figure 3.4 Comparison of Wing-Body C_L, After Ref. [9].

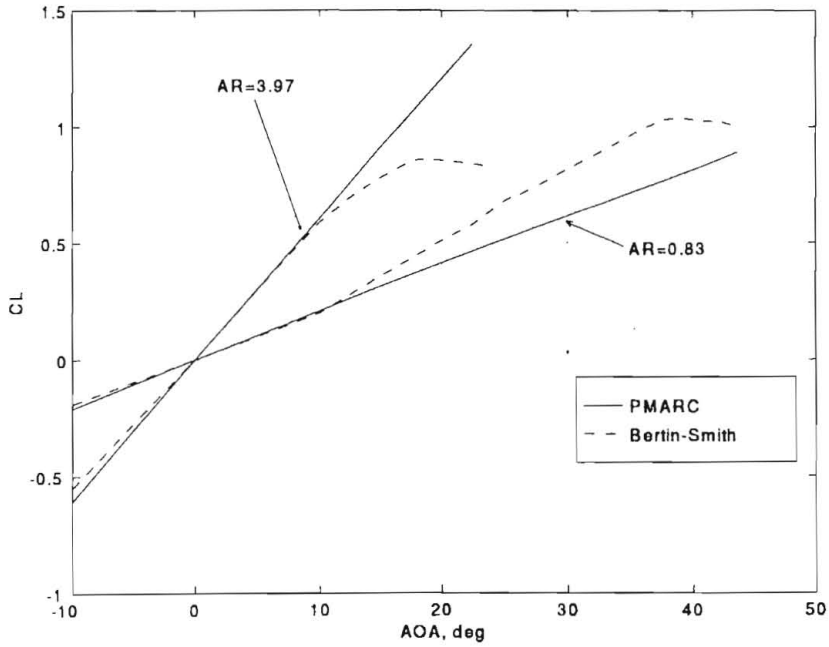

Figure 3.5 Delta Wing C_L Comparison (thickness=0.12c), After Ref. [10].

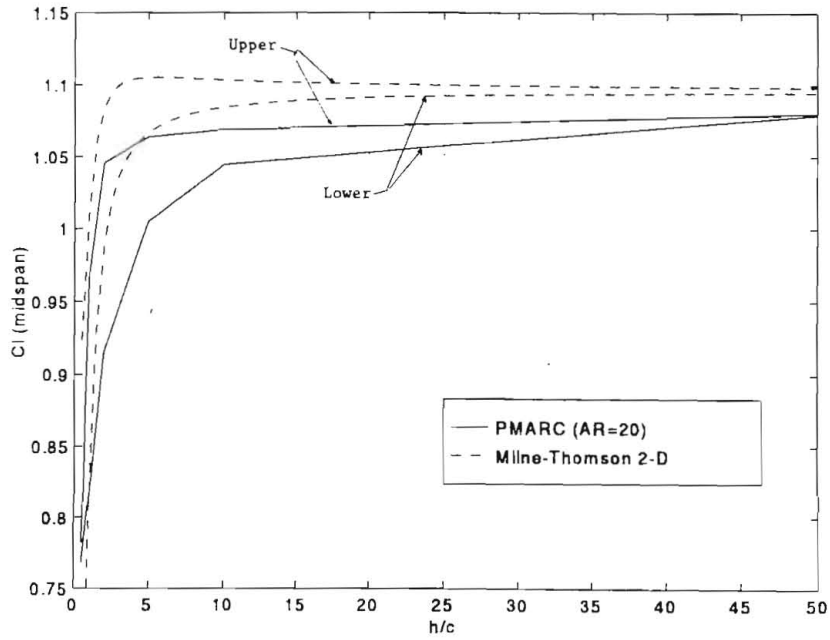

Figure 3.6 Upper and Lower Wing Mid-span C_l for Unstaggered Biwings, After Ref. [11].

4. Wings in Ground Plane Effect

The PMARC code has an internal capability to model the ground plane. This is a fairly simple task in a potential flow code since modeling a ground plane consists only of creating a symmetric model image and placing it the appropriate distance away. Difficulties are encountered in attempting to use the PMARC internal ground plane model. The data generated by PMARC in this case is not consistent with existing data. Eventually, for this analysis, a symmetric wing is modeled and placed at the appropriate distance away from the original wing in order to generate a ground plane model. The results prove reasonable as seen in the comparison made to Kohlman's data [Ref. 12] in Figure 3.7. Kohlman's data is generated from a simplified analysis based on a single horseshoe vortex.

In Kohlman's data, an increase is seen in the lift coefficient ratio at lower AOA while the wing is flying near the ground. As the AOA is increased, the lift coefficient ratio is adversely affected and in fact can be seen to fall below the no-interference lift coefficient. Although the exact C_L's are not compared, the PMARC data in general matches the Kohlman's results fairly well.

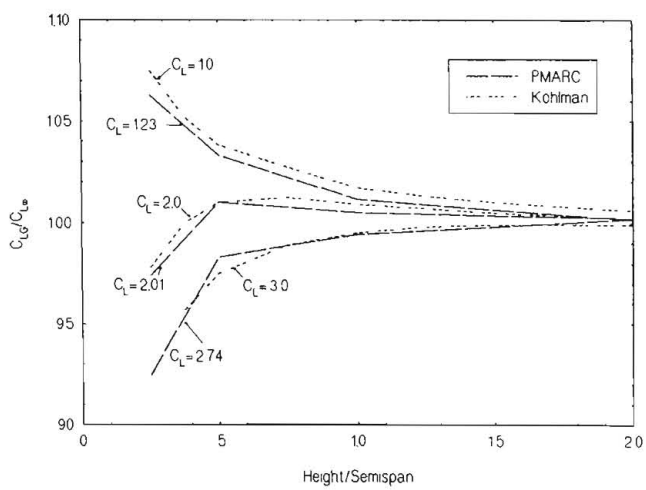

Figure 3.7 Wing in Ground Effect Comparison (NACA0007 Rectangular Wing, AR=7), After Ref. [12].

B. UNSTEADY FLOW COMPARISONS

Several comparisons are made between PMARC results and published results for oscillating wings, wings in impulsively started flows, and the wake interactions of tandem wings.

1. Pitching Wing Comparisons

Comparisons of results for wings executing harmonic pitch oscillations are made between an aspect ratio 20 wing in PMARC, Theodorsen's two-dimensional analysis [Refs. 13, 17], and the NPS two-dimensional, unsteady, panel code [Refs. 14, 15, 16]. Martin and Kroo [Ref. 13] actually make comparisons between Theodorsen's two-dimensional equations [Ref. 17] for an airfoil in pitch and plunge motion and their own runs using the PMARC code. The equation presented in Ref. [13] for the moment coefficient of a two-dimensional airfoil oscillating in pitch only is found to be in error. There is an erroneous negative sign in the first term of the equation. The corrected pitching moment equation is:

$$\begin{aligned}(C_m(t))_p &= \frac{\pi}{2}\alpha_0[(a-0.5)k+2(0.5+a)((0.5-a)kF+G]\cos(\omega t)\\ &+\frac{\pi}{2}\alpha_0[(0.125+a^2)k^2+2(0.5+a)(F-(0.5-a)kG]\sin(\omega t)\end{aligned} \tag{3.1}$$

The lift coefficient equation for a two-dimensional airfoil in pitch only is:

$$\begin{aligned}(C_l(t))_p &= \pi\alpha_0[k+2(F(0.5-a)k+G)]\cos(\omega t)\\ &+\pi\alpha_0[ak^2+2(F-(0.5-a)Gk]\sin(\omega t)\end{aligned} \tag{3.2}$$

The "F" and "G" terms in Equations 3.1 and 3.2 are the real and imaginary components from the Theodorsen function, and "α_0" is the pitch motion amplitude in radians. The reduced frequency "k" is equal to $\omega b/U_\infty$ with "b" being the airfoil half-chord, and "a" is the location of the pitching axis [Ref. 13]. Martin and Kroo examine many different parameters in their analysis of unsteady wing motions. The principal goal of this comparison is to consider the lift and pitching moment coefficients for a wing pitching about its one-half chord point.

Shown in Figure 3.8 is the comparison between Theodorsen's equations and the resulting PMARC data at a reduced frequency of k=0.3. The lift and pitching moment coefficients are matched fairly well. Shown in Figure 3.9 is the comparison between the PMARC results and those obtained by the NPS code for lift coefficient and moment coefficient at a reduced frequency of k=0.3. This comparison shows good agreement.

2. Impulsively Started Wings

The PMARC code inherently starts all runs with an impulsive start unless otherwise directed. Martin and Kroo [Ref. 13] make a brief comparison of an impulsively started rectangular wing with an aspect ratio of 6. Katz and Plotkin [Ref. 18] investigate impulsively started wings for the case of several different aspect ratios of rectangular wings and compare them with other potential flow computer codes. Shown in Figure 3.10 are indicial C_L results computed with PMARC compared to the results from Katz and Plotkin. Shown in Figure 3.11 are the induced drag coefficient (C_{Di}) comparison. An AGARD report by Lomax [Ref. 19] presents indicial lift coefficients for impulsively started wings for rectangular and delta wings. Shown in Figure 3.12 are the rectangular wing C_L comparison between Lomax and the PMARC results. Figure 3.13 provides the C_L comparison for an aspect ratio 4 delta wing. Actually Lomax plots lift curve slope ratios instead of lift coefficient ratios, but for low AOA the ratios are essentially the same as the dependence on AOA will cancel out.

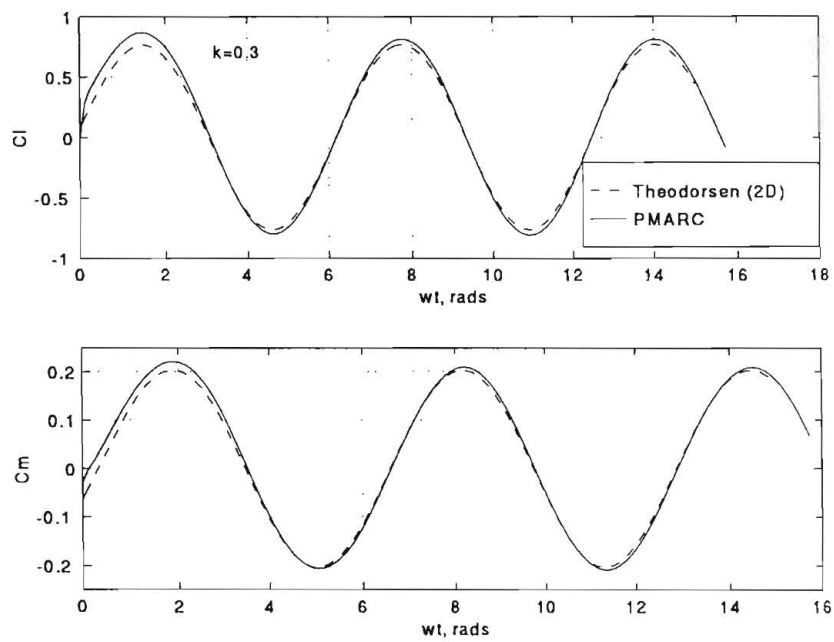

Figure 3.8 Oscillating Wing Coefficient Comparisons to Theodorsen's Equations for NACA 0007, AR=20 Rectangular Wing Pitching at the c/2 axis, After Ref. [13].

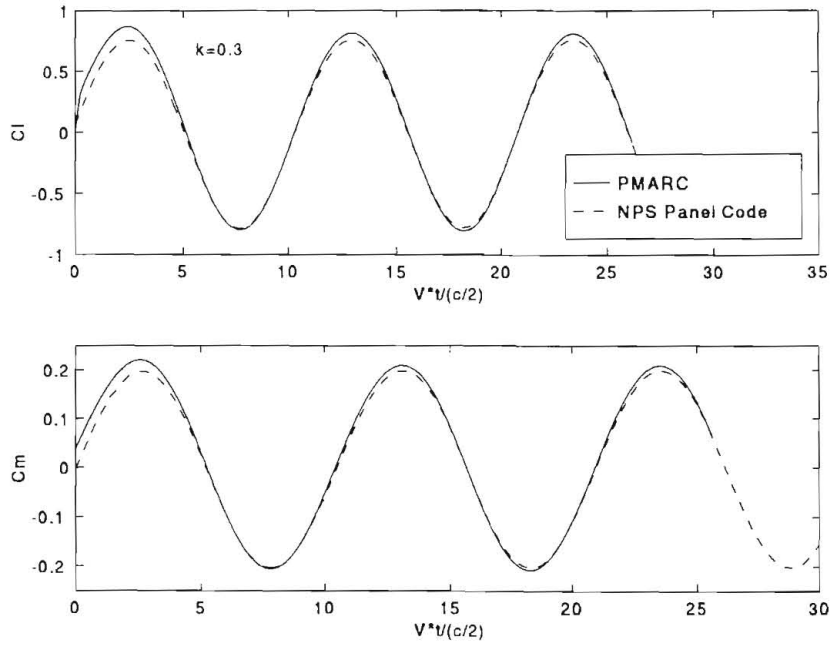

Figure 3.9 Oscillating Wing Coefficient Comparisons to the NPS Panel Code for NACA 0007, AR=20 Rectangular Wing Pitching at the c/2 axis, After Ref. [16].

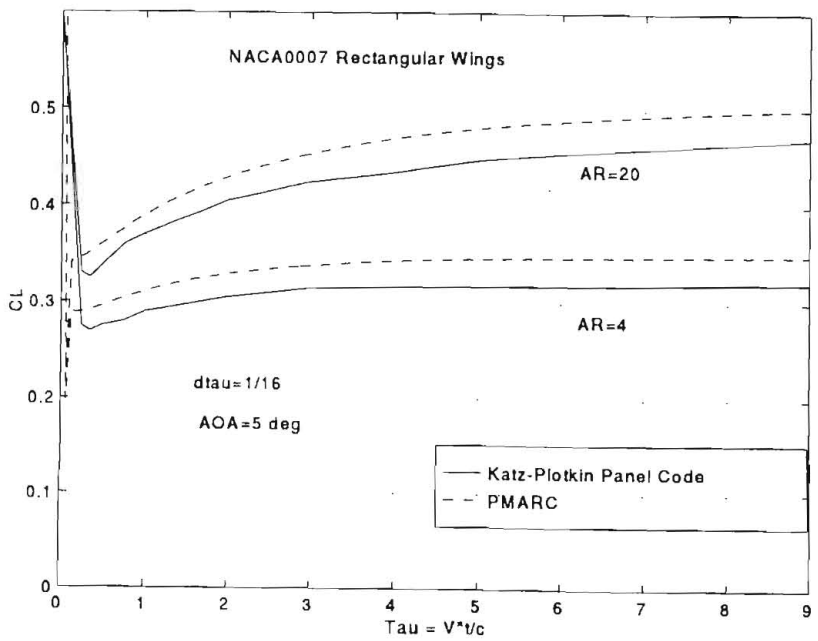

Figure 3.10 C_L Comparisons for Impulsively Started Wings, After Ref. [18].

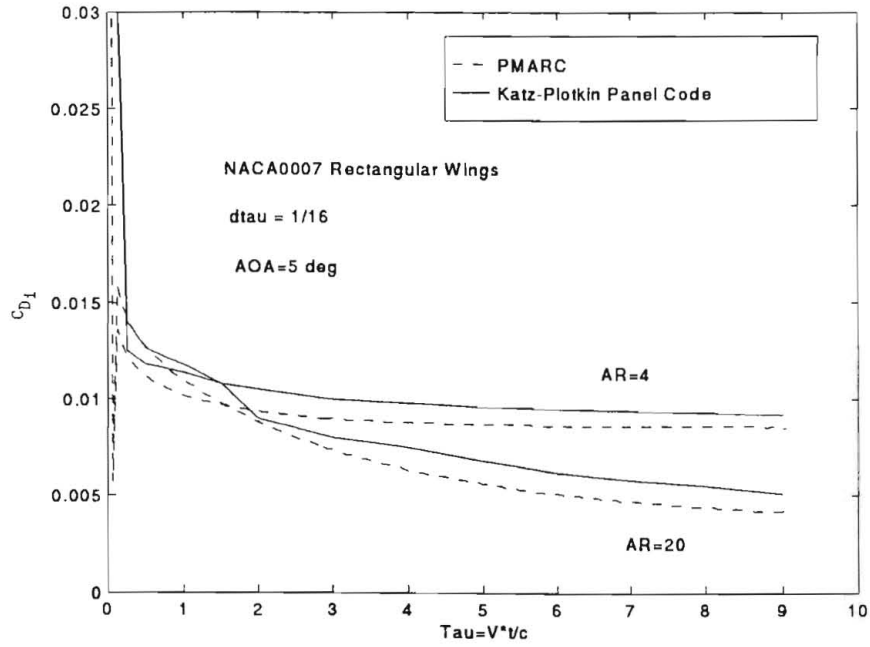

Figure 3.11 Induced C_D Comparison for an Impulsively Started Wing, After Ref. [18].

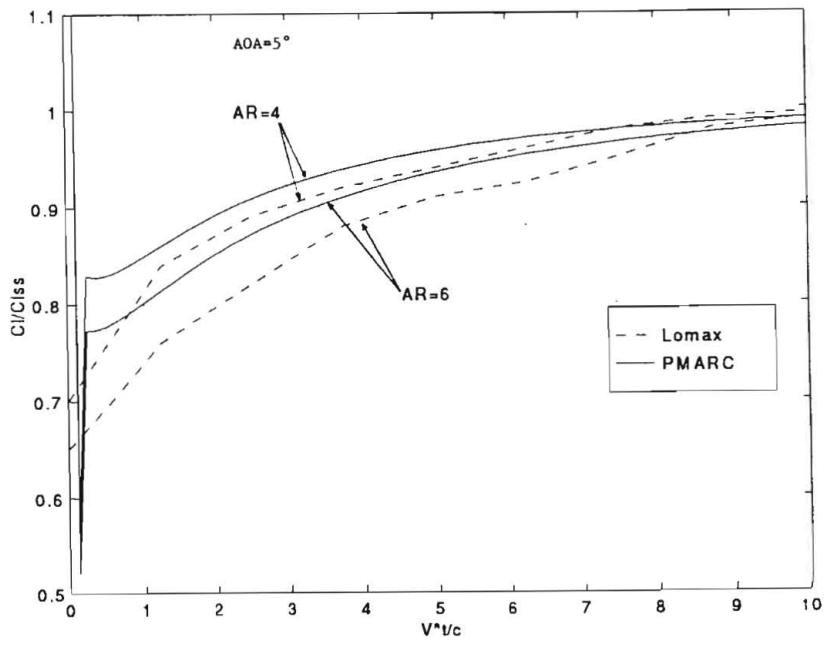

Figure 3.12 Impulsively Started Lift Coefficient Ratio Comparison for AR = 4 and 6, NACA 0007, Rectangular Wings, After Ref. [19].

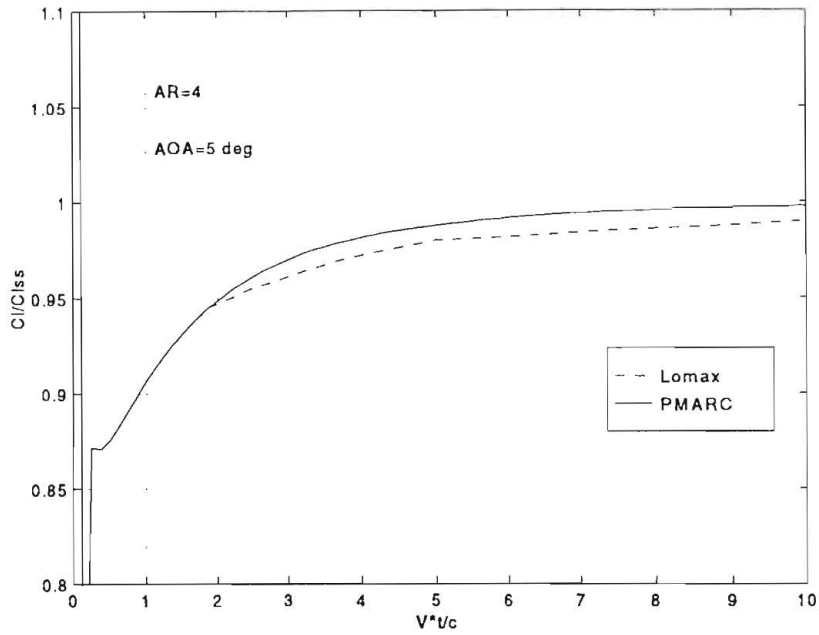

Figure 3.13 Impulsively Started Lift Coefficient Ratio Comparison for AR = 4, NACA 0007, Delta Wing, After Ref. [19].

3. Wings in Tandem

A comparison is made to an analysis of a two-dimensional pair of airfoils flying in tandem as shown by Glauert [Ref. 20]. The theoretical results predicted by Glauert for the two dimensional case indicate that an airfoil having a chord length twice that of each individual airfoil set in tandem has the average lift coefficient of the tandem pair as shown in Equation 3.3:

$$C_{L_{2c}} = \frac{C_{L_{FWD}} + C_{L_{AFT}}}{2} \tag{3.3}$$

Attempts to model this exact geometry in a three-dimensional configuration using the PMARC code meet with mixed results. The problem found is that the wake being convected downstream from the forward wing impinged upon the aft wing and penetrate the aft wing's surface during the subsequent time step. Therefore, the cases studied are those that avoided this

penetration. Jones and Platzer [Ref. 16] find for a two-dimensional wake interaction computer code that by decreasing the time step to very small relative values the convected wake will avoid the aft wing. This approached proves to be computationally unreasonable for the three-dimensional PMARC code.

Two cases are devised where the forward wing's wake passes close to the aft wing but does not actually touch it. In each case two wings are placed in tandem separated by three chord lengths measured from leading edge to leading edge. The first case places the wing system at a global AOA of 10° so that the forward wing wake passes over the aft wing. The C_L's are compared for the developing flow of the first case in Figure 3.14. In the second case, the aft wing is shifted 0.2 chord lengths above the forward wing, and each individual wing is placed at an AOA of 10° so that the forward wing wake passes below the aft wing. The C_L comparison of the second case is shown in Figure 3.15. The resulting mid-span section lift coefficients are compared to a single wing with twice the chord length of each individual wing. Wings with aspect ratios of 6 and 20 are compared although only aspect ratio 6 wings are shown in Figures 3.14 and 3.15. Table 3.1 compares the resulting values from the PMARC runs for the section lift coefficients.

AR	C_l for 2x Chord Single Wing	Average C_l for Global AOA of 10°	Average C_l for Aft Wing Shifted +0.2c
6	0.9035	0.7595	0.7419
20	1.0639	0.9969	1.0047

Table 3.1 Tandem Wings Average Section Lift Coefficient Comparisons.

The average section lift coefficients shown in Table 3.1 are calculated from the section lift coefficients from the forward wing and the aft wing as shown in Equation 3.1. The pair of wings with aspect ratio 20 have a section lift coefficient closer to the theoretical value predicted by Glauert than the aspect ratio 6 pair. Also, some deviation from theory is to be expected since it is not possible to follow the exact geometry presented by Glauert.

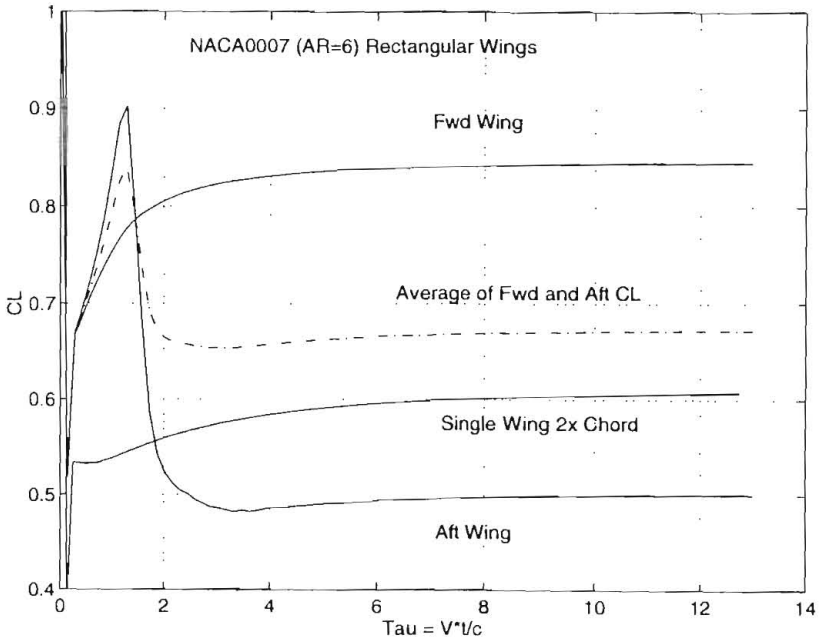

Figure 3.14 Two Wings in Tandem at a Global AOA of 10°, Separated by Three Chord Lengths Leading Edge to Leading Edge, After Ref. [20].

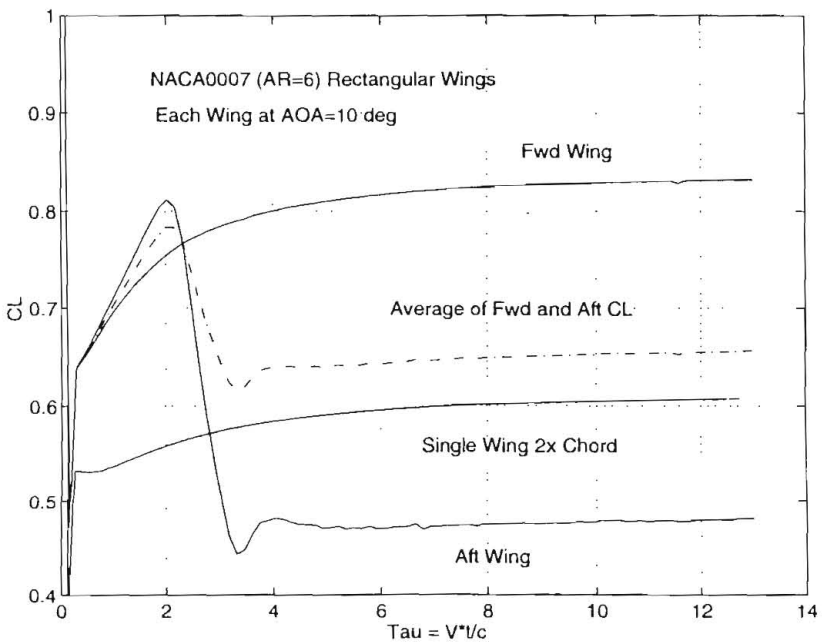

Figure 3.15 Two Wings in Tandem with the Aft Wing Three Chord Lengths (Leading Edge to Leading Edge) Behind and Shifted 0.2 Chord Lengths Up, After Ref. [20].

V. RESULTS OF MISSILE MODELING

A. MISSILE AIRFRAME DISCUSSION

The primary focus of the remaining work is to evaluate PMARC for aerodynamic missile design. To this end, the missile configurations studied by Smith et. at., [Refs. 21, 22] and by Meyer [Ref. 23] are investigated. Smith carries out a series of Mach 0.2 wind tunnel experiments on the configuration seen in Figure 4.1a. The PMARC model is shown in Figure 4.1b. Normal, moment, and axial force coefficients are found as a function of AOA. Additional parameters considered are control surface deflection and missile roll angle. Similarly, Meyer conducts wind tunnel experiments at Mach 0.1 on the configuration seen in Figure 4.2a. His primary concern centers on the effects of wing location and missile roll angle on various force coefficients. The PMARC model of the Meyer wing-body is seen in Figure 4.2b.

B. AERODYNAMIC COEFFICIENTS

A large emphasis is made in validating the aerodynamic coefficients presented in Refs. [21, 22, 23]. Meyer [Ref. 23] provides a comprehensive set of data with which to compare experimental values to PMARC generated coefficients like the pressure coefficient (Cp) and the normal force coefficient (C_N) for the missile wings and body. It is more difficult for PMARC to match the coefficients for the configuration used by Smith [Ref. 21, 22] due to canard-tail-body flow interactions. The wake modeling provided by PMARC is not found to be robust in terms of dealing with downstream interactions from other components of the body geometry. Application of the PMARC wake mechanism provide the most difficult aspect of modeling the flows although some reasonable coefficient values are obtained by applying vortex sheet type wakes to the models as discussed below.

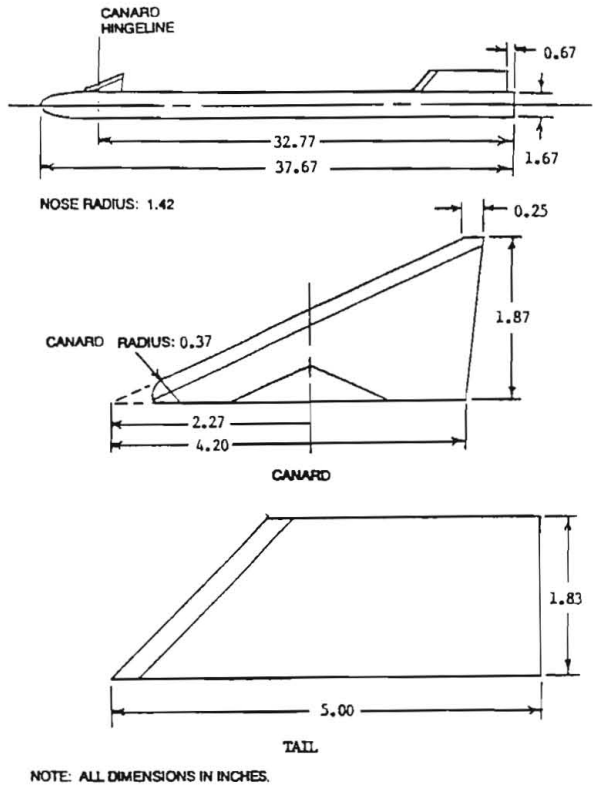

Figure 4.1a One-Third Scaled Missile Model Used for Experiments, From Ref. [21].

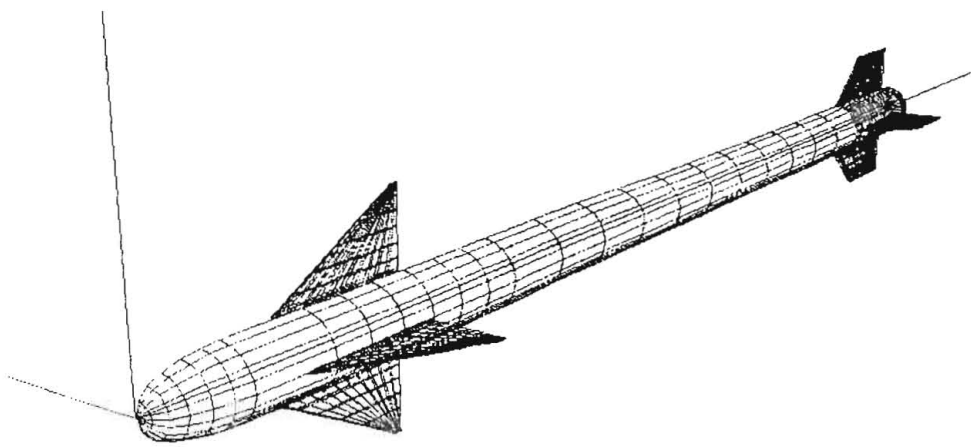

Figure 4.1b PMARC Panel Model of Smith's Missile.

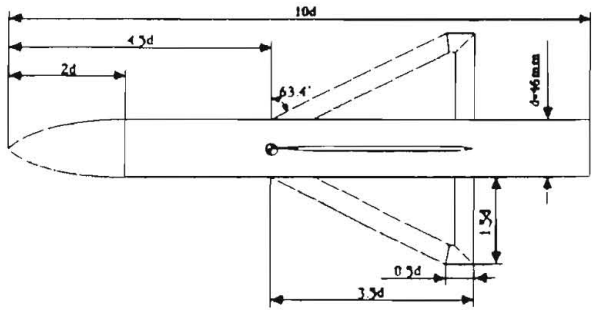

Wing B - Mid Position Configuration

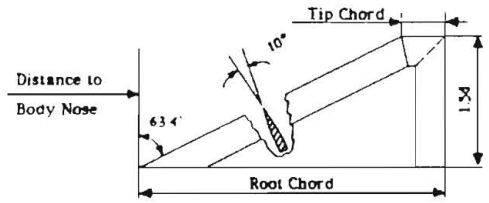

Configuration	Distance to Nose	Root Chord	Tip Chord
Wing A - Mid Position	4.5d	3.0d	0
Wing B - Fore Position	2.4d	3.5d	0.5d
Wing B - Mid Position	4.5d	3.5d	0.5d
Wing B - Back Position	6.0d	3.5d	0.5d
Wing C - Mid Position	4.5d	4.0d	1.0d

Figure 4.2a Meyer Wing-Body Model Used for Experiments, From Ref. [22].

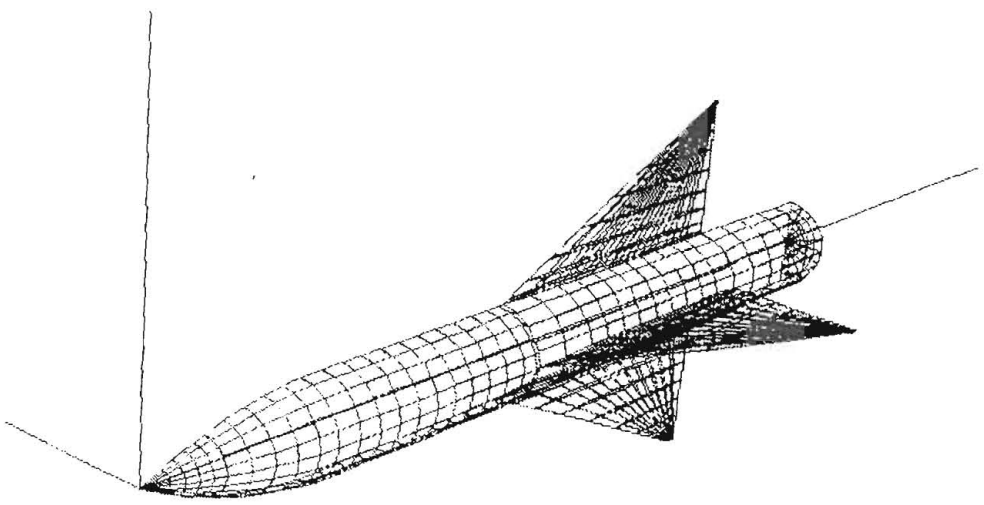

Figure 4.2b PMARC Panel Model of Meyer's Configuration.

1. Pressure Coefficient (Cp)

Comparison of the PMARC generated Cp distribution around an axisymmetric body to other data and theories provides insight to the accuracy of PMARC.

a. Nose Geometry

Many general theories predicting the pressure distribution over bodies are functions of the local slope along the bodies. Theoretical analysis of the Meyer body (Figure 4.2) and the pressure distribution around it requires that the nose geometry be mathematically defined. The nose on this body is a tangent-ogive. This is a fairly common nose configuration on many types of air-to-air missiles. A general equation [Ref. 24] used to define a tangent-ogive for missile applications is:

$$y(x) = \sqrt{R^2 - (x - L)^2} - b \tag{4.1}$$

For the case of the Meyer body with a nose length of 2d (L = 0.3018 ft) based on a body diameter of 0.1509 ft, the parameters in Equation 4.1 are R = 0.6414 ft, and b = 0.5659 ft. These parameters are found by applying the following boundary conditions to Equation 4.1.

$$y(0) = 0 \tag{4.2a}$$

$$y(L) = d/2 \tag{4.2b}$$

Figure 4.3 shows the general geometry for a tangent-ogive nose described by Equation 4.1.

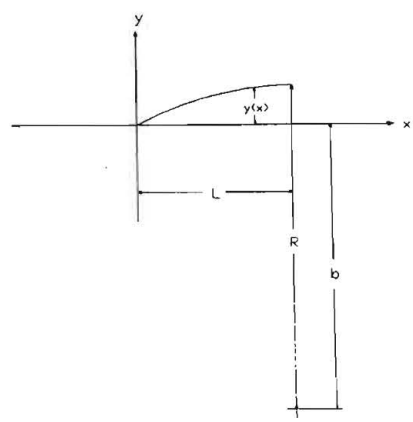

Figure 4.3 Tangent-Ogive Nose Geometry.

b. First Order Slender Body Theory

First order Slender Body Theory (SBT) predicts a Cp distribution that is linear in AOA about a body of revolution at low AOA. Equation 4.3 represents the first order equation for the Cp about a slender body [Ref. 25]. The θ body angle is referenced to zero at the six o'clock position looking at the body from the nose to the tail.

$$Cp(x) = 4\alpha y'(x)\cos(\theta) \tag{4.3}$$

For the example of the ogive nose for the Meyer body, the equation for y'(x) results from taking the derivative of Equation 4.1 which describes the shape of the nose. The derivative of Equation 4.1 gives the local slope of the ogive nose.

Shown in Figure 4.4 is the Cp comparison along the length of the body from first order SBT results to those of PMARC for the Meyer body-alone. The PMARC results are concluded to be more accurate than SBT near the nose. As seen in Figure 4.4, first order SBT predicts zero Cp at AOA when the slope of the body relative to the body axis is zero.

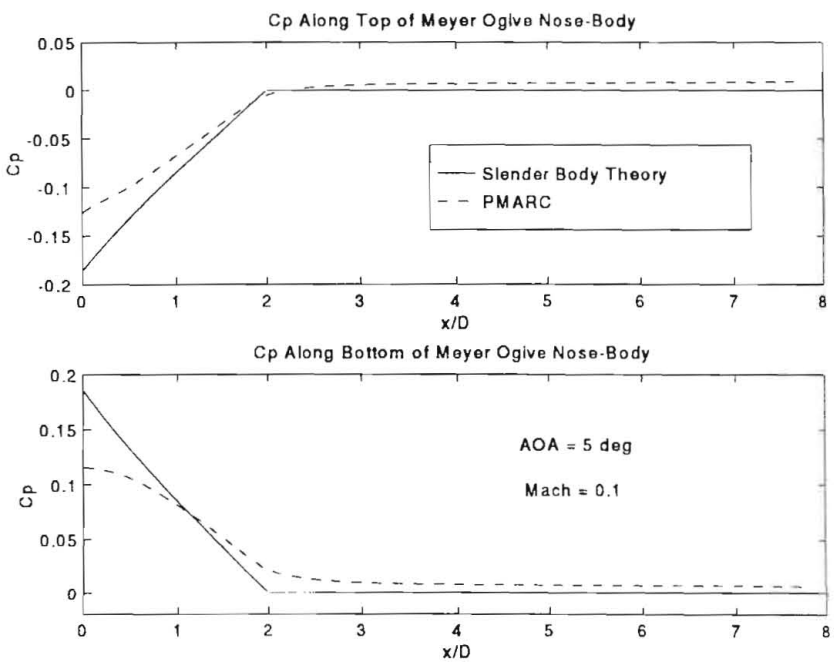

Figure 4.4 Cp Comparison Along Top and Bottom of the Meyer Body-Alone, After Ref. [24].

First order SBT only predicts pressure disturbances resulting from AOA effects. Hence at zero AOA, SBT predicts a zero pressure distribution as seen in Equation 4.3. In contrast, PMARC calculates the pressure distribution from body thickness effects as well as AOA effects. In order to make a comparison between the SBT and PMARC results, the thickness effects must be subtracted out of the PMARC results. This is done by running the body in PMARC at zero AOA, and then running it at the desired AOA (e.g., 5°). Now the Cp resulting from just AOA effects is essentially the Cp from the run at AOA minus the Cp resulting from the zero AOA run. The Cp from the zero AOA run is actually the pressure distribution generated from the body thickness effects. By subtracting its value, the remaining Cp is due to AOA effects as seen in Equation 4.4.

$$Cp_{\alpha} = Cp_{TOTAL} - Cp_{THICKNESS} \tag{4.4}$$

For the Meyer body with a tangent-ogive nose of length x/d=2, the Cp expression from first order SBT is seen in Equation 4.5.

$$Cp(x) = 4\alpha\cos(\theta)\frac{(L-x)}{\sqrt{R^2-(x-L)^2}} \qquad \text{for } x \le 2d \tag{4.5a}$$

$$Cp(x) = 0 \qquad \text{for } x \ge 2d. \tag{4.5b}$$

c. Second Order Slender Body Theory

As seen in Figure 4.5, the Cp comparison along the mid-line of the Meyer body. Obviously, the second order SBT is not matching the Cp very well near the nose of the body as it cannot account for all the disturbances that PMARC models. Equation 4.6 shows the second order theory [Refs. 25, 27]. In this case, the θ body angle is referenced from the three o'clock position looking at the body from the nose to the tail. This is different from the first order theory equation and needs to be kept in mind when comparing the two equations.

$$Cp(x) = -4\alpha y'(x)\sin(\theta) + \alpha^2[1-4\cos^2(\theta)] \tag{4.6}$$

The same local slope equation y'(x) applies to the second order Equation 4.6 as it does for the first order Equation 4.5.

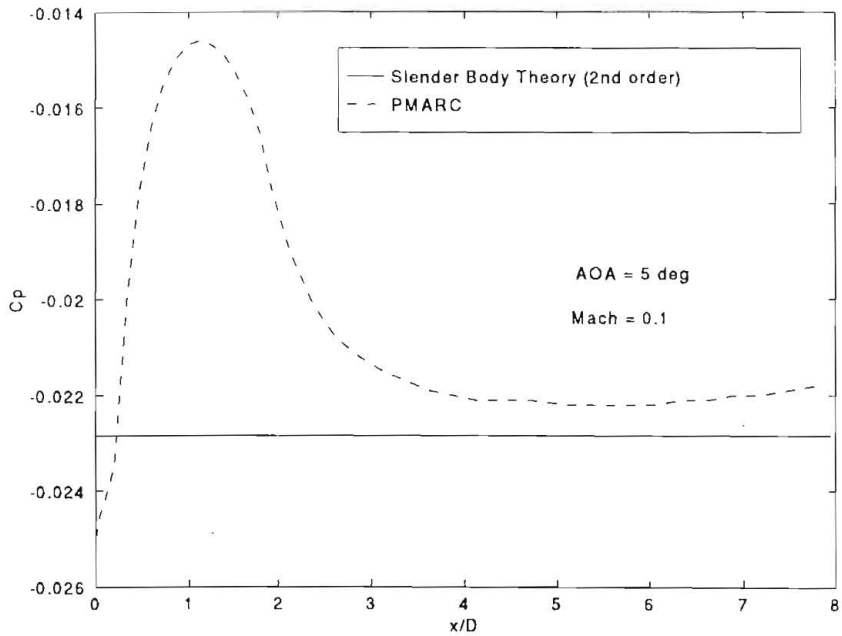

Figure 4.5 The Cp Comparison Along the Mid-line of the Meyer Body-Alone, After Ref. [23].

d. Experimental Data Comparison

Mendenhall et. al. [Ref. 26] provides data describing the Cp distribution around the body at different fuselage stations. The Mendenhall data is for a tangent-ogive nose-body with a nose length of x/d=3 and a body length of x/d=7.7. In this data, the β body angle is referenced to zero at the six o'clock position looking at the body from the nose to the tail. A comparison of the Cp distribution with the PMARC data generated at different locations along the body from PMARC is shown in Figures 4.6 and 4.7. Fair agreement is seen near the nose of the body. The agreement breaks down toward the tail of the body as nonlinear flow effects and separated flow begin to dominate.

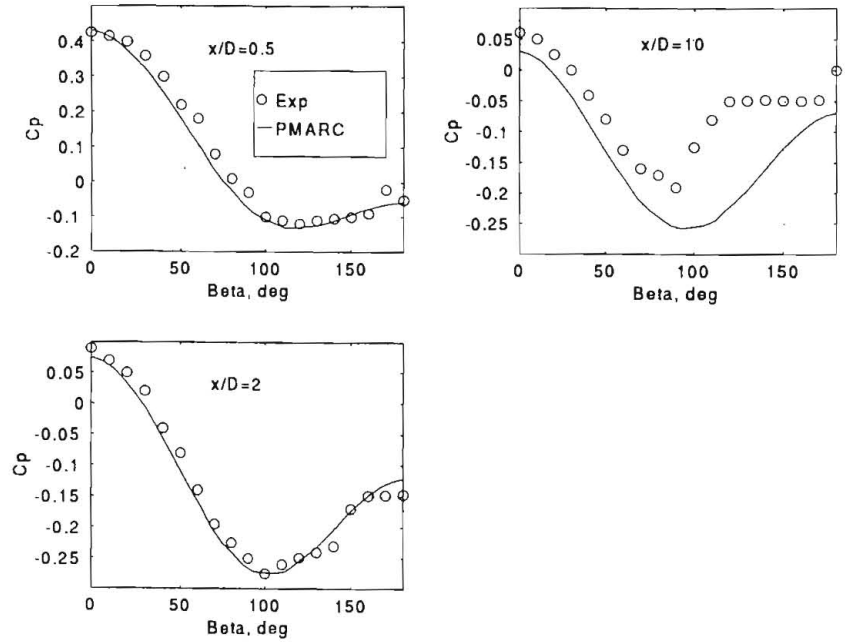

Figure 4.6 Cp Comparison for AOA=15° at Mach=0.3 of Body of Revolution, After Ref. [26].

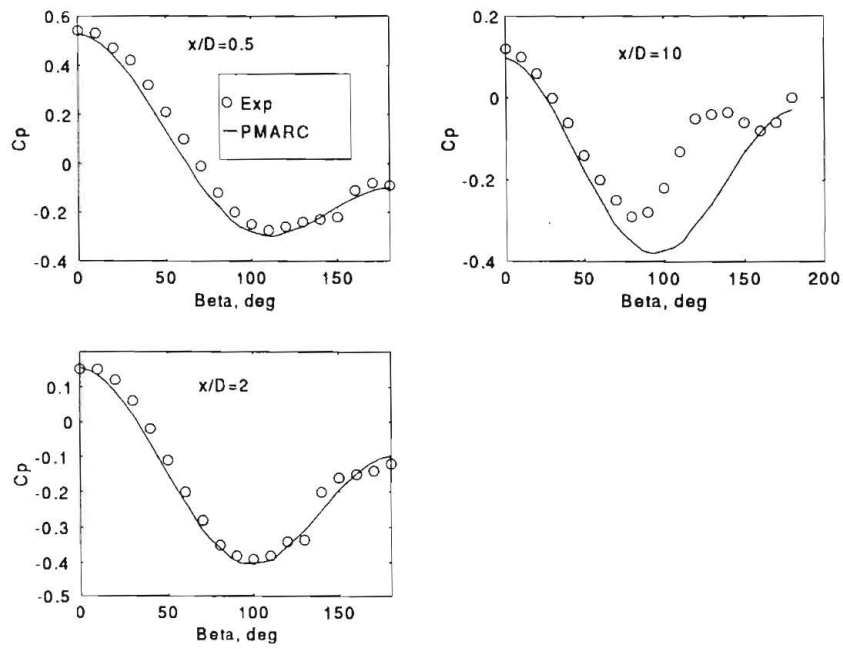

Figure 4.7 Cp Comparison for AOA=20° at Mach=0.3 of Body of Revolution, After Ref. [26].

2. Normal Force Coefficient (C_N) From Initial Wake Model

The two configurations shown in Figures 4.1 and 4.2 are initially analyzed using a simplified wake model. This wake model consists of wakes shed from the horizontal control surfaces as well as a circular-shaped wake shed from the blunt tail. This wake model proves to be inadequate for PMARC to properly calculate the C_N values. A more accurate wake model is discussed in a later section. Even though inaccurate, the results from the initial modeling attempts are still of interest, and the following is a discussion of the results.

As seen in Figure 4.8 the comparison between Meyer's data [Ref. 23] and PMARC shows general agreement at relatively low AOA for C_N of the total wing-body system at a zero roll angle (ϕ=0°). This configuration has large wings relative to body diameter. The wings generate the majority of the lifting force in this case which is modeled well by PMARC. Figure 4.9 shows the C_N comparison for the body-alone case. Apparently, the PMARC model is not accounting properly for the lift due to the body. In the later section on wake modeling a more accurate method to predict body lift is discussed. Figure 4.10 shows the C_N comparison for the wings in the presence of the body, and the body in the presence of the wings. These results are matched reasonable well at low AOA due to the presence of the wings and the lift they produce.

The C_N curve for the Smith missile configuration seen in Figure 4.11 shows that PMARC underpredicts the values compared to Smith's experimental values [Refs. 21, 22] and the AP95 data [Ref. 28]. Most likely the lift due to the body is not being fully accounted for similar to the Meyer body-alone as discussed previously. The Smith missile has small wing surfaces consistent with most tactical missiles. In this case, the majority of the lifting force comes from body lift. Since the PMARC model devised for the Smith missile does not model the body lift well, the deviation between the experimental C_N and the PMARC prediction is relatively large. In the wake modeling section to follow, a discussion is made of the use of vortex sheet wake separation lines along the body to better model the body lift contribution as well as the use of wakes shed from the canards and tail surfaces to account for the lift contribution from these components.

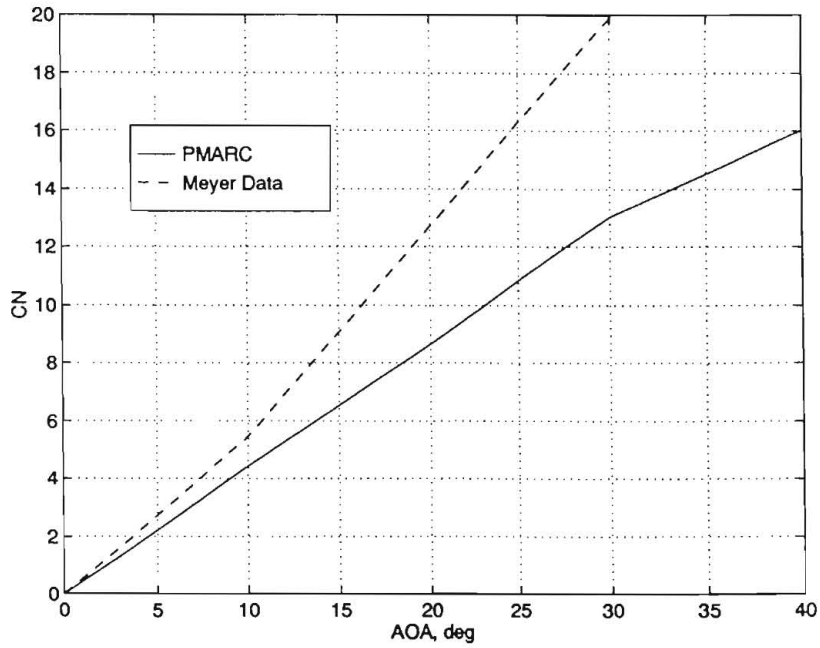

Figure 4.8 C_N for Total Wing-Body System at Zero Roll Angle, After Ref. [23].

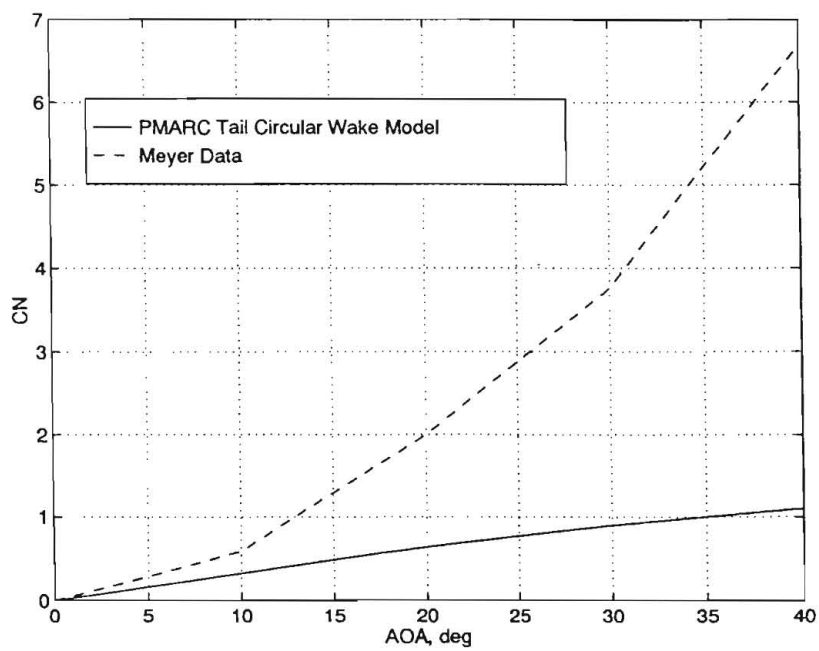

Figure 4.9 C_N Comparison for Body-Alone, After Ref. [23].

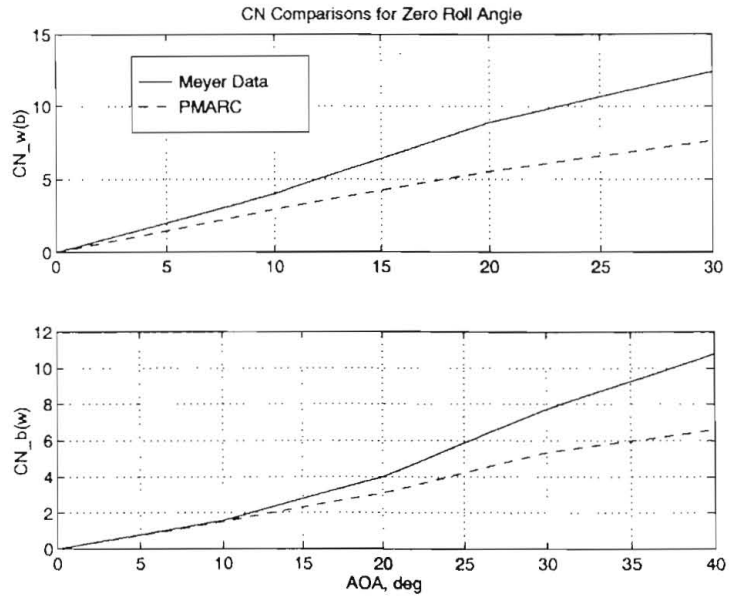

Figure 4.10 C_N Comparison for the Wing in the Presence of the Body (C_N_w(b)) and the Body in the Presence of the Wing (C_N_b(w)), After Ref. [23].

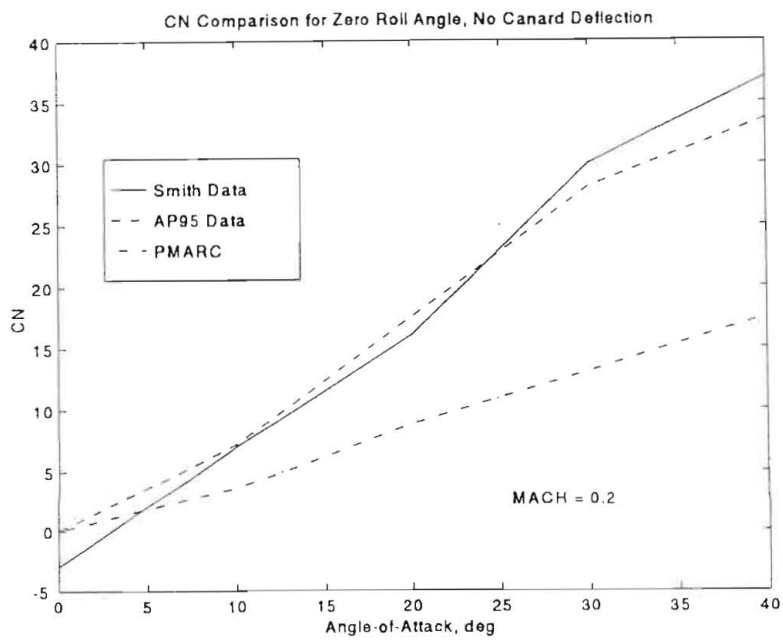

Figure 4.11 C_N Comparison of a Canard-Controlled Missile, After Ref. [21, 28].

C. WAKE MODELING

The wake modeling in PMARC is the principal component in predicting the lift force contributions of individual body components. For a basic wing model, the wake mechanism is well understood, and a shed wake is placed at the trailing edge of the wing. This type of configuration usually results in close comparisons between the lift on the wing from PMARC and other published values. In contrast, the case of a missile body with canard and tail surfaces proves more difficult in modeling an accurate wake shedding system. A majority of the wake modeling effort centers around the Meyer body-alone configuration. This configuration provides a good test base to validate the different wake modeling schemes attempted. More on this wake modeling effort follows in the next section.

It is felt more work could be done on enhancing the PMARC body lift component to further improve the correlation between the PMARC results and those from experimental methods. There is apparently a trade-off in accuracy in the modeling of the wake shed from the body. This wake shedding is the mechanism for generating lift forces in PMARC. For the cruciform missile bodies at a 0° roll angle, or in the "plus" configuration, only the horizontal control surfaces are assigned wakes since the vertical surfaces are assumed to contribute no lift to the missile system.

The wake model for the Meyer missile at a 45° roll angle, or in the "X" configuration, requires that each of the four wings shed a wake since each wing is generating lift in that orientation. Consequently, the lower two wings have wakes which penetrate the aft fuselage when the missile is placed at an AOA. This meant that these two wakes have to be truncated on each trailing edge so they will just miss the fuselage at a given AOA as they convect downstream. This causes the lift for those particular wings to be underpredicted. The alternatives in this configuration are having the wakes from the lower two wings extend along the entire wing trailing edge and penetrate the aft fuselage or truncate the trailing edge wakes causing the lift contribution from the wings to be underpredicted.

PMARC has two options within its wake model. There is the option to have a rigid wake or a flexible wake. A rigid wake is convected at the free stream velocity and is transported downstream with no distortion of the wake panel. A flexible wake is convected with the local velocity field and provides modeling of vortex roll-up as seen, for example, in a wing tip vortex

system. The flexible wake is more computationally intensive than the rigid wake and is more prone to cause problems in running a model.

1. Vortex Sheet Separation Line for the Meyer Body-Alone

In this analysis, two wake models are used in PMARC for the Meyer body-alone configuration that allowed for stable computations. The previously discussed first wake model attempted for the Meyer body-alone consists of a circular-shaped wake shed from around the edge of the blunt tail. The second wake model places two vortex sheet wake separation lines along the length of the body at general locations consistent with published vortex separation lines [Refs. 26, 27]. This second wake model provides a large amount of flexibility in controlling the C_N calculated by PMARC. The PMARC model for the Meyer body-alone consists of 2940 panels with 60 panels placed circumferentially and 49 panels placed axially. The discretization of the body is largely at the discretion of the user. This relatively large number of circumferential panels allowed flexibility with selecting wake separation lines. For the Meyer body-alone, two wake separation lines are started at the tangent point of the nose and body and continued back to the corner of the blunt tail. This is done in an attempt to simulate the actual location of the vortex shedding indicated in Refs. [26, 27].

Figure 4.12 is an excerpt from a DATA5 input file seen in Appendix E for the Meyer body-alone at an AOA of 20°. The parameters in the wake section allow the user to control the location of the wake shed line in any arbitrary manner consistent with the panel geometry.

```
&WAKE1  IDWAK=1,      IFLXW=1,      ITRFTZ= 1,    INTRW= 0,     &END
 +Y_FUSELAGE WAKE
&WAKE2  KWPACH=1,     KWSIDE=2,     KWLINE=19,    KWPAN1=19,
        KWPAN2=44,    NODEW=3,      INITIAL=0,                  &END

&WAKE1  IDWAK=1,      IFLXW=1,      ITRFTZ= 1,    INTRW= 0,     &END
 -Y_FUSELAGE WAKE
&WAKE2  KWPACH=2,     KWSIDE=2,     KWLINE=11,    KWPAN1=19,
        KWPAN2=44,    NODEW=5,      INITIAL=0,                  &END
```

Figure 4.12 Excerpt of Wake Input Parameters from a DATA5 Input File.

The KWPAN1=19 parameter indicates the wake line begins at section 19. This corresponds to the tangent point of the nose and body (i.e., there are 19 axial sections used to define the tangent-ogive nose). KWPAN2=44 indicates the wake line ends at the corner of the blunt tail which corresponds to section 44. For reference, section one is at the nose and section 49 is the last section at the tail. Figure 4.13 shows the Meyer body with wake panels being shed along the vortex sheet separation lines that are specified in the DATA5 input file for this model at an AOA of 10°. The gray-scale representation of the body in Figure 4.13 corresponds to the pressure distribution around the body for the particular time step.

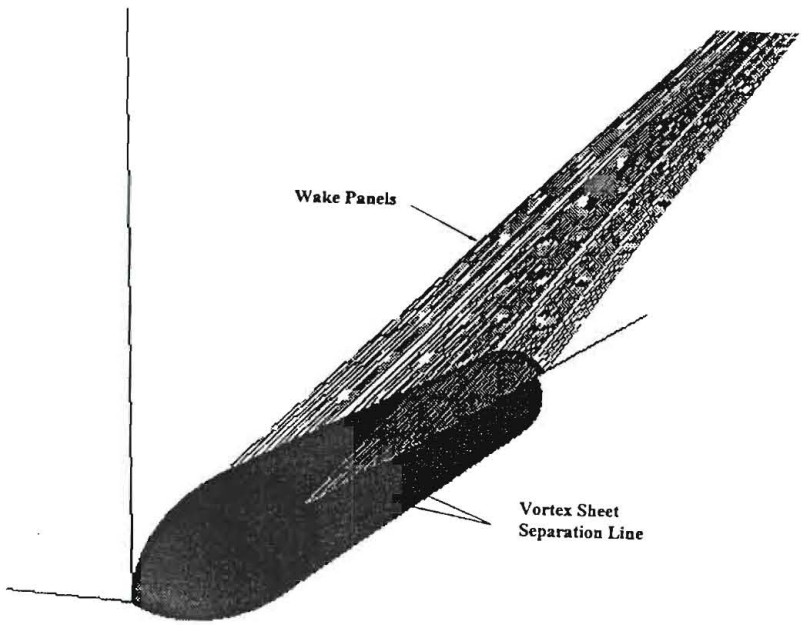

Figure 4.13 Meyer Body-Alone with Symmetric Vortex Separation Lines (AOA=10°).

The KWLINE parameter indicates where along the circumference of the body the wake separation line is positioned. The positive-Y side of the body is divided into 30 axial lines as is the negative-Y side of the body. The positive-Y side starts with line one at the bottom of the body and increments clockwise (looking nose to tail) to the top of the body at line 30. The negative-Y side starts with its line 1 at the top of the body and increments clockwise to the

bottom at its line 30 resulting in a total of 60 increments around the circumference of the body. The separation lines for the body shown in Figure 4.13 correspond to a KWLINE=17 for the positive-Y side of the body, and KWLINE=13 for the negative-Y side of the body.

With the PMARC method of modeling a lifting body, it requires the user to predict the location of body vortex separation line before actually running the code. For the comparison seen in Figure 4.14, the general locations of the vortex separation lines are initially guessed at using information from Refs. [26, 27], and then they are moved in an iterative process until the C_N values matched the experimental data from Ref. [23]. Obviously this type of process is mostly limited to investigating configurations where the coefficients are known from previous experimental or computational data. Analysis of incompletely studied configurations is possible based on some understanding of the physics of the flow and predicting the vortex separation lines from a boundary layer analysis or from Navier-Stokes computations.

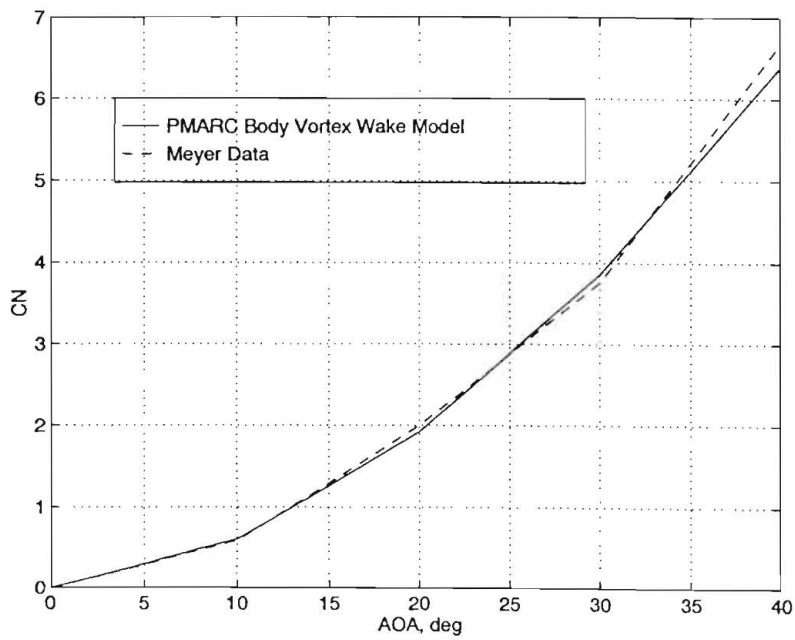

Figure 4.14 C_N Comparison for the Body-Alone, After Ref. [23].

2. Vortex Sheet Separation Line for the Smith Canard-Controlled Missile

In this analysis, two wake models are used in PMARC for the Smith missile that allowed for stable computations. The previously discussed first wake model attempt for the missile consists of wakes shed from each of the horizontal canard and tail surfaces as well as a circular-shaped wake shed from around the edge of the blunt tail. The second wake model places wakes at the control surfaces and also two vortex sheet wake separation lines along the length of the body at locations generally consistent with published vortex separation lines [Refs. 26, 27].

A representation of the PMARC model showing the wake panels and vortex separation line on the body is seen in Figure 4.15. This missile model is initially constructed with only 20 panels placed circumferentially around the body. Time constraints do not allow a more finely meshed model to be created. The existing panel distribution does not allow a large amount of flexibility in placing the vortex sheet separation line. Hence, as seen in Figure 4.16, the C_N values calculated with PMARC are not as close to the experimental data as those that are obtained for the Meyer body-alone due to its finer panel discretization.

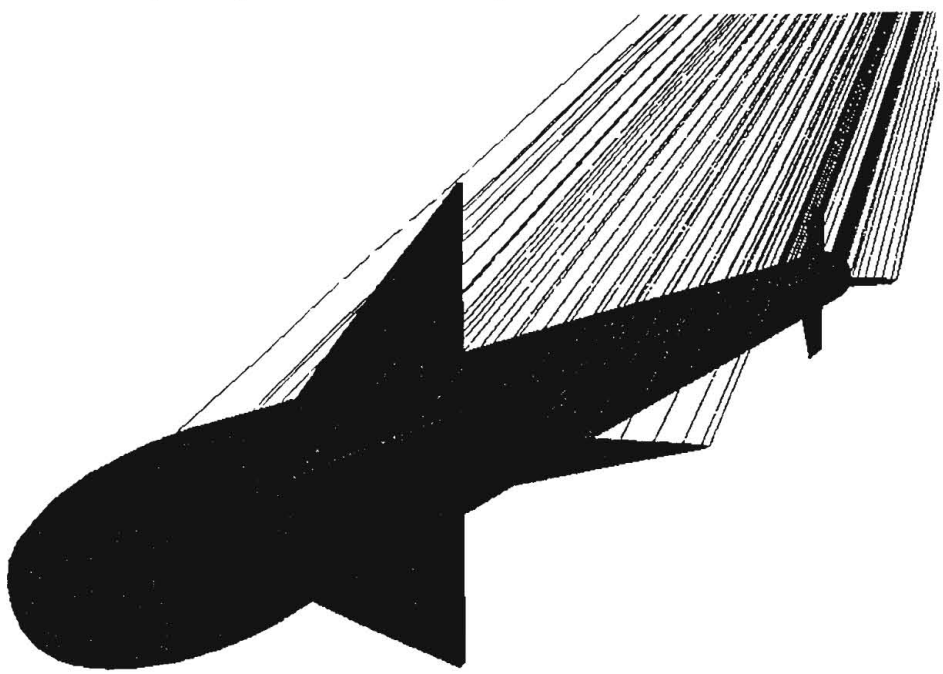

Figure 4.15 Smith Missile with Symmetric Vortex Separation Lines (AOA=20°).

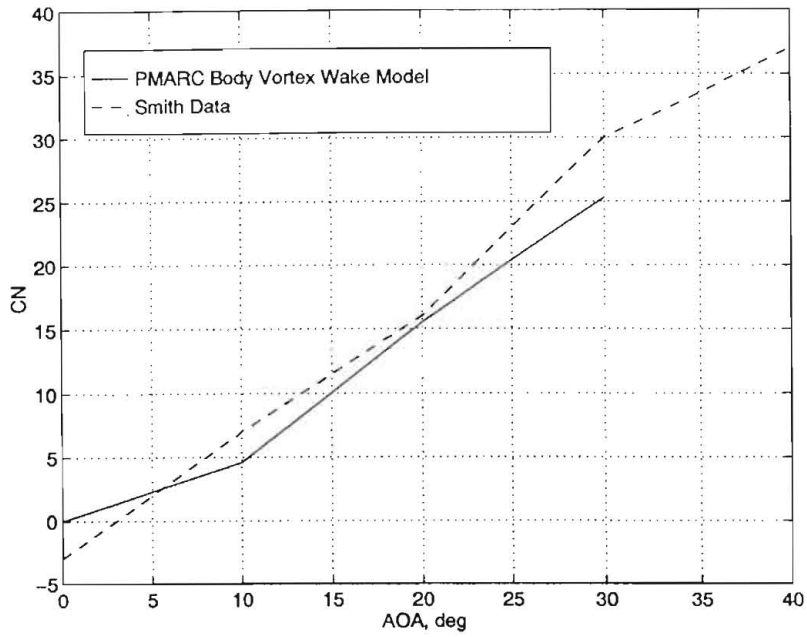

Figure 4.16 C_N Comparison of a Canard-Controlled Missile, After Ref. [21, 28].

Comparisons are also made of the pitching moment coefficient (C_M) from PMARC and those from experiments for the Smith missile. The PMARC C_M results are seen to be widely scattered and not within reasonable variation from the values published in Ref. [21], and therefore are not deemed meaningful enough to plot. Apparently the wake model used to match the C_N values is not sufficient to also match the C_M results. This is not altogether surprising since computational matching of C_M values is typically more difficult to do than matching the force coefficients. If PMARC is to be used as a complete design tool, a more detailed wake model will undoubtedly need to be constructed in order to properly match all the coefficients if possible.

VI. SUMMARY AND CONCLUSIONS

The main goal of this analysis is to determine the suitability of PMARC for initial aerodynamic missile design. To accomplish this, PMARC is compared with results available from other analyses and from experiments. This allows conclusions to be drawn on the capabilities as well as the limitations of PMARC.

It is found that PMARC, in general, can properly predict results for low AOA wing configurations as is expected from a potential flow code. The fundamental mechanism for producing lift in PMARC is the shed wake modeling. This wake-shedding process is well defined for a wing model.

The unsteady capabilities explored in PMARC prove to be an accurate tool for predicting the lift and moments of oscillating wings when compared to theory and the NPS unsteady panel code. Additional investigations of more complex configurations in an oscillatory flow are needed to fully understand the limits of PMARC's unsteady capabilities. An investigation of the indicial aerodynamic capabilities of PMARC shows reasonable results when compared to other data.

Significant challenges are encountered in attempting to model the wakes shed from bodies of revolution and bodies of revolution with control surfaces. It took several iterations to develop an intuitive scheme for the calculation of lift for bodies of revolution. Finally a wake modeling scheme using vortex separation lines along the length of the body produced normal force coefficients close to experimental data. A combination of the vortex separation lines along the body and wake shedding from the tails and canards are used for the canard-controlled missile. Although the normal force coefficient values calculated with PMARC for this configuration are close to the experimental data, reasonable values for the pitching moment coefficients are not produced. A more detailed wake model would be the next direction in the study of lift producing slender bodies with control surfaces. Further work is necessary to refine this procedure for identifying the proper location of the separation lines. This information will probably need to be provided from a boundary layer analysis or Navier-Stokes calculations.

APPENDIX A. NACA 4418 DATA5 INPUT FILE

Dec 2 1993 08:01 **planform1** Page 1

```
High Aspect Ratio Wing:  100ft Span, NACA-4418

&BIHP2    LSTIHP=2,     LSTOUT=0,     LSTFRQ=0,     LENRUN=2,     LPLTYP=1,     &END
&BIHP3    LSTGEO=0,     LSTWAB=0,     LSTWAK=0,     LSTCPV=0,                   &END
&BIHP4    MAXIT=50,     SOLRES=0.01,                                            &END
&BIHP5    DTSTPS= 10,   DTSTEP=0.5,                                             &END
&BIHP6    RSYM=1.0,     RGPR=0.0,     RFF=5.0,  RCORES=0.0080, RCOREW=0.0080,   &END
&BIHP7    VINF=558.0,   VSOUND=1116.0,                                          &END
&BIHP8    ALDEG= 2.00,  YAWDEG=0.0,   PHIDOT=0.0,  THEDOT=0.0,  PSIDOT=0.0,     &END
&BIHP8A   PHIMAX= 0.0,  THEMAX= 0.0,  PSIMAX=0.0,
          WRX=0.0,      WRY=0.0,      WRZ=0.0,                                  &END
&BIHP8B   DXMAX=0.0,    DYMAX=0.0,    DZMAX=0.0,
          WTX=0.0,      WTY=0.0,      WTZ=0.0,                                  &END
&BIHP5    CBAR=10.83,   SREF=1000.0,  SSPAN= 50.00,
          RMPX=3.75,    RMPY=0.00,    RMPZ=0.00,                                &END
&BIHP10   NGRSET=0,     NBCHGE=0,     NCZONE=0,
          NCZPCH=0,     CZDUB=0.0,    VREF=0.0,                                 &END
&BIHP11   NGRPCH=0,     NOPF=0,       NORL=0,
          NGCF=0,       NOCL=0,       VNORM=0.0,                                &END
&BIHP12   KPAN=0,       KSIDE=0,      NEWNAB=0,     NEWSID=0,                   &END
&BIHP13   NBLIT=0,                                                              &END


&ASEM1    ASEMX=0.00,       ASEMY=0.00,       ASEMZ=0.00,
          ASCAL=1.00,       ATHET=0.00,       NODEA=5,                          &END
&ASEM2    APXX=0.00,        APYY=0.00,        APZZ=0.00,
          AHXX=0.00,        AHYY=1.00,        AHZZ=0.00,                        &END


&COMP1    COMPX= 0.0000,    COMPY= 0.0000,    COMPZ= 0.0000,
          CSCAL=  1.000,    CTHET=   0.0,     NODEC= 5,                         &END
&COMP2    CPXX= 0.0000,     CPYY= 0.0000,     CPZZ= 0.0000,
          CHXX= 0.0000,     CHYY=  1.000,     CHZZ= 0.0000,                     &END


&PATCH1   IREV=  0, IDPAT= 1, MAKE=   0, KCOMP= 1, KASS= 1, IPATSYM=1,
          IPATCOP=0,                                                            &END
           WING
&SECT1    STX=    0.0000, STY= 0.0000,    STZ= 0.0000,    SCALE=  15.00 ,
          ALF=   0.0,  THETA=   0.0,
          INMODE=  5,  TNODS= 0,    TNPS=  0,    TINTS= 0.                      &END
&SECT2    RTC=    0.1800, RMC= 0.0400,    RPC= 0.4000,
          IPLANE=  2,  TNPC= 15,    TINTC= 0,                                   &END
&SECT1    STX=   0.00, STY= 50.00,    STZ= 0.0000,    SCALE=  5.00,
          ALF=   0.0,  THETA=   0.0,
          INMODE=  0,  TNODS= 3,    TNPS= 10,    TINTS= 2,                      &END


&PATCH1   IREV=  0, IDPAT= 1, MAKE=   1, KCOMP= 1, KASS= 1, IPATSYM=1,
          IPATCOP=0,                                                            &END
           WING_TIP
&PATCH2   ITYP=  2,    TNODS= 5,    TNPS=   4,    TINTS= 3,                    &END


&WAKE1    IDWAK=1,          IFLXW=1,          ITRFT2= 0,        INTRW= 0,      &END
 WING_WAKE
&WAKE2    KWPACH=2,         KWSIDE=4,         KWLINE=0,         KWPAN1=0,
          KWPAN2=0,         NODEW=0,          INITIAL=0,                       &END
&WAKE2    KWPACH=1,         KWSIDE=2,         KWLINE=0,         KWPAN1=0,
          KWPAN2=0,         NODEW=5,          INITIAL=0,                       &END


&CONSTRM  NONSL =0,  KPSL = 20,                                                 &END


&BLPARAM RN =38378000,    VISC = 0.000157, NSLBL = 1,                           &END


&VS1      NVOLR= 0,         NVOLC= 0,                                           &END
&VS2      X0=    -0.1000, Y0=     1.5000, Z0=     -0.1000, INTVSR= 1,            &END
&VS3      X1=    -0.1000, Y1=     1.5000, Z1=      0.1000, NPT1=  0,             &END
&VS4      X2=    -0.1000, Y2=     1.5000, Z2=      0.1000, NPT2= 20,             &END
&VS5      X3=     1.1000, Y3=     1.5000, Z3=     -0.1000, NPT3= 25,             &END

&VS6      XR0=    2.0000, YR0=    2.0000, ZR0=     0.0000, INTVSC= 1,            &END
```

Dec 2 1993 08:01 **planform1** Page 2

```
&VS7      XR1=    4.0000, YR1=    2.0000, ZR1=     0.0000,
          XR2=    2.0000, YR2=    2.0000, ZR2=     1.0000,                      &END
&VS8      R1=     0.1000, R2=     1.0000, PHI1=    0.0,      PHI2=360.0,        &END
&VS9      NRAD=   5,      NPHI=   12,     NLEN=    3,                          &END


&SLIN1    NSTLIN=0,                                                             &END
&SLIN2    SX0=   -2.0000, SY0=     1.0000, SZ0=    -0.5000,
          SU=     0.0000, SD=     10.0000, DS=      0.2500, INTSL= 1,           &END
&SLIN2    SX0=   -2.0000, SY0=     1.0000, SZ0=    -0.4000,
          SU=     0.0000, SD=     10.0000, DS=      0.2500, INTSL= 1,           &END
&SLIN2    SX0=   -2.0000, SY0=     1.0000, SZ0=    -0.3000,
          SU=     0.0000, SD=     10.0000, DS=      0.2500, INTSL= 1,           &END
&SLIN2    SX0=   -2.0000, SY0=     1.0000, SZ0=    -0.2000,
          SU=     0.0000, SD=     10.0000, DS=      0.2500, INTSL= 1,           &END
&SLIN2    SX0=   -2.0000, SY0=     1.0000, SZ0=    -0.1000,
          SU=     0.0000, SD=     10.0000, DS=      0.2500, INTSL= 1,           &END
&SLIN2    SX0=    2.0000, SY0=     1.0000, SZ0=     0.0000,
          SU=     0.0000, SD=     10.0000, DS=      0.2500, INTSL= 1,           &END
```

APPENDIX B. NACA 65-412 DATA5 INPUT FILE

Feb 10 1994 14:34 **NACA6digit** Page 1

```
Medium Aspect Ratio Wing:  50ft Span, NACA-65_1-412

&BINP2   LSTINP=2,      LSTOUT=0,      LSTFRQ=0,      LEINPUN=2,     LPLTTP=1,      &END
&BINP3   LSTGEO=0,      LSTWAB=0,      LSTWAK=0,      LSTCPV=0,                     &END
&BINP4   MAXIT=50,      SOLRES=0.01,                                                 &END
&BINP5   NTSTPS= 10,    DTSTEP=0.5,                                                  &END
&BINP6   RSYM=1.0,      RGPR=0.0,      RFF=5.0,   RCORES=0.0080, RCOPEW=0.0080,     &END
&BINP7   VINF=558.0,    VSOUND=1116.0,                                               &END
&BINP8   ALDEG= 2.00,   YAWDEG=0.0,    PHIDOT=0.0,   THEDOT=0.0,   PSIDOT=0.0,      &END
&BINP8A  PHIMAX= 0.0,   THEMAX= 0.0,   PSIMAX=0.0,
         WRX=0.0,       WRY=0.0,       WRZ=0.0,                                      &END
&BINP8B  DXMAX=0.0,     DYMAX=0.0,     DZMAX=0.0,
         WTX=0.0,       WTY=0.0,       WTZ=0.0,                                      &END
&BINP9   CBAR=10.50,    SREF=487,      SSPAN= 18.35,
         RMPX=3.63,     RMPY=0.00,     RMPZ=0.00,                                    &END
&BINP10  NOPSET=0,      NBCHGE=0,      NCZONE=0,
         NCZPCH=0,      CZDUB=0.0,     VREF=0.0,                                     &END
&BINP11  NORPCH=0,      NORF=0,        NORL=0,
         NOCF=0,        NOCL=0,        VNORM=0.0,                                    &END
&BINP12  KPAN=0,        KSIDE=0,       NEWNAB=0,      NEWSID=0,                     &END
&BINP13  NBLIT=0,                                                                    &END


&ASEM1   ASEMX=0.00,        ASEMY=0.00,        ASEMZ=0.00,
         ASCAL=1.00,        ATHET=0.00,        NODEA=5,                              &END
&ASEM2   APXX=0.00,         APYY=0.00,         APZZ=0.00,
         AHXX=0.00,         AHYY=1.00,         AHZZ=0.00,                            &END


&COMP1   COMPX= 0.0000,     COMPY= 0.0000,     COMPZ= 0.0000,
         CSCAL=  1.000,     CTHET=   0.0,      NODEC= 5,                             &END
&COMP2   CPXX= 0.0000,      CPYY= 0.0000,      CPZZ= 0.0000,
         CHXX= 0.0000,      CHYY=  1.000   ,   CHZZ= 0.0000,                         &END


&PATCH1  IREV=  0, IDPAT= 1, MAKE=   0, KCOMP= 1, KASS= 1, IPATSYM=1,
         IPATCOP=0,                                                                  &END
          WING
&SECT1   STX=    0.0000, STY= 0.0000,     STZ= 0.0000,     SCALE=  1.00 ,
         ALF=   0.0,  THETA=   0.0,
         INMODE=  4,  TNODS= 0,     TNPS=  0,     TINTS= 0,                          &END
14.500    0.000      0.000
13.770    0.000      0.040
13.040    0.000      0.013
12.312    0.000     -0.041
11.585    0.000     -0.109
10.859    0.000     -0.184
10.135    0.000     -0.261
9.413     0.000     -0.336
8.691     0.000     -0.406
7.970     0.000     -0.467
7.250     0.000     -0.515
6.531     0.000     -0.545
5.811     0.000     -0.559
5.092     0.000     -0.558
4.372     0.000     -0.547
3.652     0.000     -0.524
2.932     0.000     -0.490
2.210     0.000     -0.442
1.487     0.000     -0.378
1.124     0.000     -0.336
0.760     0.000     -0.285
0.394     0.000     -0.216
0.209     0.000     -0.168
0.133     0.000     -0.139
0.095     0.000     -0.117
0.000     0.000      0.000
0.050     0.000      0.146
0.084     0.000      0.179
0.154     0.000      0.230
0.331     0.000      0.324
0.690     0.000      0.468
1.051     0.000      0.581
1.413     0.000      0.677
2.140     0.000      0.832
```

Feb 10 1994 14:34 **NACA6digit** Page 2

```
2.868     0.000      0.951
3.598     0.000      1.043
4.328     0.000      1.110
5.058     0.000      1.156
5.789     0.000      1.180
6.519     0.000      1.180
7.250     0.000      1.155
7.980     0.000      1.102
8.709     0.000      1.027
9.437     0.000      0.934
10.165    0.000      0.824
10.891    0.000      0.703
11.615    0.000      0.571
12.338    0.000      0.431
13.060    0.000      0.287
13.780    0.000      0.143
14.500    0.000      0.000
&BPNODE   TNODE=3    TNPC=0     TIINTC=0     &END

&SECT1   STX=  14.43, STY= 25.00,     STZ= 0.0000,     SCALE=  0.34 ,
         ALF=   0.0,  THETA=   0.0,
         INMODE=  4,  TNODS= 3,     TNPS= 10,     TINTS= 0,                          &END
14.500    0.000      0.000
13.770    0.000      0.040
13.040    0.000      0.013
12.312    0.000     -0.041
11.585    0.000     -0.109
10.859    0.000     -0.184
10.135    0.000     -0.261
9.413     0.000     -0.336
8.691     0.000     -0.406
7.970     0.000     -0.467
7.250     0.000     -0.515
6.531     0.000     -0.545
5.811     0.000     -0.559
5.092     0.000     -0.558
4.372     0.000     -0.547
3.652     0.000     -0.524
2.932     0.000     -0.490
2.210     0.000     -0.442
1.487     0.000     -0.378
1.124     0.000     -0.336
0.760     0.000     -0.285
0.394     0.000     -0.216
0.209     0.000     -0.168
0.133     0.000     -0.139
0.095     0.000     -0.117
0.000     0.000      0.000
0.050     0.000      0.146
0.084     0.000      0.179
0.154     0.000      0.230
0.331     0.000      0.324
0.690     0.000      0.468
1.051     0.000      0.581
1.413     0.000      0.677
2.140     0.000      0.832
2.868     0.000      0.951
3.598     0.000      1.043
4.328     0.000      1.110
5.058     0.000      1.156
5.789     0.000      1.180
6.519     0.000      1.180
7.250     0.000      1.155
7.980     0.000      1.102
8.709     0.000      1.027
9.437     0.000      0.934
10.165    0.000      0.824
10.891    0.000      0.703
11.615    0.000      0.571
12.338    0.000      0.431
13.060    0.000      0.287
13.780    0.000      0.143
14.500    0.000      0.000
&BPNODE   TNODE=3    TNPC=0     TIINTC=0     &END
```

```
&PATCH1   IREV=  0, IDPAT= 1, MAKE=   1, KCOMP= 1, KASS= 1, IPATSYM=1,
          IPATCOP=0,                                                    &END
           WING_TIP
&PATCH2   ITYP=  2,    THODS= 5,    THPS=   4,   TINTS= 3,             &END


&WAKE1    IDWAK=1,         IFLXW=1,         ITRFTZ= 0,       INTRW= 0,  &END
 WING_WAKE
&WAKE2    KWPACH=2,        KWSIDE=4,        KWLINE=0,        KWPAN1=0,
          KWPAN2=0,        NODEW=0,         INITIAL=0,                  &END
&WAKE2    KWPACH=1,        KWSIDE=2,        KWLINE=0,        KWPAN1=0,
          KWPAN2=0,        NODEW=5,         INITIAL=0,                  &END


&DNSTRM   NONSL =0,  KPSL = 20,                                          &END


&BLPARAM RN =37210000,    VISC = 0.000157, NSLBL = 1,                     &END


&VS1      NVOLR= 0,        NVOLC= 0,                                     &END
&VS2      X0=    -0.1000, Y0=     1.5000, Z0=    -0.1000, INTVSR= 1,     &END
&VS3      X1=    -0.1000, Y1=     1.5000, Z1=     0.1000, NPT1=  0,      &END
&VS4      X2=    -0.1000, Y2=     1.5000, Z2=     0.1000, NPT2= 20,      &END
&VS5      X3=     1.1000, Y3=     1.5000, Z3=    -0.1000, NPT3= 25,      &END

&VS6      XR0=    2.0000, YR0=    2.0000, ZR0=    0.0000, INTVSC= 1,     &END
&VS7      XR1=    4.0000, YR1=    2.0000, ZR1=    0.0000,
          XR2=    2.0000, YR2=    2.0000, ZR2=    1.0000,                &END
&VS8      R1=     0.1000, R2=     1.0000, PHI1=  0.0,      PHI2=360.0,   &END
&VS9      NPAD=   5,      NPHI=  12,      NLEN=  3,                      &END


&SLIN1    NSTLIN=0,                                                      &END
&SLIN2    SX0=   -2.0000, SY0=    1.0000, SZ0=   -0.5000,
          SU=     0.0000, SD=    10.0000, DS=     0.2500, INTSL= 1,     &END
&SLIN2    SX0=   -2.0000, SY0=    1.0000, SZ0=   -0.4000,
          SU=     0.0000, SD=    10.0000, DS=     0.2500, INTSL= 1,     &END
&SLIN2    SX0=   -2.0000, SY0=    1.0000, SZ0=   -0.3000,
          SU=     0.0000, SD=    10.0000, DS=     0.2500, INTSL= 1,     &END
&SLIN2    SX0=   -2.0000, SY0=    1.0000, SZ0=   -0.2000,
          SU=     0.0000, SD=    10.0000, DS=     0.2500, INTSL= 1,     &END
&SLIN2    SX0=   -2.0000, SY0=    1.0000, SZ0=   -0.1000,
          SU=     0.0000, SD=    10.0000, DS=     0.2500, INTSL= 1,     &END
&SLIN2    SX0=   -2.0000, SY0=    1.0000, SZ0=    0.0000,
          SU=     0.0000, SD=    10.0000, DS=     0.2500, INTSL= 1,     &END
```

APPENDIX C. CRUCIFORM WING-BODY DATA5 INPUT FILE

Jul 24 1995 10:07 **DATA5** Page 1

```
Full CRUCIFORM AIRFRAME from Meyer (with seperate Wing & Circ Body Wakes)

&BINP2   LSTINP=2,    LSTOUT=0,    LSTFRQ=0,    LENRUN=3, LPLTYP=1,          &END

&BINP3   LSTGEO=0,    LSTWAB=0,    LSTWAK=0,    LSTCPV=0,                    &END
&BINP4   MAX1T=200,   SOLRES=0.0005,                                          &END
&BINP5   NTSTPS= 5,    DTSTEP=0.3500,                                         &END
&BINP6   RSYM=1.0,    RGPR=0.0,    RFF=5.0,     RCORES=0.005
         RCOREW=0.005,                                                        &END
&BINP7   VINF=111.6,   VSOUND=1116.0,                                         &END
&BINP8   ALDEG=  0.00,  YAWDEG=0.0,  PHIDOT=0.0, THEDOT=0.0,
         PSIDOT=0.0,                                                          &END
&BINP8A  PHIMAX=0.0, THEMAX=0.0,  PSIMAX=0.0,
         WRX=0.0,     WRY=0.0,     WRZ=0.0                                    &END
&BINP8B  DXMAX=0.0,  DYMAX=0.0,   DZMAX=0.0,
         WTX=0.0,     WTY=0.0,     WTZ=0.0,                                   &END
&BINP9   CBAR=0.1509, SREF=0.0179,  SSPAN=0.3018,
         RMPX=0.679 ,  RMPY=0.00,   RMPZ=0.00,                                &END
&BINP10   NORSET=0,   NBCHGE=0,    NCZONE=0,
          NCZPCH=0,   CZDUB=0.0,   VREF=0.0,                                  &END
&BINP11   NORPCH=0,
          NORF=0,     NORL=0,
          NOCF=0,     NOCL=0,
          VNORM=0.0,                                                          &END
&BINP12   KPAN=0,     KSIDE=0,    NEWNAB=0,    NEWSID=0,                      &END
&BINP13   NBLIT=1,                                                            &END


&ASEM1   ASEMX=0.00,       ASEMY=0.00,       ASEMZ=0.00,
         ASCAL=1.00,       ATHET=0.00,       NODEA=5,                         &END
&ASEM2   APXX=0.00,        APYY=0.00,        APZZ=0.00,
         AHXX=0.00,        AHYY=1.00,        AHZZ=0.00,                       &END

&COMP1   COMPX= 0.0000,    COMPY= 0.0000,    COMPZ= 0.0000,
         CSCAL=  1.000,    CTHET=   0.0,     NODEC= 0,                        &END
&COMP2   CPXX= 0.0000,     CPYY= 0.0000,     CPZZ= 0.0000,
         CHXX= 0.0000,     CHYY=  1.000,     CHZZ= 0.0000,                    &END

&COMP1   COMPX= 0.0000,    COMPY= 0.000,     COMPZ= 0.0000,
         CSCAL=  1.000,    CTHET=   0.0,     NODEC= 5,                        &END
&COMP2   CPXX= 0.0000,     CPYY= 0.0000,     CPZZ= 0.0000,
         CHXX= 0.0000,     CHYY=  1.000,     CHZZ= 0.0000,                    &END

&PATCH1  IREV=  0, IDPAT= 1, MAKE=   0, KCOMP=  2, KASS= 1, IPATSYM=1,
         IPATCOP=0,                                                           &END
    HORZ-WING
&SECT1   STX=    0.0000, STY= 0.0000,    STZ= 0.0000,    SCALE=  1.000 ,
         ALF=   0.0,  THETA=   0.0,
         INMODE=  4,  TNODS= 0,    TNPS=  0,    TINTS= 0,                     &END
1.207     0.0755    0.0
1.151     0.0755   -0.0049
1.107     0.0755   -0.0049
1.064     0.0755   -0.0049
1.021     0.0755   -0.0049
0.978     0.0755   -0.0049
0.934     0.0755   -0.0049
0.891     0.0755   -0.0049
0.847     0.0755   -0.0049
0.804     0.0755   -0.0049
0.742     0.0755   -0.0025
0.679     0.0755    0.0
0.742     0.0755    0.0025
0.804     0.0755    0.0049
0.847     0.0755    0.0049
0.891     0.0755    0.0049
0.934     0.0755    0.0049
0.978     0.0755    0.0049
1.021     0.0755    0.0049
1.064     0.0755    0.0049
1.107     0.0755    0.0049
1.151     0.0755    0.0049
1.207     0.0755    0.0
&BPNODE  TNODE=3    TNPC=0     TINTC=0                                        &END
&SECT1   STX= 1.175, STY= 0.302,    STZ= 0.0000,    SCALE=  0.0240,
         ALF=   0.0,  THETA=   0.0,
         INMODE=  0,  TNODS= 3,    TNPS= 10,    TINTS= 0,                     &END
```

Jul 24 1995 10:07 **DATA5** Page 2

```
&PATCH1  IREV=  0, IDPAT= 1, MAKE=   1, KCOMP= 2, KASS= 1, IPATSYM=1,
         IPATCOP=0,                                                           &END
    HORZ-WING_TIP
&PATCH2  ITYP=  1,    TNODS= 3,    TNPS=   1,   TINTS= 3,                    &END

&PATCH1  IREV=  0, IDPAT= 1, MAKE=   0, KCOMP=  2, KASS= 1, IPATSYM=0,
         IPATCOP=1,                                                           &END
    VERT-WING_UP
&PATCH3  PATX=0.0, PATY=0.0, PATZ=0.0, PSCAL=1.0, PTHET=90.0,NODEP=0
         PPXX=0.0, PPYY=0.0, PPZZ=0.0, PHXX=1.0,PHYY=0.0,PHZZ=0.0             &END

&PATCH1  IREV=  0, IDPAT= 1, MAKE=   5, KCOMP= 2, KASS= 1, IPATSYM=0,
         IPATCOP=0,                                                           &END
    VERT-UP-WING_TIP
&PATCH2  ITYP=  1,    TNODS= 3,    TNPS=   1,   TINTS= 3,                    &END

&PATCH1  IREV=  0, IDPAT= 1, MAKE=   0, KCOMP=  2, KASS= 1, IPATSYM=0,
         IPATCOP=1,                                                           &END
    VERT-WING_DOWN
&PATCH3  PATX=0.0, PATY=0.0, PATZ=0.0, PSCAL=1.0, PTHET=-90.0,NODEP=0
         PPXX=0.0, PPYY=0.0, PPZZ=0.0, PHXX=1.0,PHYY=0.0,PHZZ=0.0             &END

&PATCH1  IREV=  0, IDPAT= 1, MAKE=   7, KCOMP= 2, KASS= 1, IPATSYM=0,
         IPATCOP=0,                                                           &END
    VERT-DOWN-WING_TIP
&PATCH2  ITYP=  1,    TNODS= 3,    TNPS=   1,   TINTS= 3,                    &END

&PATCH1  IREV=  0, IDPAT= 2, MAKE=   0, KCOMP= 1, KASS= 1, IPATSYM=1,
         IPATCOP=0,                                                           &END
    FORWARD FUSELAGE
&SECT1   STX= 0.000, STY= 0.00,    STZ= 0.0000,    SCALE=  0.000,
         ALF=   0.0,  THETA=   0.0,
         INMODE=  1,  TNODS= 0,    TNPS= 0,    TINTS= 0,                     &END
0.0000    -0.0755    0.0
0.0131    -0.0743    0.0
0.0258    -0.071     0.0
0.0377    -0.0653    0.0
0.0485    -0.0578    0.0
0.0578    -0.0485    0.0
0.0633    -0.0377    0.0
0.071     -0.0258    0.0
0.0743    -0.0131    0.0
0.0755     0.0000    0.0
0.0743     0.0131    0.0
0.071      0.0258    0.0
0.0633     0.0377    0.0
0.0578     0.0485    0.0
0.0485     0.0578    0.0
0.0377     0.0653    0.0
0.0258     0.071     0.0
0.0131     0.0743    0.0
0.0000     0.0755    0.0
&BPNODE  TNODE=3,   TNPC=10,    TINTC=1,
&SECT1   STX= 0.0066, STY= 0.0000,    STZ= 0.0000,    SCALE=  0.0457,
         ALF=   0.0,  THETA=   0.0,
         INMODE=  0,  TNODS= 0,    TNPS= 0,    TINTS= 0,                     &END
&SECT1   STX= 0.0164, STY= 0.0000,    STZ= 0.0000,    SCALE=  0.1120,
         ALF=   0.0,  THETA=   0.0,
         INMODE=  0,  TNODS= 0,    TNPS= 0,    TINTS= 0,                     &END
&SECT1   STX= 0.0328, STY= 0.0000,    STZ= 0.0000,    SCALE=  0.2162,
         ALF=   0.0,  THETA=   0.0,
         INMODE=  0,  TNODS= 0,    TNPS= 0,    TINTS= 0,                     &END
&SECT1   STX= 0.0492, STY= 0.0000,    STZ= 0.0000,    SCALE=  0.3129,
         ALF=   0.0,  THETA=   0.0,
         INMODE=  0,  TNODS= 0,    TNPS= 0,    TINTS= 0,                     &END
&SECT1   STX= 0.0656, STY= 0.0000,    STZ= 0.0000,    SCALE=  0.4026,
         ALF=   0.0,  THETA=   0.0,
         INMODE=  0,  TNODS= 0,    TNPS= 0,    TINTS= 0,                     &END
&SECT1   STX= 0.082 , STY= 0.0000,    STZ= 0.0000,    SCALE=  0.4952,
         ALF=   0.0,  THETA=   0.0,
         INMODE=  0,  TNODS= 0,    TNPS= 0,    TINTS= 0,                     &END
&SECT1   STX= 0.0980, STY= 0.0000,    STZ= 0.0000,    SCALE=  0.56120,
         ALF=   0.0,  THETA=   0.0,
         INMODE=  0,  TNODS= 0,    TNPS= 0,    TINTS= 0,                     &END
&SECT1   STX= 0.1310, STY= 0.0000,    STZ= 0.0000,    SCALE=  0.6938,
         ALF=   0.0,  THETA=   0.0,
```

```
          INMODE= 0,  TNODS= 0,    TNPS= 0,    TINTS= 0,                    &END
&SECT1    STX= 0.1640, STY= 0.0000,    STZ= 0.0000,    SCALE= 0.8015,
          ALF= 0.0,  THETA= 0.0,
          INMODE= 0,  TNODS= 0,    TNPS= 0,    TINTS= 0,                    &END
&SECT1    STX= 0.1970, STY= 0.0000,    STZ= 0.0000,    SCALE= 0.8854,
          ALF= 0.0,  THETA= 0.0,
          INMODE= 0,  TNODS= 0,    TNPS= 0,    TINTS= 0,                    &END
&SECT1    STX= 0.2300, STY= 0.0000,    STZ= 0.0000,    SCALE= 0.946,
          ALF= 0.0,  THETA= 0.0,
          INMODE= 0,  TNODS= 0,    TNPS= 0,    TINTS= 0,                    &END
&SECT1    STX= 0.2620, STY= 0.0000,    STZ= 0.0000,    SCALE= 0.984,
          ALF= 0.0,  THETA= 0.0,
          INMODE= 0,  TNODS= 0,    TNPS= 0,    TINTS= 0,                    &END
&SECT1    STX= 0.3020, STY= 0.0000,    STZ= 0.0000,    SCALE= 1.000,
          ALF= 0.0,  THETA= 0.0,
          INMODE= 0,  TNODS= 0,    TNPS= 0,    TINTS= 0,                    &END
&SECT1    STX= 0.3397, STY= 0.0000,    STZ= 0.0000,    SCALE= 1.000,
          ALF= 0.0,  THETA= 0.0,
          INMODE= 0,  TNODS= 0,    TNPS= 0,    TINTS= 0,                    &END
&SECT1    STX= 0.3774, STY= 0.0000,    STZ= 0.0000,    SCALE= 1.000,
          ALF= 0.0,  THETA= 0.0,
          INMODE= 0,  TNODS= 0,    TNPS= 0,    TINTS= 0,                    &END
&SECT1    STX= 0.4151, STY= 0.0000,    STZ= 0.0000,    SCALE= 1.000,
          ALF= 0.0,  THETA= 0.0,
          INMODE= 0,  TNODS= 0,    TNPS= 0,    TINTS= 0,                    &END
&SECT1    STX= 0.4528, STY= 0.0000,    STZ= 0.0000,    SCALE= 1.000,
          ALF= 0.0,  THETA= 0.0,
          INMODE= 0,  TNODS= 0,    TNPS= 0,    TINTS= 0,                    &END
&SECT1    STX= 0.4905, STY= 0.0000,    STZ= 0.0000,    SCALE= 1.000,
          ALF= 0.0,  THETA= 0.0,
          INMODE= 0,  TNODS= 0,    TNPS= 0,    TINTS= 0,                    &END
&SECT1    STX= 0.5282, STY= 0.0000,    STZ= 0.0000,    SCALE= 1.000,
          ALF= 0.0,  THETA= 0.0,
          INMODE= 0,  TNODS= 0,    TNPS= 0,    TINTS= 0,                    &END
&SECT1    STX= 0.5659, STY= 0.0000,    STZ= 0.0000,    SCALE= 1.000,
          ALF= 0.0,  THETA= 0.0,
          INMODE= 0,  TNODS= 0,    TNPS= 0,    TINTS= 0,                    &END
&SECT1    STX= 0.6036, STY= 0.0000,    STZ= 0.0000,    SCALE= 1.000,
          ALF= 0.0,  THETA= 0.0,
          INMODE= 0,  TNODS= 0,    TNPS= 0,    TINTS= 0,                    &END
&SECT1    STX= 0.6413, STY= 0.0000,    STZ= 0.0000,    SCALE= 1.000,
          ALF= 0.0,  THETA= 0.0,
          INMODE= 0,  TNODS= 0,    TNPS= 0,    TINTS= 0,                    &END
&SECT1    STX= 0.6690, STY= 0.0000,    STZ= 0.0000,    SCALE= 1.000,
          ALF= 0.0,  THETA= 0.0,
          INMODE= 0,  TNODS= 0,    TNPS= 0,    TINTS= 0,                    &END
&SECT1    STX= 0.0000, STY= 0.0000,    STZ= 0.0000,    SCALE= 1.000,
          ALF= 0.0,  THETA= 0.0,
          INMODE= 4,  TNODS= 3,    TNPS= 0,    TINTS= 0,                    &END
0.679       0.0        -0.0755
0.679       0.0258     -0.071
0.679       0.0485     -0.0578
0.679       0.0633     -0.0377
0.679       0.0710     -0.0258
0.679       0.0755      0.0000
0.679       0.0710      0.0258
0.679       0.0633      0.0377
0.679       0.0485      0.0578
0.679       0.0258      0.071
0.679       0.0000      0.0755
&BPNODE   TNODE=3,   TNPC=0,    TINTC=3,                                    &END

&PATCH1   IREV= 0, IDPAT= 2, MAKE= 0, KCOMP= 1, KASS= 1, IPATSYM=1,
          IPATCOP=0,                                                       &END
    LOWER AFT FUSELAGE
&SECT1    STX= 0.0000, STY= 0.0000,    STZ= 0.0000,    SCALE= 1.000,
          ALF= 0.0,  THETA= 0.0,
          INMODE= 4,  TNODS= 0,    TNPS= 0,    TINTS= 0,                    &END
0.679       0.0        -0.0755
0.679       0.0258     -0.071
0.679       0.0485     -0.0578
0.679       0.0633     -0.0377
0.679       0.0710     -0.0258
0.679       0.0755      0.0000
&BPNODE   TNODE=3,   TNPC=0,    TINTC=0,                                    &END
&SECT1    STX= 0.0000, STY= 0.0000,    STZ= 0.0000,    SCALE= 1.000,
```



```
          ALF= 0.0,  THETA= 0.0,
          INMODE= 4,  TNODS= 0,    TNPS= 0,    TINTS= 0,                    &END
0.742       0.0025     -0.0755
0.742       0.0258     -0.071
0.742       0.0485     -0.0578
0.742       0.0633     -0.0377
0.742       0.0710     -0.0258
0.742       0.0755     -0.0025
&BPNODE   TNODE=3,   TNPC=0,    TINTC=0,                                    &END
&SECT1    STX= 0.0000, STY= 0.0000,    STZ= 0.0000,    SCALE= 1.000,
          ALF= 0.0,  THETA= 0.0,
          INMODE= 4,  TNODS= 0,    TNPS= 0,    TINTS= 0,                    &END
0.804       0.0049     -0.0755
0.804       0.0258     -0.071
0.804       0.0485     -0.0578
0.804       0.0633     -0.0377
0.804       0.0710     -0.0258
0.804       0.0755     -0.0049
&BPNODE   TNODE=3,   TNPC=0,    TINTC=0,                                    &END
&SECT1    STX= 0.0000, STY= 0.0000,    STZ= 0.0000,    SCALE= 1.000,
          ALF= 0.0,  THETA= 0.0,
          INMODE= 4,  TNODS= 0,    TNPS= 0,    TINTS= 0,                    &END
0.847       0.0049     -0.0755
0.847       0.0258     -0.071
0.847       0.0485     -0.0578
0.847       0.0633     -0.0377
0.847       0.0710     -0.0258
0.847       0.0755     -0.0049
&BPNODE   TNODE=3,   TNPC=0,    TINTC=0,                                    &END
&SECT1    STX= 0.0000, STY= 0.0000,    STZ= 0.0000,    SCALE= 1.000,
          ALF= 0.0,  THETA= 0.0,
          INMODE= 4,  TNODS= 0,    TNPS= 0,    TINTS= 0,                    &END
0.891       0.0049     -0.0755
0.891       0.0258     -0.071
0.891       0.0485     -0.0578
0.891       0.0633     -0.0377
0.891       0.0710     -0.0258
0.891       0.0755     -0.0049
&BPNODE   TNODE=3,   TNPC=0,    TINTC=0,                                    &END
&SECT1    STX= 0.0000, STY= 0.0000,    STZ= 0.0000,    SCALE= 1.000,
          ALF= 0.0,  THETA= 0.0,
          INMODE= 4,  TNODS= 0,    TNPS= 0,    TINTS= 0,                    &END
0.934       0.0049     -0.0755
0.934       0.0258     -0.071
0.934       0.0485     -0.0578
0.934       0.0633     -0.0377
0.934       0.0710     -0.0258
0.934       0.0755     -0.0049
&BPNODE   TNODE=3,   TNPC=0,    TINTC=0,                                    &END
&SECT1    STX= 0.0000, STY= 0.0000,    STZ= 0.0000,    SCALE= 1.000,
          ALF= 0.0,  THETA= 0.0,
          INMODE= 4,  TNODS= 0,    TNPS= 0,    TINTS= 0,                    &END
0.978       0.0049     -0.0755
0.978       0.0258     -0.071
0.978       0.0485     -0.0578
0.978       0.0633     -0.0377
0.978       0.0710     -0.0258
0.978       0.0755     -0.0049
&BPNODE   TNODE=3,   TNPC=0,    TINTC=0,                                    &END
&SECT1    STX= 0.0000, STY= 0.0000,    STZ= 0.0000,    SCALE= 1.000,
          ALF= 0.0,  THETA= 0.0,
          INMODE= 4,  TNODS= 0,    TNPS= 0,    TINTS= 0,                    &END
1.021       0.0049     -0.0755
1.021       0.0258     -0.071
1.021       0.0485     -0.0578
1.021       0.0633     -0.0377
1.021       0.0710     -0.0258
1.021       0.0755     -0.0049
&BPNODE   TNODE=3,   TNPC=0,    TINTC=0,                                    &END
&SECT1    STX= 0.0000, STY= 0.0000,    STZ= 0.0000,    SCALE= 1.000,
          ALF= 0.0,  THETA= 0.0,
          INMODE= 4,  TNODS= 0,    TNPS= 0,    TINTS= 0,                    &END
1.064       0.0049     -0.0755
1.064       0.0258     -0.071
1.064       0.0485     -0.0578
1.064       0.0633     -0.0377
```

```
1.064      0.0710    -0.0258
1.064      0.0755    -0.0049
&BPNODE   TNODE=3,   TNPC=0,    TINTC=0,                                  &END
&SECT1   STX= 0.0000, STY= 0.0000,    STZ= 0.0000,    SCALE=  1.000,
         ALF=   0.0,  THETA=   0.0,
         INMODE=  4,  TNODS= 0,    TNPS= 0,    TINTS= 0,                  &END
1.107      0.0049    -0.0755
1.107      0.0258    -0.071
1.107      0.0485    -0.0578
1.107      0.0633    -0.0377
1.107      0.0710    -0.0258
1.107      0.0755    -0.0049
&BPNODE   TNODE=3,   TNPC=0,    TINTC=0,                                  &END
&SECT1   STX= 0.0000, STY= 0.0000,    STZ= 0.0000,    SCALE=  1.000,
         ALF=   0.0,  THETA=   0.0,
         INMODE=  4,  TNODS= 0,    TNPS= 0,    TINTS= 0,                  &END
1.151      0.0049    -0.0755
1.151      0.0258    -0.071
1.151      0.0485    -0.0578
1.151      0.0633    -0.0377
1.151      0.0710    -0.0258
1.151      0.0755    -0.0049
&BPNODE   TNODE=3,   TNPC=0,    TINTC=0,                                  &END
&SECT1   STX= 0.0000, STY= 0.0000,    STZ= 0.0000,    SCALE=  1.000,
         ALF=   0.0,  THETA=   0.0,
         INMODE=  4,  TNODS= 3,    TNPS= 0,    TINTS= 0,                  &END
1.207      0.0000    -0.0755
1.207      0.0258    -0.071
1.207      0.0485    -0.0578
1.207      0.0633    -0.0377
1.207      0.0710    -0.0258
1.207      0.0755     0.0000
&BPNODE   TNODE=3,   TNPC=0,    TINTC=0,                                  &END

&PATCH1  IREV=  0, IDPAT= 2, MAKE= 0, KCOMP= 1, KASS= 1, IPATSYM=1,
         IPATCOP=0,                                                       &END
    UPPER AFT FUSELAGE
&SECT1   STX= 0.0000, STY= 0.0000,    STZ= 0.0000,    SCALE=  1.000,
         ALF=   0.0,  THETA=   0.0,
         INMODE=  4,  TNODS= 0,    TNPS= 0,    TINTS= 0,                  &END
0.679      0.0755    0.0000
0.679      0.0710    0.0258
0.679      0.0633    0.0377
0.679      0.0485    0.0578
0.679      0.0258    0.071
0.679      0.0       0.0755
&BPNODE   TNODE=3,   TNPC=0,    TINTC=0,                                  &END
&SECT1   STX= 0.0000, STY= 0.0000,    STZ= 0.0000,    SCALE=  1.000,
         ALF=   0.0,  THETA=   0.0,
         INMODE=  4,  TNODS= 0,    TNPS= 0,    TINTS= 0,                  &END
0.742      0.0755    0.0025
0.742      0.0710    0.0258
0.742      0.0633    0.0377
0.742      0.0485    0.0578
0.742      0.0258    0.071
0.742      0.0025    0.0755
&BPNODE   TNODE=3,   TNPC=0,    TINTC=0,                                  &END
&SECT1   STX= 0.0000, STY= 0.0000,    STZ= 0.0000,    SCALE=  1.000,
         ALF=   0.0,  THETA=   0.0,
         INMODE=  4,  TNODS= 0,    TNPS= 0,    TINTS= 0,                  &END
0.804      0.0755    0.0049
0.804      0.0710    0.0258
0.804      0.0633    0.0377
0.804      0.0485    0.0578
0.804      0.0258    0.071
0.804      0.0049    0.0755
&BPNODE   TNODE=3,   TNPC=0,    TINTC=0,                                  &END
&SECT1   STX= 0.0000, STY= 0.0000,    STZ= 0.0000,    SCALE=  1.000,
         ALF=   0.0,  THETA=   0.0,
         INMODE=  4,  TNODS= 0,    TNPS= 0,    TINTS= 0,                  &END
0.847      0.0755    0.0049
0.847      0.0710    0.0258
0.847      0.0633    0.0377
0.847      0.0485    0.0578
0.847      0.0258    0.071
0.847      0.0049    0.0755
```



```
&BPNODE   TNODE=3,   TNPC=0,    TINTC=0,                                  &END
&SECT1   STX= 0.0000, STY= 0.0000,    STZ= 0.0000,    SCALE=  1.000,
         ALF=   0.0,  THETA=   0.0,
         INMODE=  4,  TNODS= 0,    TNPS= 0,    TINTS= 0,                  &END
0.891      0.0755    0.0049
0.891      0.0710    0.0258
0.891      0.0633    0.0377
0.891      0.0485    0.0578
0.891      0.0258    0.071
0.891      0.0049    0.0755
&BPNODE   TNODE=3,   TNPC=0,    TINTC=0,                                  &END
&SECT1   STX= 0.0000, STY= 0.0000,    STZ= 0.0000,    SCALE=  1.000,
         ALF=   0.0,  THETA=   0.0,
         INMODE=  4,  TNODS= 0,    TNPS= 0,    TINTS= 0,                  &END
0.934      0.0755    0.0049
0.934      0.0710    0.0258
0.934      0.0633    0.0377
0.934      0.0485    0.0578
0.934      0.0258    0.071
0.934      0.0049    0.0755
&BPNODE   TNODE=3,   TNPC=0,    TINTC=0,                                  &END
&SECT1   STX= 0.0000, STY= 0.0000,    STZ= 0.0000,    SCALE=  1.000,
         ALF=   0.0,  THETA=   0.0,
         INMODE=  4,  TNODS= 0,    TNPS= 0,    TINTS= 0,                  &END
0.978      0.0755    0.0049
0.978      0.0710    0.0258
0.978      0.0633    0.0377
0.978      0.0485    0.0578
0.978      0.0258    0.071
0.978      0.0049    0.0755
&BPNODE   TNODE=3,   TNPC=0,    TINTC=0,                                  &END
&SECT1   STX= 0.0000, STY= 0.0000,    STZ= 0.0000,    SCALE=  1.000,
         ALF=   0.0,  THETA=   0.0,
         INMODE=  4,  TNODS= 0,    TNPS= 0,    TINTS= 0,                  &END
1.021      0.0755    0.0049
1.021      0.0710    0.0258
1.021      0.0633    0.0377
1.021      0.0485    0.0578
1.021      0.0258    0.071
1.021      0.0049    0.0755
&BPNODE   TNODE=3,   TNPC=0,    TINTC=0,                                  &END
&SECT1   STX= 0.0000, STY= 0.0000,    STZ= 0.0000,    SCALE=  1.000,
         ALF=   0.0,  THETA=   0.0,
         INMODE=  4,  TNODS= 0,    TNPS= 0,    TINTS= 0,                  &END
1.064      0.0755    0.0049
1.064      0.0710    0.0258
1.064      0.0633    0.0377
1.064      0.0485    0.0578
1.064      0.0258    0.071
1.064      0.0049    0.0755
&BPNODE   TNODE=3,   TNPC=0,    TINTC=0,                                  &END
&SECT1   STX= 0.0000, STY= 0.0000,    STZ= 0.0000,    SCALE=  1.000,
         ALF=   0.0,  THETA=   0.0,
         INMODE=  4,  TNODS= 0,    TNPS= 0,    TINTS= 0,                  &END
1.107      0.0755    0.0049
1.107      0.0710    0.0258
1.107      0.0633    0.0377
1.107      0.0485    0.0578
1.107      0.0258    0.071
1.107      0.0049    0.0755
&BPNODE   TNODE=3,   TNPC=0,    TINTC=0,                                  &END
&SECT1   STX= 0.0000, STY= 0.0000,    STZ= 0.0000,    SCALE=  1.000,
         ALF=   0.0,  THETA=   0.0,
         INMODE=  4,  TNODS= 0,    TNPS= 0,    TINTS= 0,                  &END
1.151      0.0755    0.0049
1.151      0.0710    0.0258
1.151      0.0633    0.0377
1.151      0.0485    0.0578
1.151      0.0258    0.071
1.151      0.0049    0.0755
&BPNODE   TNODE=3,   TNPC=0,    TINTC=0,                                  &END
&SECT1   STX= 0.0000, STY= 0.0000,    STZ= 0.0000,    SCALE=  1.000,
         ALF=   0.0,  THETA=   0.0,
         INMODE=  4,  TNODS= 3,    TNPS= 0,    TINTS= 0,                  &END
1.207      0.0755    0.00
1.207      0.0710    0.0258
```

```
1.207      0.0633    0.0377
1.207      0.0485    0.0578
1.207      0.0258    0.071
1.207      0.0000    0.0755
&BPNODE   TNODE=3,   TNPC=0,    TINTC=0,                                  &END

&PATCH1   IREV=  0, IDPAT= 2, MAKE= 0, KCOMP= 1, KASS= 1, IPATSYM=1,
          IPATCOP=0,                                                     &END
    AFT FUSELAGE
&SECT1    STX= 0.000, STY= 0.00,    STZ= 0.0000,    SCALE=  1.000,
          ALF=   0.0,  THETA=   0.0,
          INMODE=  4,  TNODS= 0,    TNPS= 0,    TINTS= 0,                &END
1.2070       0.0       -0.0755
1.2070       0.0258    -0.071
1.2070       0.0485    -0.0578
1.2070       0.0633    -0.0377
1.2070       0.0710    -0.0258
1.2070       0.0755     0.0000
1.2070       0.0710     0.0258
1.2070       0.0633     0.0377
1.2070       0.0485     0.0578
1.2070       0.0258     0.071
1.2070       0.0000     0.0755
&BPNODE   TNODE=3,   TNPC=0,    TINTC=0,                                  &END
&SECT1    STX= 1.267, STY= 0.00,    STZ= 0.0000,    SCALE=  1.00,
          ALF=   0.0,  THETA=   0.0,
          INMODE=  1,  TNODS= 0,    TNPS= 0,    TINTS= 0,                &END
0.0000     -0.0755    0.0
0.0131     -0.0743    0.0
0.0258     -0.071     0.0
0.0377     -0.0653    0.0
0.0485     -0.0578    0.0
0.0578     -0.0485    0.0
0.0633     -0.0377    0.0
0.071      -0.0258    0.0
0.0743     -0.0131    0.0
0.0755      0.0000    0.0
0.0743      0.0131    0.0
0.071       0.0258    0.0
0.0633      0.0377    0.0
0.0578      0.0485    0.0
0.0485      0.0578    0.0
0.0377      0.0653    0.0
0.0258      0.071     0.0
0.0131      0.0743    0.0
0.0000      0.0755    0.0
&BPNODE   TNODE=3,   TNPC=10,   TINTC=3,                                  &END
&SECT1    STX= 1.328, STY= 0.00,    STZ= 0.0000,    SCALE=  1.00,
          ALF=   0.0,  THETA=   0.0,
          INMODE=  0,  TNODS= 0,    TNPS= 0,    TINTS= 0,                &END
&SECT1    STX=1.388, STY= 0.00,    STZ= 0.0000,    SCALE=  1.000,
          ALF=   0.0,  THETA=   0.0,
          INMODE=  0,  TNODS= 0,    TNPS= 0,    TINTS= 0,                &END
&SECT1    STX=1.449, STY= 0.00,    STZ= 0.0000,    SCALE=  1.000,
          ALF=   0.0,  THETA=   0.0,
          INMODE=  0,  TNODS= 0,    TNPS= 0,    TINTS= 0,                &END
&SECT1    STX=1.509, STY= 0.00,    STZ= 0.0000,    SCALE=  1.000,
          ALF=   0.0,  THETA=   0.0,
          INMODE=  0,  TNODS= 0,    TNPS= 0,    TINTS= 0,                &END
&SECT1    STX=1.509, STY= 0.00,    STZ= 0.0000,    SCALE=  0.800,
          ALF=   0.0,  THETA=   0.0,
          INMODE=  0,  TNODS= 0,    TNPS= 0,    TINTS= 0,                &END
&SECT1    STX=1.509, STY= 0.00,    STZ= 0.0000,    SCALE=  0.600,
          ALF=   0.0,  THETA=   0.0,
          INMODE=  0,  TNODS= 0,    TNPS= 0,    TINTS= 0,                &END
&SECT1    STX=1.509, STY= 0.00,    STZ= 0.0000,    SCALE=  0.400,
          ALF=   0.0,  THETA=   0.0,
          INMODE=  0,  TNODS= 0,    TNPS= 0,    TINTS= 0,                &END
&SECT1    STX=1.509, STY= 0.00,    STZ= 0.0000,    SCALE=  0.200,
          ALF=   0.0,  THETA=   0.0,
          INMODE=  0,  TNODS= 0,    TNPS= 0,    TINTS= 0,                &END
&SECT1    STX=1.509, STY= 0.00,    STZ= 0.0000,    SCALE=  0.000,
          ALF=   0.0,  THETA=   0.0,
          INMODE=  0,  TNODS= 5,    TNPS= 0,    TINTS= 0,                &END

&WAKE1    IDWAK=1,        IFLXW=1,        ITRFTZ= 1,      INTRW= 1,      &END
```



```
  RGHT_WING_WAKE
&WAKE2    KWPACH=1,       KWSIDE=2,       KWLINE=0,       KWPAN1=0,
          KWPAN2=0,       NODEW=3,        INITIAL=0,                     &END

&WAKE1    IDWAK=1,        IFLXW=1,        ITRFTZ= 1,      INTRW= 1,      &END
  LEFT_WING_WAKE
&WAKE2    KWPACH=2,       KWSIDE=4,       KWLINE=0,       KWPAN1=0,
          KWPAN2=0,       NODEW=3,        INITIAL=0,                     &END

&WAKE1    IDWAK=1,        IFLXW=1,        ITRFTZ= 1,      INTRW= 1,      &END
  CIRC_AFT_BODY_WAKE
&WAKE2    KWPACH=15,      KWSIDE=1,       KWLINE=6,       KWPAN1=0,
          KWPAN2=0,       NODEW=0,        INITIAL=0,                     &END
&WAKE2    KWPACH=16,      KWSIDE=1,       KWLINE=6,       KWPAN1=0,
          KWPAN2=0,       NODEW=5,        INITIAL=0,                     &END

&CNSTRM   NONSL =0,  KPSL = 20,50,80,                                    &END


&BLPARAM  RN =2000000,     VISC = 0.00016,  NSLBL = 1,2,3,               &END


&VS1      NVOLR= 0,       NVOLC= 0,                                      &END
&VS2      X0=    3.00000, Y0=     2.0000, Z0=    -2.0000, INTVSR= 1,     &END
&VS3      X1=    18.0000, Y1=     2.0000, Z1-    -2.0000, NPT1= 16,      &END
&VS4      X2=     3.0000, Y2=     16.000, Z2=    -2.0000, NPT2= 3,       &END
&VS5      X3=     3.0000, Y3=     2.0000, Z3=     2.0000, NPT3= 18,      &END

&VS6      XR0=    0.0000, YR0=    0.0000, ZR0=    0.0000, INTVSC= 1,     &END
&VS7      XR1=    0.0000, YR1=   10.0000, ZR1=    0.0000,
          XR2=    0.0000, YR2=    0.0000, ZR2=    1.0000,                &END
&VS8      R1=     0.5000, R2=     5.0000, PHI1=  0.0,     PHI2=330.0,    &END
&VS9      NRAD=  10,      NPHI=  12,      NLEN=  5,                      &END


&SLIN1    NSTLIN=0,                                                      &END
&SLIN2    SX0=    2.0000, SY0=    5.0000, SZ0=   -0.5000,
          SU=     0.0000, SD=    15.0000, DS=     0.1000, INTSL= 1,      &END
&SLIN2    SX0=    2.0000, SY0=    5.0000, SZ0=   -0.4000,
          SU=     0.0000, SD=    15.0000, DS=     0.1000, INTSL= 1,      &END
&SLIN2    SX0=    2.0000, SY0=    5.0000, SZ0=   -0.3000,
          SU=     0.0000, SD=    15.0000, DS=     0.1000, INTSL= 1,      &END
&SLIN2    SX0=    2.0000, SY0=    5.0000, SZ0=   -0.2000,
          SU=     0.0000, SD=    15.0000, DS=     0.1000, INTSL= 1,      &END
&SLIN2    SX0=    2.0000, SY0=    5.0000, SZ0=   -0.1000,
          SU=     0.0000, SD=    15.0000, DS=     0.1000, INTSL= 1,      &END
```

APPENDIX D. CANARD CRUCIFORM MISSILE DATA5 INPUT FILE


```
 Full AIM-TYPE AIRFRAME (w/ Canard, Tail, Vortex-Body wake attempt)

&BINP2   LSTINP=2,   LSTOUT=0,   LSTFRQ=0,   LENRUN=0, LPLTYP=1,          &END

&BINP3   LSTGEO=0,   LSTNAB=0,   LSTWAK=0,   LSTCPV=0,                    &END
&BINP4   MAXIT=200,  SOLRES=0.0005,                                       &END
&BINP5   NTSTPS= 3,  DTSTEP=0.3500,                                       &END
&BINP6   RSYM=1.0,   RGPR=0.0,   RFF=5.0,    RCORES=0.005
         RCOREW=0.005,                                                     &END
&BINP7   VINF=223.2,   VSOUND=1116.0,                                      &END
&BINP8   ALDEG= 10.00,  YAWDEG=0.0,  PHIDOT=0.0, THEDOT=0.0,
         PSIDOT=0.0,                                                      &END
&BINP8A  PHIMAX=0.0, THEMAX=0.0,  PSIMAX=0.0,
         WRX=0.0,    WRY=0.0,     WRZ=0.0                                 &END
&BINP8B  DXMAX=0.0,  DYMAX=0.0,   DZMAX=0.0,
         WTX=0.0,    WTY=0.0,     WTZ=0.0,                                &END
&BINP9   CBAR=0.4167, SREF=0.1364,  SSPAN=0.6658,
         RMPX=4.7917,  RMPY=0.00,   RMPZ=0.00,                             &END
&BINP10   NORSET=0,   NBCHGE=0,    NCZONE=0,
          NCZPCH=0,   CZDUB=0.0,   VREF=0.0,                               &END
&BINP11   NORPCH=0,
          NORF=0,     NORL=0,
          NOCF=0,     NOCL=0,
          VNORM=0.0,                                                      &END
&BINP12   KPAN=0,     KSIDE=0,    NEWNAB=0,    NEWSID=0,                  &END
&BINP13   NBLIT=1,                                                        &END


&ASEM1   ASEMX=0.00,       ASEMY=0.00,       ASEMZ=0.00,
         ASCAL=1.00,       ATHET=0.00,       NODEA=5,                     &END
&ASEM2   APXX=0.00,        APYY=0.00,        APZZ=0.00,
         AHXX=0.00,        AHYY=1.00,        AHZZ=0.00,                   &END

&COMP1   COMPX= 0.0000,    COMPY= 0.0000,    COMPZ= 0.0000,
         CSCAL=  1.000,    CTHET=   0.0,     NODEC= 0,                    &END
&COMP2   CPXX= 0.0000,     CPYY= 0.0000,     CPZZ= 0.0000,
         CHXX= 0.0000,     CHYY=  1.000,     CHZZ= 0.0000,                &END

&COMP1   COMPX= 0.0000,    COMPY= 0.000,     COMPZ= 0.0000,
         CSCAL=  1.000,    CTHET=   0.0,     NODEC= 0,                    &END
&COMP2   CPXX= 0.0000,     CPYY= 0.0000,     CPZZ= 0.0000,
         CHXX= 0.0000,     CHYY=  1.000,     CHZZ= 0.0000,                &END

&COMP1   COMPX= 1.2250,    COMPY= 0.2183,    COMPZ= 0.0000,
         CSCAL=  1.000,    CTHET=   0.0,     NODEC= 0,                    &END
&COMP2   CPXX= 0.0000,     CPYY= 0.0000,     CPZZ= 0.0000,
         CHXX= 0.0000,     CHYY=  1.000,     CHZZ= 0.0000,                &END

&COMP1   COMPX= 1.2250,    COMPY= 0.2183,    COMPZ= 0.0000,
         CSCAL=  1.000,    CTHET=   0.0,     NODEC= 5,                    &END
&COMP2   CPXX= 0.0000,     CPYY= 0.0000,     CPZZ= 0.0000,
         CHXX= 0.0000,     CHYY=  0.000,     CHZZ= 1.0000,                &END

&PATCH1  IREV=  0, IDPAT= 1, MAKE=   0, KCOMP=  2, KASS= 1, IPATSYM=1,
         IPATCOP=0,                                                       &END
    HORZ-TAIL
&SECT1   STX=    0.0000, STY= 0.0000,    STZ= 0.0000,    SCALE=  1.000 ,
         ALF=   0.0,  THETA=   0.0,
         INMODE=  4,  TNODS= 0,    TNPS=  0,    TINTS= 0,                  &END
9.2500     0.20822    0.0
9.1667     0.20822   -0.0071
9.0833     0.20822   -0.0071
9.0000     0.20822   -0.0071
8.9167     0.20822   -0.0071
8.8333     0.20822   -0.0071
8.7500     0.20822   -0.0071
8.6667     0.20822   -0.0071
8.5833     0.20822   -0.0071
8.5000     0.20822   -0.0071
8.4167     0.20822   -0.0071
8.3333     0.20822   -0.0071
8.2500     0.20822   -0.0071
8.1667     0.20822   -0.0071
8.1317     0.20822   -0.0071
8.0696     0.20826   -0.0056
8.0000     0.20833    0.0
```



```
8.0696     0.20826    0.0056
8.1317     0.20822    0.0071
8.1667     0.20822    0.0071
8.2500     0.20822    0.0071
8.3333     0.20822    0.0071
8.4167     0.20822    0.0071
8.5000     0.20822    0.0071
8.5833     0.20822    0.0071
8.6667     0.20822    0.0071
8.7500     0.20822    0.0071
8.8333     0.20822    0.0071
8.9167     0.20822    0.0071
9.0000     0.20822    0.0071
9.0833     0.20822    0.0071
9.1667     0.20822    0.0071
9.2500     0.20822    0.0
&BPNODE  TNODE=3    TNPC=0     TINTC=0                                    &END
&SECT1   STX= 3.7, STY= 0.4667,    STZ= 0.0000,    SCALE=  0.600,
         ALF=   0.0,  THETA=   0.0,
         INMODE=  0,  TNODS= 3,    TNPS= 8,    TINTS= 0,                  &END
&PATCH1  IREV=  0, IDPAT= 1, MAKE=   1, KCOMP= 2, KASS= 1, IPATSYM=1,
         IPATCOP=0,                                                       &END
    HORZ-TAIL_TIP
&PATCH2  ITYP=  1,    TNODS= 3,    TNPS=   1,    TINTS= 3,                &END

&PATCH1  IREV=  0, IDPAT= 1, MAKE=   0, KCOMP=  2, KASS= 1, IPATSYM=0,
         IPATCOP=1,                                                       &END
    VERT-TAIL_UP
&PATCH3  PATX=0.0, PATY=0.0, PATZ=0.0, PSCAL=1.0, PTHET=90.0,NODEP=0
         PPXX=0.0, PPYY=0.0, PPZZ=0.0, PHXX=1.0,PHYY=0.0,PHZZ=0.0         &END
&PATCH1  IREV=  0, IDPAT= 1, MAKE=   5, KCOMP= 2, KASS= 1, IPATSYM=0,
         IPATCOP=0,                                                       &END
    VERT-UP-TAIL_TIP
&PATCH2  ITYP=  1,    TNODS= 3,    TNPS=   1,    TINTS= 3,                &END
&PATCH3  PATX=0.0, PATY=0.0, PATZ=0.0, PSCAL=1.0, PTHET=-90.0,NODEP=0
         PPXX=0.0, PPYY=0.0, PPZZ=0.0, PHXX=1.0,PHYY=0.0,PHZZ=0.0         &END
&PATCH1  IREV=  0, IDPAT= 1, MAKE=   0, KCOMP=  2, KASS= 1, IPATSYM=0,
         IPATCOP=1,                                                       &END
    VERT-TAIL_DOWN
&PATCH3  PATX=0.0, PATY=0.0, PATZ=0.0, PSCAL=1.0, PTHET=-90.0,NODEP=0
         PPXX=0.0, PPYY=0.0, PPZZ=0.0, PHXX=1.0,PHYY=0.0,PHZZ=0.0         &END
&PATCH1  IREV=  0, IDPAT= 1, MAKE=   7, KCOMP= 2, KASS= 1, IPATSYM=0,
         IPATCOP=0,                                                       &END
    VERT-DOWN-TAIL_TIP
&PATCH2  ITYP=  1,    TNODS= 3,    TNPS=   1,    TINTS= 3,                &END
&PATCH3  PATX=0.0, PATY=0.0, PATZ=0.0, PSCAL=1.0, PTHET=-90.0,NODEP=0
         PPXX=0.0, PPYY=0.0, PPZZ=0.0, PHXX=1.0,PHYY=0.0,PHZZ=0.0         &END


&PATCH1  IREV=  0, IDPAT= 1, MAKE=   0, KCOMP= 3, KASS= 1, IPATSYM=1,
         IPATCOP=0,                                                       &END
    HORZ-CANARD
&SECT1   STX=    0.0000, STY= 0.0000,    STZ= 0.0000,    SCALE=  1.000 ,
         ALF=   0.0,  THETA=   0.0,
         INMODE=  4,  TNODS= 0,    TNPS=  0,    TINTS= 0,                  &END
0.4825  0  0
0.3938  0 -0.0113
0.3050  0 -0.0113
0.2163  0 -0.0113
0.1275  0 -0.0113
0.0388  0 -0.0113
-0.0500 0 -0.0113
-0.1388 0 -0.0113
-0.2275 0 -0.0113
-0.3163 0 -0.0113
-0.4050 0 -0.0113
-0.4175 0 -0.0070
-0.4300 0  0.0
-0.4175 0  0.0070
-0.4050 0  0.0113
-0.3163 0  0.0113
-0.2275 0  0.0113
-0.1388 0  0.0113
-0.0500 0  0.0113
0.0388  0  0.0113
0.1275  0  0.0113
```

```
 0.2163  0  0.0113
 0.3050  0  0.0113
 0.3938  0  0.0113
 0.4825  0  0.0
 &BPNODE   TNODE=3    TNPC=0     TINTC=0                                          &END
 &SECT1   STX= 0.46, STY= 0.4675,    STZ= 0.0000,    SCALE=  0.0500,
          ALF=   0.0,  THETA=   0.0,
          INMODE=  0,  TNODS= 3,    TNPS= 8,    TINTS= 0,                         &END
 &PATCH1  IREV=  0, IDPAT= 1, MAKE=   9, KCOMP= 3, KASS= 1, IPATSYM=1,
          IPATCOP=0,                                                              &END
     H-CANARD_TIP
 &PATCH2  ITYP=  1,    TNODS= 3,    TNPS=   1,   TINTS= 3,                       &END

 &PATCH1  IREV=  0, IDPAT= 1, MAKE= -9, KCOMP= 3, KASS= 1, IPATSYM=1,
          IPATCOP=0,                                                              &END
     H-CANARD_ROOT
 &PATCH2  ITYP=  1,    TNODS= 3,    TNPS=   1,   TINTS= 3,                       &END

 &PATCH1  IREV=  0, IDPAT= 1, MAKE=   0, KCOMP= 4, KASS= 1, IPATSYM=0,
          IPATCOP=9,                                                              &END
     VERT-CANARD_UP
 &PATCH3  PATX=0.0, PATY=0.0, PATZ=0.0, PSCAL=1.0, PTHET=90.0,NODEP=0
          PPXX=0.0, PPYY=0.0, PPZZ=0.0, PHXX=1.0,PHYY=0.0,PHZZ=0.0                &END
 &PATCH1  IREV=  0, IDPAT= 1, MAKE=   15, KCOMP= 4, KASS= 1, IPATSYM=0,
          IPATCOP=0,                                                              &END
     VUP-CANARD_TIP
 &PATCH2  ITYP=  1,    TNODS= 3,    TNPS=   1,   TINTS= 3,                       &END
 &PATCH3  PATX=0.0, PATY=0.0, PATZ=0.0, PSCAL=1.0, PTHET=90.0,NODEP=0
          PPXX=0.0, PPYY=0.0, PPZZ=0.0, PHXX=1.0,PHYY=0.0,PHZZ=0.0                &END
 &PATCH1  IREV=  0, IDPAT= 1, MAKE= -15, KCOMP= 4, KASS= 1, IPATSYM=0,
          IPATCOP=0,                                                              &END
     VUP-CANARD_ROOT
 &PATCH2  ITYP=  1,    TNODS= 3,    TNPS=   1,   TINTS= 3,                       &END
 &PATCH3  PATX=0.0, PATY=0.0, PATZ=0.0, PSCAL=1.0, PTHET=-90.0,NODEP=0
          PPXX=0.0, PPYY=0.0, PPZZ=0.0, PHXX=1.0,PHYY=0.0,PHZZ=0.0                &END
 &PATCH1  IREV=  0, IDPAT= 1, MAKE=   0, KCOMP= 4, KASS= 1, IPATSYM=0,
          IPATCOP=9,                                                              &END
     VERT-CANARD_DOWN
 &PATCH3  PATX=0.0, PATY=0.0, PATZ=0.0, PSCAL=1.0, PTHET=-90.0,NODEP=0
          PPXX=0.0, PPYY=0.0, PPZZ=0.0, PHXX=1.0,PHYY=0.0,PHZZ=0.0                &END
 &PATCH1  IREV=  0, IDPAT= 1, MAKE=   18, KCOMP= 4, KASS= 1, IPATSYM=0,
          IPATCOP=0,                                                              &END
     VDOWN-CANARD_TIP
 &PATCH2  ITYP=  1,    TNODS= 3,    TNPS=   1,   TINTS= 3,                       &END
 &PATCH3  PATX=0.0, PATY=0.0, PATZ=0.0, PSCAL=1.0, PTHET=-90.0,NODEP=0
          PPXX=0.0, PPYY=0.0, PPZZ=0.0, PHXX=1.0,PHYY=0.0,PHZZ=0.0                &END
 &PATCH1  IREV=  0, IDPAT= 1, MAKE= -18, KCOMP= 4, KASS= 1, IPATSYM=0,
          IPATCOP=0,                                                              &END
     VDOWN-CANARD_ROOT
 &PATCH2  ITYP=  1,    TNODS= 3,    TNPS=   1,   TINTS= 3,                       &END
 &PATCH3  PATX=0.0, PATY=0.0, PATZ=0.0, PSCAL=1.0, PTHET=-90.0,NODEP=0
          PPXX=0.0, PPYY=0.0, PPZZ=0.0, PHXX=1.0,PHYY=0.0,PHZZ=0.0                &END

 &PATCH1  IREV=  0, IDPAT= 2, MAKE=   0, KCOMP= 1, KASS= 1, IPATSYM=1,
          IPATCOP=0,                                                              &END
     FORWARD FUSELAGE
 &SECT1   STX= 0.000, STY= 0.00,    STZ= 0.0000,    SCALE=  0.000,
          ALF=   0.0,  THETA=   0.0,
          INMODE=  1,  TNODS= 0,    TNPS= 0,    TINTS= 0,                         &END
 0.0000    -0.2083    0.0
 0.0361    -0.2051    0.0
 0.0712    -0.1957    0.0
 0.1042    -0.1804    0.0
 0.1339    -0.1596    0.0
 0.1596    -0.1339    0.0
 0.1804    -0.1042    0.0
 0.1957    -0.0712    0.0
 0.2051    -0.0361    0.0
 0.2083     0.0000    0.0
 0.2051     0.0361    0.0
 0.1957     0.0712    0.0
 0.1804     0.1042    0.0
 0.1596     0.1339    0.0
 0.1339     0.1596    0.0
 0.1042     0.1804    0.0
 0.0712     0.1957    0.0
```



```
 0.0361     0.2051    0.0
 0.0000     0.2083    0.0
 &BPNODE   TNODE=3,   TNPC=10,    TINTC=3,                                        &END
 &SECT1   STX= 0.0181, STY= 0.0000,    STZ= 0.0000,    SCALE=  0.3488,
          ALF=   0.0,  THETA=   0.0,
          INMODE=  0,  TNODS= 0,    TNPS= 0,    TINTS= 0,                         &END
 &SECT1   STX= 0.0681, STY= 0.0000,    STZ= 0.0000,    SCALE=  0.6163,
          ALF=   0.0,  THETA=   0.0,
          INMODE=  0,  TNODS= 0,    TNPS= 0,    TINTS= 0,                         &END
 &SECT1   STX= 0.1475, STY= 0.0000,    STZ= 0.0000,    SCALE=  0.7682,
          ALF=   0.0,  THETA=   0.0,
          INMODE=  0,  TNODS= 0,    TNPS= 0,    TINTS= 0,                         &END
 &SECT1   STX= 0.2578, STY= 0.0000,    STZ= 0.0000,    SCALE=  0.8966,
          ALF=   0.0,  THETA=   0.0,
          INMODE=  0,  TNODS= 0,    TNPS= 0,    TINTS= 0,                         &END
 &SECT1   STX= 0.3700, STY= 0.0000,    STZ= 0.0000,    SCALE=  0.9741,
          ALF=   0.0,  THETA=   0.0,
          INMODE=  0,  TNODS= 0,    TNPS= 0,    TINTS= 0,                         &END
 &SECT1   STX= 0.4833, STY= 0.0000,    STZ= 0.0000,    SCALE=  1.000,
          ALF=   0.0,  THETA=   0.0,
          INMODE=  0,  TNODS= 0,    TNPS= 0,    TINTS= 0,                         &END
 &SECT1   STX= 1.0000, STY= 0.0000,    STZ= 0.0000,    SCALE=  1.000,
          ALF=   0.0,  THETA=   0.0,
          INMODE=  0,  TNODS= 0,    TNPS= 0,    TINTS= 0,                         &END
 &SECT1   STX= 1.2500, STY= 0.0000,    STZ= 0.0000,    SCALE=  1.000,
          ALF=   0.0,  THETA=   0.0,
          INMODE=  0,  TNODS= 0,    TNPS= 0,    TINTS= 0,                         &END
 &SECT1   STX= 1.5000, STY= 0.0000,    STZ= 0.0000,    SCALE=  1.000,
          ALF=   0.0,  THETA=   0.0,
          INMODE=  0,  TNODS= 0,    TNPS= 0,    TINTS= 0,                         &END
 &SECT1   STX= 1.7500, STY= 0.0000,    STZ= 0.0000,    SCALE=  1.000,
          ALF=   0.0,  THETA=   0.0,
          INMODE=  0,  TNODS= 0,    TNPS= 0,    TINTS= 0,                         &END
 &SECT1   STX= 2.0000, STY= 0.0000,    STZ= 0.0000,    SCALE=  1.000,
          ALF=   0.0,  THETA=   0.0,
          INMODE=  0,  TNODS= 0,    TNPS= 0,    TINTS= 0,                         &END
 &SECT1   STX= 2.2500, STY= 0.0000,    STZ= 0.0000,    SCALE=  1.000,
          ALF=   0.0,  THETA=   0.0,
          INMODE=  0,  TNODS= 0,    TNPS= 0,    TINTS= 0,                         &END
 &SECT1   STX= 2.5000, STY= 0.0000,    STZ= 0.0000,    SCALE=  1.000,
          ALF=   0.0,  THETA=   0.0,
          INMODE=  0,  TNODS= 0,    TNPS= 0,    TINTS= 0,                         &END
 &SECT1   STX= 3.0000, STY= 0.0000,    STZ= 0.0000,    SCALE=  1.000,
          ALF=   0.0,  THETA=   0.0,
          INMODE=  0,  TNODS= 0,    TNPS= 0,    TINTS= 0,                         &END
 &SECT1   STX= 3.5000, STY= 0.0000,    STZ= 0.0000,    SCALE=  1.000,
          ALF=   0.0,  THETA=   0.0,
          INMODE=  0,  TNODS= 0,    TNPS= 0,    TINTS= 0,                         &END
 &SECT1   STX= 4.0000, STY= 0.0000,    STZ= 0.0000,    SCALE=  1.000,
          ALF=   0.0,  THETA=   0.0,
          INMODE=  0,  TNODS= 0,    TNPS= 0,    TINTS= 0,                         &END
 &SECT1   STX= 4.5000, STY= 0.0000,    STZ= 0.0000,    SCALE=  1.000,
          ALF=   0.0,  THETA=   0.0,
          INMODE=  0,  TNODS= 0,    TNPS= 0,    TINTS= 0,                         &END
 &SECT1   STX= 5.0000, STY= 0.0000,    STZ= 0.0000,    SCALE=  1.000,
          ALF=   0.0,  THETA=   0.0,
          INMODE=  0,  TNODS= 0,    TNPS= 0,    TINTS= 0,                         &END
 &SECT1   STX= 5.5000, STY= 0.0000,    STZ= 0.0000,    SCALE=  1.000,
          ALF=   0.0,  THETA=   0.0,
          INMODE=  0,  TNODS= 0,    TNPS= 0,    TINTS= 0,                         &END
 &SECT1   STX= 6.0000, STY= 0.0000,    STZ= 0.0000,    SCALE=  1.000,
          ALF=   0.0,  THETA=   0.0,
          INMODE=  0,  TNODS= 0,    TNPS= 0,    TINTS= 0,                         &END
 &SECT1   STX= 6.5000, STY= 0.0000,    STZ= 0.0000,    SCALE=  1.000,
          ALF=   0.0,  THETA=   0.0,
          INMODE=  0,  TNODS= 0,    TNPS= 0,    TINTS= 0,                         &END
 &SECT1   STX= 7.0000, STY= 0.0000,    STZ= 0.0000,    SCALE=  1.000,
          ALF=   0.0,  THETA=   0.0,
          INMODE=  0,  TNODS= 0,    TNPS= 0,    TINTS= 0,                         &END
 &SECT1   STX= 7.5000, STY= 0.0000,    STZ= 0.0000,    SCALE=  1.000,
          ALF=   0.0,  THETA=   0.0,
          INMODE=  0,  TNODS= 0,    TNPS= 0,    TINTS= 0,                         &END
 &SECT1   STX= 0.0000, STY= 0.0000,    STZ= 0.0000,    SCALE=  1.000,
          ALF=   0.0,  THETA=   0.0,
          INMODE=  4,  TNODS= 3,    TNPS= 0,    TINTS= 0,                         &END
 8.0   0.0      -0.2083
```

```
 8.0   0.0644   -0.1981
 8.0   0.I225   -0.1685
 8.0   0.1685   -0.1175
 8.0   0.1981   -0.0644
 8.0   0.2083    0.0000
 8.0   0.1981    0.0644
 8.0   0.1685    0.1175
 8.0   0.1225    0.1685
 8.0   0.0644    0.1981
 8.0   0.0       0.2083
&BPNODE   TNODE=3,   TNPC=0,    TINTC=0,                                  &END

&PATCH1  IREV=  0, IDPAT= 2, MAKE= 0, KCOMP= 1, KASB= 1, IPATSYM=1,
         IPATCOP=0,                                                      &END
    LOWER AFT FUSELAGE
&SECT1   STX= 0.0000, STY= 0.0000,    STZ= 0.0000,    SCALE=  1.000,
         ALF=   0.0,  THETA=   0.0,
         INMODE=  4,  TNODS= 0,    TNPS= 0,    TINTS= 0,                 &END
 8.0   0.0       -0.2083
 8.0   0.0644    -0.1981
 8.0   0.1225    -0.1685
 8.0   0.1685    -0.1175
 8.0   0.1981    -0.0644
 8.0   0.2083     0.0000
&BPNODE   TNODE=3,   TNPC=0,    TINTC=0,                                  &END
&SECT1   STX= 0.0000, STY= 0.0000,    STZ= 0.0000,    SCALE=  1.000,
         ALF=   0.0,  THETA=   0.0,
         INMODE=  4,  TNODS= 0,    TNPS= 0,    TINTS= 0,                 &END
 8.0696  0.0056 -0.2083
 8.0696  0.0633 -0.1984
 8.0696  0.1206 -0.1699
 8.0696  0.1665 -0.1252
 8.0696  0.1967 -0.0686
 8.0696  0.2083 -0.0056
&BPNODE   TNODE=3,   TNPC=0,    TINTC=0,                                  &END
&SECT1   STX= 0.0000, STY= 0.0000,    STZ= 0.0000,    SCALE=  1.000,
         ALF=   0.0,  THETA=   0.0,
         INMODE=  4,  TNODS= 0,    TNPS= 0,    TINTS= 0,                 &END
 8.1317  0.0071 -0.2082
 8.1317  0.0630 -0.1986
 8.1317  0.1202 -0.1702
 8.1317  0.1660 -0.1259
 8.1317  0.1963 -0.0697
 8.1317  0.2082 -0.0071
&BPNODE   TNODE=3,   TNPC=0,    TINTC=0,                                  &END
&SECT1   STX= 0.0000, STY= 0.0000,    STZ= 0.0000,    SCALE=  1.000,
         ALF=   0.0,  THETA=   0.0,
         INMODE=  4,  TNODS= 0,    TNPS= 0,    TINTS= 0,                 &END
 8.1667  0.0071 -0.2082
 8.1667  0.0630 -0.1986
 8.1667  0.1202 -0.1702
 8.1667  0.1660 -0.1259
 8.1667  0.1963 -0.0697
 8.1667  0.2082 -0.0071
&BPNODE   TNODE=3,   TNPC=0,    TINTC=0,                                  &END
&SECT1   STX= 0.0000, STY= 0.0000,    STZ= 0.0000,    SCALE=  1.000,
         ALF=   0.0,  THETA=   0.0,
         INMODE=  4,  TNODS= 0,    TNPS= 0,    TINTS= 0,                 &END
 8.2500  0.0071 -0.2082
 8.2500  0.0630 -0.1986
 8.2500  0.1202 -0.1702
 8.2500  0.1660 -0.1259
 8.2500  0.1963 -0.0697
 8.2500  0.2082 -0.0071
&BPNODE   TNODE=3,   TNPC=0,    TINTC=0,                                  &END
&SECT1   STX= 0.0000, STY= 0.0000,    STZ= 0.0000,    SCALE=  1.000,
         ALF=   0.0,  THETA=   0.0,
         INMODE=  4,  TNODS= 0,    TNPS= 0,    TINTS= 0,                 &END
 8.3333  0.0071 -0.2082
 8.3333  0.0630 -0.1986
 8.3333  0.1202 -0.1702
 8.3333  0.1660 -0.1259
 8.3333  0.1963 -0.0697
 8.3333  0.2082 -0.0071
&BPNODE   TNODE=3,   TNPC=0,    TINTC=0,                                  &END
&SECT1   STX= 0.0000, STY= 0.0000,    STZ= 0.0000,    SCALE=  1.000,
```



```
         ALF=   0.0,  THETA=   0.0,
         INMODE=  4,  TNODS= 0,    TNPS= 0,    TINTS= 0,                 &END
 8.4167  0.0071 -0.2082
 8.4167  0.0630 -0.1986
 8.4167  0.1202 -0.1702
 8.4167  0.1660 -0.1259
 8.4167  0.1963 -0.0697
 8.4167  0.2082 -0.0071
&BPNODE   TNODE=3,   TNPC=0,    TINTC=0,                                  &END
&SECT1   STX= 0.0000, STY= 0.0000,    STZ= 0.0000,    SCALE=  1.000,
         ALF=   0.0,  THETA=   0.0,
         INMODE=  4,  TNODS= 0,    TNPS= 0,    TINTS= 0,                 &END
 8.5000  0.0071 -0.2082
 8.5000  0.0630 -0.1986
 8.5000  0.1202 -0.1702
 8.5000  0.1660 -0.1259
 8.5000  0.1963 -0.0697
 8.5000  0.2082 -0.0071
&BPNODE   TNODE=3,   TNPC=0,    TINTC=0,                                  &END
&SECT1   STX= 0.0000, STY= 0.0000,    STZ= 0.0000,    SCALE=  1.000,
         ALF=   0.0,  THETA=   0.0,
         INMODE=  4,  TNODS= 0,    TNPS= 0,    TINTS= 0,                 &END
 8.5833  0.0071 -0.2082
 8.5833  0.0630 -0.1986
 8.5833  0.1202 -0.1702
 8.5833  0.1660 -0.1259
 8.5833  0.1963 -0.0697
 8.5833  0.2082 -0.0071
&BPNODE   TNODE=3,   TNPC=0,    TINTC=0,                                  &END
&SECT1   STX= 0.0000, STY= 0.0000,    STZ= 0.0000,    SCALE=  1.000,
         ALF=   0.0,  THETA=   0.0,
         INMODE=  4,  TNODS= 0,    TNPS= 0,    TINTS= 0,                 &END
 8.6667  0.0071 -0.2082
 8.6667  0.0630 -0.1986
 8.6667  0.1202 -0.1702
 8.6667  0.1660 -0.1259
 8.6667  0.1963 -0.0697
 8.6667  0.2082 -0.0071
&BPNODE   TNODE=3,   TNPC=0,    TINTC=0,                                  &END
&SECT1   STX= 0.0000, STY= 0.0000,    STZ= 0.0000,    SCALE=  1.000,
         ALF=   0.0,  THETA=   0.0,
         INMODE=  4,  TNODS= 0,    TNPS= 0,    TINTS= 0,                 &END
 8.7500  0.0071 -0.2082
 8.7500  0.0630 -0.1986
 8.7500  0.1202 -0.1702
 8.7500  0.1660 -0.1259
 8.7500  0.1963 -0.0697
 8.7500  0.2082 -0.0071
&BPNODE   TNODE=3,   TNPC=0,    TINTC=0,                                  &END
&SECT1   STX= 0.0000, STY= 0.0000,    STZ= 0.0000,    SCALE=  1.000,
         ALF=   0.0,  THETA=   0.0,
         INMODE=  4,  TNODS= 0,    TNPS= 0,    TINTS= 0,                 &END
 8.8333  0.0071 -0.2082
 8.8333  0.0630 -0.1986
 8.8333  0.1202 -0.1702
 8.8333  0.1660 -0.1259
 8.8333  0.1963 -0.0697
 8.8333  0.2082 -0.0071
&BPNODE   TNODE=3,   TNPC=0,    TINTC=0,                                  &END
&SECT1   STX= 0.0000, STY= 0.0000,    STZ= 0.0000,    SCALE=  1.000,
         ALF=   0.0,  THETA=   0.0,
         INMODE=  4,  TNODS= 0,    TNPS= 0,    TINTS= 0,                 &END
 8.9167  0.0071 -0.2082
 8.9167  0.0630 -0.1986
 8.9167  0.1202 -0.1702
 8.9167  0.1660 -0.1259
 8.9167  0.1963 -0.0697
 8.9167  0.2082 -0.0071
&BPNODE   TNODE=3,   TNPC=0,    TINTC=0,                                  &END
&SECT1   STX= 0.0000, STY= 0.0000,    STZ= 0.0000,    SCALE=  1.000,
         ALF=   0.0,  THETA=   0.0,
         INMODE=  4,  TNODS= 0,    TNPS= 0,    TINTS= 0,                 &END
 9.0000  0.0071 -0.2082
 9.0000  0.0630 -0.1986
 9.0000  0.1202 -0.1702
 9.0000  0.1660 -0.1259
```

```
9.0000  0.1963 -0.0697
9.0000  0.2082 -0.0071
&BPNODE   TNODE=3,   TNPC=0,    TINTC=0,                                  &END
&SECT1   STX= 0.0000, STY= 0.0000,    STZ= 0.0000,    SCALE=  1.000,
         ALF=   0.0,  THETA=   0.0,
         INMODE=  4,  TNODS= 0,    TNPS= 0,    TINTS= 0,                  &END
9.0833  0.0071 -0.2082
9.0833  0.0630 -0.1986
9.0833  0.1202 -0.1702
9.0833  0.1660 -0.1259
9.0833  0.1963 -0.0697
9.0833  0.2082 -0.0071
&BPNODE   TNODE=3,   TNPC=0,    TINTC=0,                                  &END
&SECT1   STX= 0.0000, STY= 0.0000,    STZ= 0.0000,    SCALE=  1.000,
         ALF=   0.0,  THETA=   0.0,
         INMODE=  4,  TNODS= 0,    TNPS= 0,    TINTS= 0,                  &END
9.1667  0.0071 -0.2082
9.1667  0.0630 -0.1986
9.1667  0.1202 -0.1702
9.1667  0.1660 -0.1259
9.1667  0.1963 -0.0697
9.1667  0.2082 -0.0071
&BPNODE   TNODE=3,   TNPC=0,    TINTC=0,                                  &END
&SECT1   STX= 0.0000, STY= 0.0000,    STZ= 0.0000,    SCALE=  1.000,
         ALF=   0.0,  THETA=   0.0,
         INMODE=  4,  TNODS= 3,    TNPS= 0,    TINTS= 0,                  &END
9.2500  0.0    -0.2083
9.2500  0.0630 -0.1986
9.2500  0.1202 -0.1702
9.2500  0.1660 -0.1259
9.2500  0.1963 -0.0697
9.2500  0.2083  0.0
&BPNODE   TNODE=3,   TNPC=0,    TINTC=0,                                  &END
&PATCH1  IREV=  0, IDPAT= 2, MAKE= 0, KCOMP= 1, KASS= 1, IPATSYM=1,
         IPATCOP=0,                                                      &END
    UPPER AFT FUSELAGE
&SECT1   STX= 0.0000, STY= 0.0000,    STZ= 0.0000,    SCALE=  1.000,
         ALF=   0.0,  THETA=   0.0,
         INMODE=  4,  TNODS= 0,    TNPS= 0,    TINTS= 0,                  &END
8.0   0.2083    0.0000
8.0   0.1981    0.0644
8.0   0.1685    0.1175
8.0   0.1225    0.1685
8.0   0.0644    0.1981
8.0   0.0       0.2083
&BPNODE   TNODE=3,   TNPC=0,    TINTC=0,                                  &END
&SECT1   STX= 0.0000, STY= 0.0000,    STZ= 0.0000,    SCALE=  1.000,
         ALF=   0.0,  THETA=   0.0,
         INMODE=  4,  TNODS= 0,    TNPS= 0,    TINTS= 0,                  &END
8.0696  0.2083  0.0056
8.0696  0.1967  0.0686
8.0696  0.1665  0.1252
8.0696  0.1206  0.1699
8.0696  0.0633  0.1984
8.0696  0.0056  0.2083
&BPNODE   TNODE=3,   TNPC=0,    TINTC=0,                                  &END
&SECT1   STX= 0.0000, STY= 0.0000,    STZ= 0.0000,    SCALE=  1.000,
         ALF=   0.0,  THETA=   0.0,
         INMODE=  4,  TNODS= 0,    TNPS= 0,    TINTS= 0,                  &END
8.1317  0.2082  0.0071
8.1317  0.1963  0.0697
8.1317  0.1660  0.1259
8.1317  0.1202  0.1702
8.1317  0.0630  0.1986
8.1317  0.0071  0.2082
&BPNODE   TNODE=3,   TNPC=0,    TINTC=0,                                  &END
&SECT1   STX= 0.0000, STY= 0.0000,    STZ= 0.0000,    SCALE=  1.000,
         ALF=   0.0,  THETA=   0.0,
         INMODE=  4,  TNODS= 0,    TNPS= 0,    TINTS= 0,                  &END
8.1667  0.2082  0.0071
8.1667  0.1963  0.0697
8.1667  0.1660  0.1259
8.1667  0.1202  0.1702
8.1667  0.0630  0.1986
8.1667  0.0071  0.2082
&BPNODE   TNODE=3,   TNPC=0,    TINTC=0,                                  &END
```



```
&SECT1   STX= 0.0000, STY= 0.0000,    STZ= 0.0000,    SCALE=  1.000,
         ALF=   0.0,  THETA=   0.0,
         INMODE=  4,  TNODS= 0,    TNPS= 0,    TINTS= 0,                  &END
8.2500  0.2082  0.0071
8.2500  0.1963  0.0697
8.2500  0.1660  0.1259
8.2500  0.1202  0.1702
8.2500  0.0630  0.1986
8.2500  0.0071  0.2082
&BPNODE   TNODE=3,   TNPC=0,    TINTC=0,                                  &END
&SECT1   STX= 0.0000, STY= 0.0000,    STZ= 0.0000,    SCALE=  1.000,
         ALF=   0.0,  THETA=   0.0,
         INMODE=  4,  TNODS= 0,    TNPS= 0,    TINTS= 0,                  &END
8.3333  0.2082  0.0071
8.3333  0.1963  0.0697
8.3333  0.1660  0.1259
8.3333  0.1202  0.1702
8.3333  0.0630  0.1986
8.3333  0.0071  0.2082
&BPNODE   TNODE=3,   TNPC=0,    TINTC=0,                                  &END
&SECT1   STX= 0.0000, STY= 0.0000,    STZ= 0.0000,    SCALE=  1.000,
         ALF=   0.0,  THETA=   0.0,
         INMODE=  4,  TNODS= 0,    TNPS= 0,    TINTS= 0,                  &END
8.4167  0.2082  0.0071
8.4167  0.1963  0.0697
8.4167  0.1660  0.1259
8.4167  0.1202  0.1702
8.4167  0.0630  0.1986
8.4167  0.0071  0.2082
&BPNODE   TNODE=3,   TNPC=0,    TINTC=0,                                  &END
&SECT1   STX= 0.0000, STY= 0.0000,    STZ= 0.0000,    SCALE=  1.000,
         ALF=   0.0,  THETA=   0.0,
         INMODE=  4,  TNODS= 0,    TNPS= 0,    TINTS= 0,                  &END
8.5000  0.2082  0.0071
8.5000  0.1963  0.0697
8.5000  0.1660  0.1259
8.5000  0.1202  0.1702
8.5000  0.0630  0.1986
8.5000  0.0071  0.2082
&BPNODE   TNODE=3,   TNPC=0,    TINTC=0,                                  &END
&SECT1   STX= 0.0000, STY= 0.0000,    STZ= 0.0000,    SCALE=  1.000,
         ALF=   0.0,  THETA=   0.0,
         INMODE=  4,  TNODS= 0,    TNPS= 0,    TINTS= 0,                  &END
8.5833  0.2082  0.0071
8.5833  0.1963  0.0697
8.5833  0.1660  0.1259
8.5833  0.1202  0.1702
8.5833  0.0630  0.1986
8.5833  0.0071  0.2082
&BPNODE   TNODE=3,   TNPC=0,    TINTC=0,                                  &END
&SECT1   STX= 0.0000, STY= 0.0000,    STZ= 0.0000,    SCALE=  1.000,
         ALF=   0.0,  THETA=   0.0,
         INMODE=  4,  TNODS= 0,    TNPS= 0,    TINTS= 0,                  &END
8.6667  0.2082  0.0071
8.6667  0.1963  0.0697
8.6667  0.1660  0.1259
8.6667  0.1202  0.1702
8.6667  0.0630  0.1986
8.6667  0.0071  0.2082
&BPNODE   TNODE=3,   TNPC=0,    TINTC=0,                                  &END
&SECT1   STX= 0.0000, STY= 0.0000,    STZ= 0.0000,    SCALE=  1.000,
         ALF=   0.0,  THETA=   0.0,
         INMODE=  4,  TNODS= 0,    TNPS= 0,    TINTS= 0,                  &END
8.7500  0.2082  0.0071
8.7500  0.1963  0.0697
8.7500  0.1660  0.1259
8.7500  0.1202  0.1702
8.7500  0.0630  0.1986
8.7500  0.0071  0.2082
&BPNODE   TNODE=3,   TNPC=0,    TINTC=0,                                  &END
&SECT1   STX= 0.0000, STY= 0.0000,    STZ= 0.0000,    SCALE=  1.000,
         ALF=   0.0,  THETA=   0.0,
         INMODE=  4,  TNODS= 0,    TNPS= 0,    TINTS= 0,                  &END
8.8333  0.2082  0.0071
8.8333  0.1963  0.0697
8.8333  0.1660  0.1259
```

```
8.8333  0.1202  0.1702
8.8333  0.0630  0.1986
8.8333  0.0071  0.2082
&BPNODE   TNODE=3,   TNPC=0,    TINTC=0,                                    &END
&SECT1    STX= 0.0000, STY= 0.0000,    STZ= 0.0000,    SCALE=  1.000,
          ALF=   0.0,  THETA=   0.0,
          INMODE=  4,  TNODS= 0,    TNPS= 0,    TINTS= 0,                   &END
8.9167  0.2082  0.0071
8.9167  0.1963  0.0697
8.9167  0.1660  0.1259
8.9167  0.1202  0.1702
8.9167  0.0630  0.1986
8.9167  0.0071  0.2082
&BPNODE   TNODE=3,   TNPC=0,    TINTC=0,                                    &END
&SECT1    STX= 0.0000, STY= 0.0000,    STZ= 0.0000,    SCALE=  1.000,
          ALF=   0.0,  THETA=   0.0,
          INMODE=  4,  TNODS= 0,    TNPS= 0,    TINTS= 0,                   &END
9.0000  0.2082  0.0071
9.0000  0.1963  0.0697
9.0000  0.1660  0.1259
9.0000  0.1202  0.1702
9.0000  0.0630  0.1986
9.0000  0.0071  0.2082
&BPNODE   TNODE=3,   TNPC=0,    TINTC=0,                                    &END
&SECT1    STX= 0.0000, STY= 0.0000,    STZ= 0.0000,    SCALE=  1.000,
          ALF=   0.0,  THETA=   0.0,
          INMODE=  4,  TNODS= 0,    TNPS= 0,    TINTS= 0,                   &END
9.0833  0.2082  0.0071
9.0833  0.1963  0.0697
9.0833  0.1660  0.1259
9.0833  0.1202  0.1702
9.0833  0.0630  0.1986
9.0833  0.0071  0.2082
&BPNODE   TNODE=3,   TNPC=0,    TINTC=0,                                    &END
&SECT1    STX= 0.0000, STY= 0.0000,    STZ= 0.0000,    SCALE=  1.000,
          ALF=   0.0,  THETA=   0.0,
          INMODE=  4,  TNODS= 0,    TNPS= 0,    TINTS= 0,                   &END
9.1667  0.2082  0.0071
9.1667  0.1963  0.0697
9.1667  0.1660  0.1259
9.1667  0.1202  0.1702
9.1667  0.0630  0.1986
9.1667  0.0071  0.2082
&BPNODE   TNODE=3,   TNPC=0,    TINTC=0,                                    &END
&SECT1    STX= 0.0000, STY= 0.0000,    STZ= 0.0000,    SCALE=  1.000,
          ALF=   0.0,  THETA=   0.0,
          INMODE=  4,  TNODS= 3,    TNPS= 0,    TINTS= 0,                   &END
9.2500  0.2083  0.0000
9.2500  0.1963  0.0697
9.2500  0.1660  0.1259
9.2500  0.1202  0.1702
9.2500  0.0630  0.1986
9.2500  0.0     0.2083
&BPNODE   TNODE=3,   TNPC=0,    TINTC=0,                                    &END

&PATCH1   IREV=  0, IDPAT= 2, MAKE= 0, KCOMP= 1, KASS= 1, IPATSYM=1,
          IPATCOP=0,                                                        &END
    AFT FUSELAGE
&SECT1    STX= 0.000, STY= 0.00,    STZ= 0.0000,    SCALE=  1.000,
          ALF=   0.0,  THETA=   0.0,
          INMODE=  4,  TNODS= 0,    TNPS= 0,    TINTS= 0,                   &END
9.2500  0.0     -0.2083
9.2500  0.0630  -0.1986
9.2500  0.1202  -0.1702
9.2500  0.1660  -0.1259
9.2500  0.1963  -0.0697
9.2500  0.2082  0.0000
9.2500  0.1963  0.0697
9.2500  0.1660  0.1259
9.2500  0.1202  0.1702
9.2500  0.0630  0.1986
9.2500  0.0     0.2083
&BPNODE   TNODE=3,   TNPC=0,    TINTC=0,                                    &END
&SECT1    STX= 9.3333, STY= 0.00,    STZ= 0.0000,    SCALE=  1.000,
          ALF=   0.0,  THETA=   0.0,
          INMODE=  1,  TNODS= 0,    TNPS= 0,    TINTS= 0,                   &END
```



```
0.0000    -0.2083    0.0
0.0361    -0.2051    0.0
0.0712    -0.1957    0.0
0.1042    -0.1804    0.0
0.1339    -0.1596    0.0
0.1596    -0.1339    0.0
0.1804    -0.1042    0.0
0.1957    -0.0712    0.0
0.2051    -0.0361    0.0
0.2083     0.0000    0.0
0.2051     0.0361    0.0
0.1957     0.0712    0.0
0.1804     0.1042    0.0
0.1596     0.1339    0.0
0.1339     0.1596    0.0
0.1042     0.1804    0.0
0.0712     0.1957    0.0
0.0361     0.2051    0.0
0.0000     0.2083    0.0
&BPNODE   TNODE=3,   TNPC=10,    TINTC=3,                                   &END
&SECT1    STX= 9.3755, STY= 0.00,    STZ= 0.0000,    SCALE=  1.000,
          ALF=   0.0,  THETA=   0.0,
          INMODE=  0,  TNODS= 0,    TNPS= 0,    TINTS= 0,                   &END
&SECT1    STX= 9.4167, STY= 0.00,    STZ= 0.0000,    SCALE=  1.000,
          ALF=   0.0,  THETA=   0.0,
          INMODE=  0,  TNODS= 0,    TNPS= 0,    TINTS= 0,                   &END
&SECT1    STX= 9.4167, STY= 0.00,    STZ= 0.0000,    SCALE=  0.800,
          ALF=   0.0,  THETA=   0.0,
          INMODE=  0,  TNODS= 0,    TNPS= 0,    TINTS= 0,                   &END
&SECT1    STX=9.4167, STY= 0.00,    STZ= 0.0000,    SCALE=  0.600,
          ALF=   0.0,  THETA=   0.0,
          INMODE=  0,  TNODS= 0,    TNPS= 0,    TINTS= 0,                   &END
&SECT1    STX=9.4167, STY= 0.00,    STZ= 0.0000,    SCALE=  0.400,
          ALF=   0.0,  THETA=   0.0,
          INMODE=  0,  TNODS= 0,    TNPS= 0,    TINTS= 0,                   &END
&SECT1    STX=9.4167, STY= 0.00,    STZ= 0.0000,    SCALE=  0.200,
          ALF=   0.0,  THETA=   0.0,
          INMODE=  0,  TNODS= 0,    TNPS= 0,    TINTS= 0,                   &END
&SECT1    STX=9.4167, STY= 0.00,    STZ= 0.0000,    SCALE=  0.000,
          ALF=   0.0,  THETA=   0.0,
          INMODE=  0,  TNODS= 5,    TNPS= 0,    TINTS= 0,                   &END

&WAKE1    IDWAK=1,        IFLXW=1,        ITRFTZ= 1,      INTRW= 1,         &END
  TAIL1_WAKE
&WAKE2    KWPACH=1,       KWSIDE=2,       KWLINE=0,       KWPAN1=0,
          KWPAN2=0,       NODEW=3,        INITIAL=0,                        &END

&WAKE1    IDWAK=1,        IFLXW=1,        ITRFTZ= 1,      INTRW= 1,         &END
  TAIL2_WAKE
&WAKE2    KWPACH=2,       KWSIDE=2,       KWLINE=0,       KWPAN1=0,
          KWPAN2=0,       NODEW=3,        INITIAL=0,                        &END

&WAKE1    IDWAK=1,        IFLXW=1,        ITRFTZ= 1,      INTRW= 1,         &END
  CANARD1_WAKE
&WAKE2    KWPACH=9,       KWSIDE=2,       KWLINE=0,       KWPAN1=0,
          KWPAN2=0,       NODEW=3,        INITIAL=0,                        &END

&WAKE1    IDWAK=1,        IFLXW=1,        ITRFTZ= 1,      INTRW= 1,         &END
  CANARD2_WAKE
&WAKE2    KWPACH=10,       KWSIDE=4,       KWLINE=0,       KWPAN1=0,
          KWPAN2=0,       NODEW=3,        INITIAL=0,                        &END

&WAKE1    IDWAK=1,        IFLXW=1,        ITRFTZ= 1,      INTRW= 1,         &END
  +Y-BODY-VORTEX-WAKE
&WAKE2    KWPACH=21,      KWSIDE=2,       KWLINE=5,       KWPAN1=7,
          KWPAN2=0,       NODEW=0,        INITIAL=0,                        &END
&WAKE2    KWPACH=25,      KWSIDE=2,       KWLINE=1,       KWPAN1=0,
          KWPAN2=0,       NODEW=0,        INITIAL=0,                        &END
&WAKE2    KWPACH=27,      KWSIDE=2,       KWLINE=5,       KWPAN1=0,
          KWPAN2=3,       NODEW=3,        INITIAL=0,                        &END

&WAKE1    IDWAK=1,        IFLXW=1,        ITRFTZ= 1,      INTRW= 1,         &END
  -Y-BODY-VORTEX-WAKE
&WAKE2    KWPACH=22,      KWSIDE=2,       KWLINE=5,       KWPAN1=7,
          KWPAN2=0,       NODEW=0,        INITIAL=0,                        &END
&WAKE2    KWPACH=26,      KWSIDE=2,       KWLINE=5,       KWPAN1=0,
```

```
         KWPAN2=0,        NODEW=0,        INITIAL=0,                          &END
&WAKE2   KWPACH=28,       KWSIDE=2,       KWLINE=5,       KWPAN1=0,
         KWPAN2=3,        NODEW=5,        INITIAL=0,                          &END

&ONSTRM  NONSL =0,  KPSL = 20,50,80,                                          &END


&BLPARAM RN =2000000,     VISC = 0.00016,  NSLBL = 1,2,3,                     &END


&VS1     NVOLR= 0,        NVOLC= 0,                                           &END
&VS2     X0=    3.00000, Y0=     2.0000, Z0=    -2.0000, INTVSR= 1,           &END
&VS3     X1=    18.0000, Y1=     2.0000, Z1=    -2.0000, NPT1= 16,            &END
&VS4     X2=     3.0000, Y2=     16.000, Z2=    -2.0000, NPT2= 3,             &END
&VS5     X3=     3.0000, Y3=     2.0000, Z3=     2.0000, NPT3= 18,            &END

&VS6     XR0=    0.0000, YR0=    0.0000, ZR0=    0.0000, INTVSC= 1,           &END
&VS7     XR1=    0.0000, YR1=   10.0000, ZR1=    0.0000,
         XR2=    0.0000, YR2=    0.0000, ZR2=    1.0000,                      &END
&VS8     R1=     0.5000, R2=     5.0000, PHI1=  0.0,     PHI2=330.0,          &END
&VS9     NRAD=  10,       NPHI=  12,      NLEN=  5,                            &END


&SLIN1   NSTLIN=0,                                                            &END
&SLIN2   SX0=    2.0000, SY0=    5.0000, SZ0=   -0.5000,
         SU=     0.0000, SD=    15.0000, DS=     0.1000, INTSL= 1,            &END
&SLIN2   SX0=    2.0000, SY0=    5.0000, SZ0=   -0.4000,
         SU=     0.0000, SD=    15.0000, DS=     0.1000, INTSL= 1,            &END
&SLIN2   SX0=    2.0000, SY0=    5.0000, SZ0=   -0.3000,
         SU=     0.0000, SD=    15.0000, DS=     0.1000, INTSL= 1,            &END
&SLIN2   SX0=    2.0000, SY0=    5.0000, SZ0=   -0.2000,
         SU=     0.0000, SD=    15.0000, DS=     0.1000, INTSL= 1,            &END
&SLIN2   SX0=    2.0000, SY0=    5.0000, SZ0=   -0.1000,
         SU=     0.0000, SD=    15.0000, DS=     0.1000, INTSL= 1,            &END
```

APPENDIX E. TANGENT-OGIVE NOSE BODY DATA5 INPUT FILE

Aug 1 1995 13:53 **DATA5** Page 1

```
  MISSILE BODY ONLY from Meyer (Blunt Tail Body & Fuselage Wake)

&BINP2   LSTINP=2,    LSTOUT=0, LSTFRQ=0,    LENRUN=0, LPLTYP=1,          &END

&BINP3   LSTGEO=0,    LSTNAB=0,    LSTWAK=0,    LSTCPV=0,                  &END
&BINP4   MAXIT=200,   SOLRES=0.0005,                                        &END
&BINP5   NTSTPS=4,    DTSTEP=0.350,                                        &END
&BINP6   RSYM=1.0,    RGPR=0.0,    RFF=5.0,     RCORES=0.005
         RCOREW=0.005,                                                      &END
&BINP7   VINF=111.6,    VSOUND=1116.0,                                      &END
&BINP8   ALDEG=20.00,  YAWDEG=0.0,  PHIDOT=0.0, THEDOT=0.0,
         PSIDOT=0.0,                                                        &END
&BINP8A  PHIMAX=0.0, THEMAX=0.0,  PSIMAX=0.0,
         WRX=0.0,    WRY=0.0,     WRZ=0.0                                   &END
&BINP8B  DXMAX=0.0,  DYMAX=0.0,   DZMAX=0.0,
         WTX=0.0,    WTY=0.0,     WTZ=0.0,                                  &END
&BINP9   CBAR=0.1509, SREF=0.0179,  SSPAN=0.3018,
         RMPX=0.679 ,  RMPY=0.00,   RMPZ=0.00,                              &END
&BINP10   NORSET=0,    NBCHGE=0,    NCZONE=0,
          NCZPCH=0,    CZDUB=0.0,   VREF=0.0,                               &END
&BINP11   NORPCH=0,
          NORF=0,      NORL=0,
          NOCF=0,      NOCL=0,
          VNORM=0.0,                                                        &END
&BINP12   KPAN=0,      KSIDE=0,     NEWNAB=0,    NEWSID=0,                  &END
&BINP13   NBLIT=1,                                                          &END


&ASEM1   ASEMX=0.00,       ASEMY=0.00,       ASEMZ=0.00,
         ASCAL=1.00,       ATHET=0.00,       NODEA=5,                       &END
&ASEM2   APXX=0.00,        APYY=0.00,        APZZ=0.00,
         AHXX=0.00,        AHYY=1.00,        AHZZ=0.00,                     &END

&COMP1   COMPX= 0.0000,    COMPY= 0.0000,    COMPZ= 0.0000,
         CSCAL=  1.000,    CTHET=   0.0,     NODEC= 5,                      &END
&COMP2   CPXX= 0.0000,     CPYY= 0.0000,     CPZZ= 0.0000,
         CHXX= 0.0000,     CHYY=  1.000,     CHZZ= 0.0000,                  &END

&PATCH1  IREV=  0, IDPAT= 2, MAKE=   0, KCOMP= 1, KASS= 1, IPATSYM=1,
         IPATCOP=0,                                                         &END
    FORWARD FUSELAGE
&SECT1   STX= 0.000, STY= 0.00,    STZ= 0.0000,    SCALE=  0.010,
         ALF=   0.0,  THETA=   0.0,
         INMODE=  1,  TNODS= 0,    TNPS= 0,    TINTS= 0,                    &END
0.0000    -0.0755    0.0
0.0131    -0.0743    0.0
0.0258    -0.071     0.0
0.0377    -0.0653    0.0
0.0485    -0.0578    0.0
0.0578    -0.0485    0.0
0.0653    -0.0377    0.0
0.071     -0.0258    0.0
0.0743    -0.0131    0.0
0.0755     0.0000    0.0
0.0743     0.0131    0.0
0.071      0.0258    0.0
0.0653     0.0377    0.0
0.0578     0.0485    0.0
0.0485     0.0578    0.0
0.0377     0.0653    0.0
0.0258     0.071     0.0
0.0131     0.0743    0.0
0.0000     0.0755    0.0
&BPNODE   TNODE=3,    TNPC=30,    TINTC=3,                                 &END
&SECT1   STX= 0.0020, STY= 0.0000,    STZ= 0.0000,    SCALE=  0.0141,
         ALF=   0.0,  THETA=   0.0,
         INMODE=  0,  TNODS= 0,    TNPS= 0,    TINTS= 0,                    &END
&SECT1   STX= 0.0040, STY= 0.0000,    STZ= 0.0000,    SCALE=  0.0280,
         ALF=   0.0,  THETA=   0.0,
         INMODE=  0,  TNODS= 0,    TNPS= 0,    TINTS= 0,                    &END
&SECT1   STX= 0.0100, STY= 0.0000,    STZ= 0.0000,    SCALE=  0.0692,
         ALF=   0.0,  THETA=   0.0,
         INMODE=  0,  TNODS= 0,    TNPS= 0,    TINTS= 0,                    &END
&SECT1   STX= 0.0200, STY= 0.0000,    STZ= 0.0000,    SCALE=  0.1355,
         ALF=   0.0,  THETA=   0.0,
         INMODE=  0,  TNODS= 0,    TNPS= 0,    TINTS= 0,                    &END
```

Aug 1 1995 13:53 **DATA5** Page 2

```
&SECT1   STX= 0.0400, STY= 0.0000,    STZ= 0.0000,    SCALE=  0.2595
         ALF=   0.0,  THETA=   0.0,
         INMODE=  0,  TNODS= 0,    TNPS= 0,    TINTS= 0,                    &END
&SECT1   STX= 0.0600, STY= 0.0000,    STZ= 0.0000,    SCALE=  0.3727,
         ALF=   0.0,  THETA=   0.0,
         INMODE=  0,  TNODS= 0,    TNPS= 0,    TINTS= 0,                    &END
&SECT1   STX= 0.0800, STY= 0.0000,    STZ= 0.0000,    SCALE=  0.4754,
         ALF=   0.0,  THETA=   0.0,
         INMODE=  0,  TNODS= 0,    TNPS= 0,    TINTS= 0,                    &END
&SECT1   STX= 0.1000, STY= 0.0000,    STZ= 0.0000,    SCALE=  0.5682,
         ALF=   0.0,  THETA=   0.0,
         INMODE=  0,  TNODS= 0,    TNPS= 0,    TINTS= 0,                    &END
&SECT1   STX= 0.120 , STY= 0.0000,    STZ= 0.0000,    SCALE=  0.6513,
         ALF=   0.0,  THETA=   0.0,
         INMODE=  0,  TNODS= 0,    TNPS= 0,    TINTS= 0,                    &END
&SECT1   STX= 0.1400, STY= 0.0000,    STZ= 0.0000,    SCALE=  0.7250 ,
         ALF=   0.0,  THETA=   0.0,
         INMODE=  0,  TNODS= 0,    TNPS= 0,    TINTS= 0,                    &END
&SECT1   STX= 0.1600, STY= 0.0000,    STZ= 0.0000,    SCALE=  0.7896,
         ALF=   0.0,  THETA=   0.0,
         INMODE=  0,  TNODS= 0,    TNPS= 0,    TINTS= 0,                    &END
&SECT1   STX= 0.1800, STY= 0.0000,    STZ= 0.0000,    SCALE=  0.8452,
         ALF=   0.0,  THETA=   0.0,
         INMODE=  0,  TNODS= 0,    TNPS= 0,    TINTS= 0,                    &END
&SECT1   STX= 0.2000, STY= 0.0000,    STZ= 0.0000,    SCALE=  0.8922,
         ALF=   0.0,  THETA=   0.0,
         INMODE=  0,  TNODS= 0,    TNPS= 0,    TINTS= 0,                    &END
&SECT1   STX= 0.2200, STY= 0.0000,    STZ= 0.0000,    SCALE=  0.9305,
         ALF=   0.0,  THETA=   0.0,
         INMODE=  0,  TNODS= 0,    TNPS= 0,    TINTS= 0,                    &END
&SECT1   STX= 0.2400, STY= 0.0000,    STZ= 0.0000,    SCALE=  0.9604,
         ALF=   0.0,  THETA=   0.0,
         INMODE=  0,  TNODS= 0,    TNPS= 0,    TINTS= 0,                    &END
&SECT1   STX= 0.2600, STY= 0.0000,    STZ= 0.0000,    SCALE=  0.9819
         ALF=   0.0,  THETA=   0.0,
         INMODE=  0,  TNODS= 0,    TNPS= 0,    TINTS= 0,                    &END
&SECT1   STX= 0.2800, STY= 0.0000,    STZ= 0.0000,    SCALE=  0.9951,
         ALF=   0.0,  THETA=   0.0,
         INMODE=  0,  TNODS= 0,    TNPS= 0,    TINTS= 0,                    &END
&SECT1   STX= 0.3020, STY= 0.0000,    STZ= 0.0000,    SCALE=  1.000,
         ALF=   0.0,  THETA=   0.0,
         INMODE=  0,  TNODS= 0,    TNPS= 0,    TINTS= 0,                    &END
&SECT1   STX= 0.3397, STY= 0.0000,    STZ= 0.0000,    SCALE=  1.000,
         ALF=   0.0,  THETA=   0.0,
         INMODE=  0,  TNODS= 0,    TNPS= 0,    TINTS= 0,                    &END
&SECT1   STX= 0.3774, STY= 0.0000,    STZ= 0.0000,    SCALE=  1.000,
         ALF=   0.0,  THETA=   0.0,
         INMODE=  0,  TNODS= 0,    TNPS= 0,    TINTS= 0,                    &END
&SECT1   STX= 0.4151, STY= 0.0000,    STZ= 0.0000,    SCALE=  1.000,
         ALF=   0.0,  THETA=   0.0,
         INMODE=  0,  TNODS= 0,    TNPS= 0,    TINTS= 0,                    &END
&SECT1   STX= 0.4528, STY= 0.0000,    STZ= 0.0000,    SCALE=  1.000,
         ALF=   0.0,  THETA=   0.0,
         INMODE=  0,  TNODS= 0,    TNPS= 0,    TINTS= 0,                    &END
&SECT1   STX= 0.4905, STY= 0.0000,    STZ= 0.0000,    SCALE=  1.000,
         ALF=   0.0,  THETA=   0.0,
         INMODE=  0,  TNODS= 0,    TNPS= 0,    TINTS= 0,                    &END
&SECT1   STX= 0.5282, STY= 0.0000,    STZ= 0.0000,    SCALE=  1.000,
         ALF=   0.0,  THETA=   0.0,
         INMODE=  0,  TNODS= 0,    TNPS= 0,    TINTS= 0,                    &END
&SECT1   STX= 0.5659, STY= 0.0000,    STZ= 0.0000,    SCALE=  1.000,
         ALF=   0.0,  THETA=   0.0,
         INMODE=  0,  TNODS= 0,    TNPS= 0,    TINTS= 0,                    &END
&SECT1   STX= 0.6036, STY= 0.0000,    STZ= 0.0000,    SCALE=  1.000,
         ALF=   0.0,  THETA=   0.0,
         INMODE=  0,  TNODS= 0,    TNPS= 0,    TINTS= 0,                    &END
&SECT1   STX= 0.6413, STY= 0.0000,    STZ= 0.0000,    SCALE=  1.000,
         ALF=   0.0,  THETA=   0.0,
         INMODE=  0,  TNODS= 0,    TNPS= 0,    TINTS= 0,                    &END
&SECT1   STX= 0.6790, STY= 0.0000,    STZ= 0.0000,    SCALE=  1.000,
         ALF=   0.0,  THETA=   0.0,
         INMODE=  0,  TNODS= 0,    TNPS= 0,    TINTS= 0,                    &END
&SECT1   STX= 0.7420, STY= 0.0000,    STZ= 0.0000,    SCALE=  1.000,
         ALF=   0.0,  THETA=   0.0,
         INMODE=  0,  TNODS= 0,    TNPS= 0,    TINTS= 0,                    &END
&SECT1   STX= 0.8040, STY= 0.0000,    STZ= 0.0000,    SCALE=  1.000,
```

```
          ALF=   0.0,  THETA=   0.0,
          INMODE=  0,  TNODS= 0,    TNPS= 0,    TINTS= 0,                    &END
&SECT1    STX= 0.8470, STY= 0.0000,    STZ= 0.0000,    SCALE=  1.000,
          ALF=   0.0,  THETA=   0.0,
          INMODE=  0,  TNODS= 0,    TNPS= 0,    TINTS= 0,                    &END
&SECT1    STX= 0.8910, STY= 0.0000,    STZ= 0.0000,    SCALE=  1.000,
          ALF=   0.0,  THETA=   0.0,
          INMODE=  0,  TNODS= 0,    TNPS= 0,    TINTS= 0,                    &END
&SECT1    STX= 0.9340, STY= 0.0000,    STZ= 0.0000,    SCALE=  1.000,
          ALF=   0.0,  THETA=   0.0,
          INMODE=  0,  TNODS= 0,    TNPS= 0,    TINTS= 0,                    &END
&SECT1    STX= 0.9780, STY= 0.0000,    STZ= 0.0000,    SCALE=  1.000,
          ALF=   0.0,  THETA=   0.0,
          INMODE=  0,  TNODS= 0,    TNPS= 0,    TINTS= 0,                    &END
&SECT1    STX= 1.0210, STY= 0.0000,    STZ= 0.0000,    SCALE=  1.000,
          ALF=   0.0,  THETA=   0.0,
          INMODE=  0,  TNODS= 0,    TNPS= 0,    TINTS= 0,                    &END
&SECT1    STX= 1.0640, STY= 0.0000,    STZ= 0.0000,    SCALE=  1.000,
          ALF=   0.0,  THETA=   0.0,
          INMODE=  0,  TNODS= 0,    TNPS= 0,    TINTS= 0,                    &END
&SECT1    STX= 1.1070, STY= 0.0000,    STZ= 0.0000,    SCALE=  1.000,
          ALF=   0.0,  THETA=   0.0,
          INMODE=  0,  TNODS= 0,    TNPS= 0,    TINTS= 0,                    &END
&SECT1    STX= 1.1510, STY= 0.0000,    STZ= 0.0000,    SCALE=  1.000,
          ALF=   0.0,  THETA=   0.0,
          INMODE=  0,  TNODS= 0,    TNPS= 0,    TINTS= 0,                    &END
&SECT1    STX= 1.20, STY= 0.0000,    STZ= 0.0000,    SCALE=  1.000,
          ALF=   0.0,  THETA=   0.0,
          INMODE=  0,  TNODS= 0,    TNPS= 0,    TINTS= 0,                    &END
&SECT1    STX= 1.260, STY= 0.00,    STZ= 0.0000,    SCALE=  1.00,
          ALF=   0.0,  THETA=   0.0,
          INMODE=  0,  TNODS= 0,    TNPS= 0,    TINTS= 0,                    &END
&SECT1    STX= 1.328, STY= 0.00,    STZ= 0.0000,    SCALE=  1.00,
          ALF=   0.0,  THETA=   0.0,
          INMODE=  0,  TNODS= 0,    TNPS= 0,    TINTS= 0,                    &END
&SECT1    STX=1.388, STY= 0.00,    STZ= 0.0000,    SCALE= 1.000,
          ALF=   0.0,  THETA=   0.0,
          INMODE=  0,  TNODS= 0,    TNPS= 0,    TINTS= 0,                    &END
&SECT1    STX=1.449, STY= 0.00,    STZ= 0.0000,    SCALE=  1.00,
          ALF=   0.0,  THETA=   0.0,
          INMODE=  0,  TNODS= 0,    TNPS= 0,    TINTS= 0,                    &END
&SECT1    STX=1.509, STY= 0.00,    STZ= 0.0000,    SCALE=  1.000,
          ALF=   0.0,  THETA=   0.0,
          INMODE=  0,  TNODS= 0,    TNPS= 0,    TINTS= 0,                    &END
&SECT1    STX=1.509, STY= 0.00,    STZ= 0.0000,    SCALE=  0.800,
          ALF=   0.0,  THETA=   0.0,
          INMODE=  0,  TNODS= 0,    TNPS= 0,    TINTS= 0,                    &END
&SECT1    STX=1.509, STY= 0.00,    STZ= 0.0000,    SCALE=  0.600,
          ALF=   0.0,  THETA=   0.0,
          INMODE=  0,  TNODS= 0,    TNPS= 0,    TINTS= 0,                    &END
&SECT1    STX=1.509, STY= 0.00,    STZ= 0.0000,    SCALE=  0.400,
          ALF=   0.0,  THETA=   0.0,
          INMODE=  0,  TNODS= 0,    TNPS= 0,    TINTS= 0,                    &END
&SECT1    STX=1.509, STY= 0.00,    STZ= 0.0000,    SCALE=  0.200,
          ALF=   0.0,  THETA=   0.0,
          INMODE=  0,  TNODS= 0,    TNPS= 0,    TINTS= 0,                    &END
&SECT1    STX=1.509, STY= 0.00,    STZ= 0.0000,    SCALE=  0.000,
          ALF=   0.0,  THETA=   0.0,
          INMODE=  0,  TNODS= 5,    TNPS= 0,    TINTS= 0,                    &END

&WAKE1    IDWAK=1,        IFLXW=1,        ITRFTZ= 1,      INTRW= 0,          &END
  +Y_FUSELAGE WAKE
&WAKE2    KWPACH=1,       KWSIDE=2,       KWLINE=19,      KWPAN1=19,
          KWPAN2=44,      NODEW=3,        INITIAL=0,                         &END

&WAKE1    IDWAK=1,        IFLXW=1,        ITRFTZ= 1,      INTRW= 0,          &END
  -Y_FUSELAGE WAKE
&WAKE2    KWPACH=2,       KWSIDE=2,       KWLINE=11,      KWPAN1=19,
          KWPAN2=44,      NODEW=5,        INITIAL=0,                         &END


&ONSTRM   NONSL =0,  KPSL = 20,50,80,                                        &END

&RLPARAM  RN =2000000,     VISC = 0.00016,  NSLBL = 1,2,3,                   &END

&VS1      NVOLR= 0,       NVOLC= 0,                                          &END
```



```
&VS2      X0=    3.00000, Y0=     2.0000, Z0=    -2.0000, INTVSR= 1,        &END
&VS3      X1=    18.0000, Y1=     2.0000, Z1=    -2.0000, NPT1= 16,         &END
&VS4      X2=     3.0000, Y2=    16.000, Z2=     -2.0000, NPT2= 3,          &END
&VS5      X3=     3.0000, Y3=     2.0000, Z3=     2.0000, NPT3= 18,         &END

&VS6      XR0=    0.0000, YR0=    0.0000, ZR0=    0.0000, INTVSC= 1,        &END
&VS7      XR1=    0.0000, YR1=   10.0000, ZR1=    0.0000,
          XR2=    0.0000, YR2=    0.0000, ZR2=    1.0000,                   &END
&VS8      R1=     0.5000, R2=     5.0000, PHI1=  0.0,     PHI2=330.0,       &END
&VS9      NRAD=  10,      NPHI=  12,      NLEN=  5,                         &END

&SLIN1    NSTLIN=0,                                                         &END
&SLIN2    SX0=     2.0000, SY0=    5.0000, SZ0=   -0.5000,
          SU=      0.0000, SD=    15.0000, DS=     0.1000, INTSL= 1,        &END
&SLIN2    SX0=     2.0000, SY0=    5.0000, SZ0=   -0.4000,
          SU=      0.0000, SD=    15.0000, DS=     0.1000, INTSL= 1,        &END
&SLIN2    SX0=     2.0000, SY0=    5.0000, SZ0=   -0.3000,
          SU=      0.0000, SD=    15.0000, DS=     0.1000, INTSL= 1,        &END
&SLIN2    SX0=     2.0000, SY0=    5.0000, SZ0=   -0.2000,
          SU=      0.0000, SD=    15.0000, DS=     0.1000, INTSL= 1,        &END
&SLIN2    SX0=     2.0000, SY0=    5.0000, SZ0=   -0.1000,
          SU=      0.0000, SD=    15.0000, DS=     0.1000, INTSL= 1,        &END
```

APPENDIX F. SAMPLE PARAM.DAT FILE


```
C
C  CODE DIMENSIONING PARAMETERS
C
C  NUMBER OF SURFACE PANELS ALLOWED
C
      PARAMETER (NSPDIM = 10000)
C
C  NUMBER OF NEUMANN PANELS ALLOWED
C
      PARAMETER (NNPDIM = 10)
C
C  NUMBER OF PATCHES ALLOWED
C
      PARAMETER (NPDIM = 30)
C
C  NUMBER OF BASIC POINTS ALLOWED FOR SECTION DEFINITION
C  (ALSO NUMBER OF SECTIONS ALLOWED PER PATCH)
C  (ALSO NUMBER OF ROWS OR COLUMNS + 1 ALLOWED ON A PATCH)
C  CAUTION:  DO NOT SET THIS PARAMETER TO LESS THAN 50!
C
      PARAMETER (NBPDIM = 500)
C
C  NUMBER OF WAKE PANELS ALLOWED
C
      PARAMETER (NWPDIM = 4900)
C
C  NUMBER OF WAKE COLUMNS OR ROWS ALLOWED ON EACH WAKE
C
      PARAMETER (NWCDIM = 1000)
C
C  NUMBER OF WAKES ALLOWED
C
      PARAMETER (NWDIM = 50)
C
C  NUMBER OF SCAN VOLUMES OF EACH TYPE ALLOWED
C
      PARAMETER (NSVDIM = 19)
C
C  NUMBER OF POINTS PER OFF-BODY STREAMLINE ALLOWED
C
      PARAMETER (NSLPDIM = 2000)
C
C  NUMBER OF POINTS PER ON-BODY STREAMLINE ALLOWED
C
      PARAMETER (NONSLPDIM = 2000)
C
C  NUMBER OF GROUPS OF PANELS ON WHICH NONZERO NORMAL VELOCITY IS PRESCRIBED
C
      PARAMETER (NVELDIM = 20)
C
C  NUMBER OF WAKE CORNER POINTS ALLOWED
C
      PARAMETER (NWCPDIM=(NWPDIM + 1)*2)
C
C  NUMBER OF SURFACE CORNER POINTS ALLOWED
C
      PARAMETER (NSCPDIM=(NSPDIM + 1)*2)
C
C  NUMBER OF EDGE PANELS ALLOWED ON A PATCH
C
      PARAMETER (NEPDIM = NBPDIM * 4)
C
C  PARAMETER CONTROLLING WHETHER THE DOUBLET INFL. COEFF. MATRIX IS STORED
C  ON DISK OR IN RAM.  IF INRAM IS SET TO 1, MATRIX IS STORED ON DISK.
C  IF INRAM IS SET TO NSPDIM, MATRIX IS STORED IN RAM. NOTE THESE ARE THE
C  ONLY TWO CHOICES!!!!  IF ANY OTHER VALUE IS ENTERED, THE CODE WILL FAIL!!!
C
      PARAMETER (INRAM = 1)
```

APPENDIX G. SAMPLE COMMON.F FILE


```
      COMMON/ BLDATA    / FSVEL,RH,BLS(NONSLPDIM),
     +                    BLCP(NONSLPDIM),BLX(NONSLPDIM),BLY(NONSLPDIM),
     +                    BLZ(NONSLPDIM),BLU(NONSLPDIM),
     +                    VISC,DSTAR(NONSLPDIM),
     +                    BLTHETA(NONSLPDIM),RH(NONSLPDIM),
     +                    CF(NONSLPDIM),
     +                    DUDN(NONSLPDIM),DEL(NONSLPDIM)
      COMMON/ BLDATAI   / NBLIT,NSLPTS,LAMSEP,ITRAN,ITRBSEP
      COMMON/ CONST     / PI,     EPS,   FOURPI, CBAR,
     +                    SSPAN, SREF, RMPX,    RMPY,    RMPZ,
     +                    SOLRES,RCORS,RFF,RCORW
      COMMON/ CONSTI    / MAXIT
      COMMON/ INTERNAL  / CZDUB,VREF
      COMMON/ INTERNALI / NCZONE,NCZPCH
      COMMON/ TSTEP     / NTSTPS, ITSTEP
      COMMON/ NEWNAB    / KPAN(NSPDIM),KSIDE(NSPDIM),NEWNAB(NSPDIM),
     +                    NEWSID(NSPDIM),NBCHGE
      COMMON/ PNABOR    / NABOR(4,NSPDIM),NABSID(4,NSPDIM)
      COMMON/ NUM       / NPAN,NPATCH,NWPAN,NWAKE,NCOMP,NASSEM
      COMMON/ ONSET     / ALPHA,ALDEG,YAW,YAWDEG,
     +                    WIND(3,3),VINF,VSOUND
      COMMON/ SYMMETRY  / SYM, GPR
      COMMON/ PATNAM    / PNAME(6,NPDIM)
      COMMON/ PATCHES   / IDENT(NPDIM), IPAN(NPDIM), KLASS(NPDIM),
     +                    KOMP(NPDIM),  LPAN(NPDIM), NCOL(NPDIM),
     +                    NPANS(NPDIM), NROW(NPDIM)
      COMMON/ PRINT     / LSTINP,    LSTOUT, LSTGEO, LSTNAB, LSTWAK,
     +                    LSTFRQ, LSTCPV ,LSTHLD, LPLTYP
      COMMON/ VELSETI   / NOCF(NVELDIM),NOCL(NVELDIM),NORF(NVELDIM),
     +                    NORL(NVELDIM),NORPCH(NVELDIM),NORSET
      COMMON/ VELSET    / VNORM(NVELDIM)
      COMMON/ RUNCNTRL  / LENRUN
      COMMON/ SOLUTION  / SIG(NSPDIM), DUB(NSPDIM), PDUB(NSPDIM),
     +                    WDUB(NWPDIM), VX(NSPDIM), VY(NSPDIM),
     +                    VZ(NSPDIM), VXR(NNPDIM), VYR(NNPDIM),
     +                    VZR(NNPDIM),DIAG(NSPDIM),
     +                    PHSV(NSPDIM), VNORMAL(NSPDIM), CPDUB(NSCPDIM),
     +                    VCPX(NSCPDIM),VCPY(NSCPDIM),VCPZ(NSCPDIM),
     +                    CPPDUB(NSCPDIM)
      COMMON/ SPANEL    / XC(NSPDIM), YC(NSPDIM), ZC(NSPDIM),
     +                    PCS(3,3,NSPDIM), AREA(NSPDIM), PFF(NSPDIM),
     +                    CPSX(NSCPDIM), CPSY(NSCPDIM), CPSZ(NSCPDIM),
     +                    SMP(NSPDIM),SMQ(NSPDIM)
      COMMON/ SPANELI   / ICPS(NPDIM),KPTYP(NSPDIM)
      COMMON/ SCRFILES  / JPLOT, JDUBIC,
     +                    JSORIC, IMU, JSL
      COMMON/ INTRSCT   / INTW(NWDIM)
      COMMON/ UNSTDY    / OMEGA(3),VFR(3),DTSTEP,
     +                    PHIDOT,THEDOT,PSIDOT,
     +                    PHIMAX,THEMAX,PSIMAX,WRX,WRY,WRZ,
     +                    DXMAX,DYMAX,DZMAX,WTX,WTY,WTZ
      COMMON/ WAKNAM    / WNAME(6,NWDIM)
      COMMON/ WAKESI    / NWCOL(NWDIM), NWROW(NWDIM), IWPAN(NWDIM),
     +                    LWPAN(NWDIM), IDENTW(NWDIM),
     +                    KWPU(NWCDIM,NWDIM), KWPL(NWCDIM,NWDIM),
     +                    IFLEXW(NWDIM), ITRFZ(NWDIM)
      COMMON/ WAKES     / PHIU(NWCDIM,NWDIM), PHIL(NWCDIM,NWDIM)
      COMMON/ WPANEL    / XCW(NWPDIM), YCW(NWPDIM), ZCW(NWPDIM),
     +                    PCSW(3,3,NWPDIM), AREAW(NWPDIM),
     +                    PFFW(NWPDIM),
     +                    CPWX(NWCPDIM), CPWY(NWCPDIM), CPWZ(NWCPDIM)
      COMMON/ WPANELI   / ICPW(NWDIM)
      COMMON/ MDUBIC    / DUBICWW(INRAM,NSPDIM)
      COMMON/ ONSTRML   / NONSL
C
C  TYPE DECLARATIONS
C
      LOGICAL SYM,GPR,FAR,CLOSED
      CHARACTER*4 PNAME,WNAME,TITL
      INTEGER TNODS,TNPS,TINTS,TNODE,TNPC,TINTC
      INTEGER UPNABOR,UPNABSID,DNNABOR,DNNABSID
C
```

LIST OF REFERENCES

1. Ashby, D., Dudley, M., Iguchi, S., Browne, L., and Katz, J., "Potential Flow Theory and Operation Guide for the Panel Code PMARC_12," NASA TM-102851, Ames Research Center, Moffett Field, CA., December 1992.

2. Ashby, D., Dudley, M. R., and Iguchi, S. K., "Development and Validation of an Advanced Low-Order Panel Method," NASA TM 101024, October 1988.

3. Keith, S., "General Visualization System, Version 3.1," Sterling Software, Palo Alto, CA, 1992.

4. Burris, S., "Subsonic Load Analysis Manual," Developed for use by Naval Postgraduate School Aerospace Engineering Department, Monterey, CA, 1994.

5. Edge, D., and Perkins, J., "Three-Dimensional Aerodynamic Analysis of a Subsonic High-Lift Transport Configuration Using PMARC," AIAA Paper 95-0039, 33rd Aerospace Sciences Meeting, Reno, NV, January 1995.

6. Dougherty, D., Sed and Awk, O'Reilly and Associates, Inc., Sebastopol, CA, 1990.

7. Aho, A., Kernighan, B., and Weinberger, P., The Awk Programming Language, Addison-Wesley, 1988.

8. Loving, D. L., Estabrooks, B. B., "Analysis of Pressure Distribution of Wing-Fuselage Configuration Having a Wing of 45° Sweepback, Aspect Ratio 4, Taper Ratio 0.6, and NACA 65A006 Airfoil Section," NACA RM L51F07, September 1951.

9. Rom, J., High Angle-of-Attack Aerodynamics, Subsonic, Transonic, and Supersonic Flows, Spring-Verlag, 1992.

10. Bertin, J. J., and Smith, M. L., Aerodynamics for Engineers, 2d ed., Prentice-Hall, 1989.

11. Milne-Thomson, L. M., Theoretical Aerodynamics, Dover Publications Inc., 1955.

12. Kohlman, D. Introduction to VSTOL Airplanes, Iowa State University Press, 1981.

13. Martin, D. M., and Kroo, I., "Comparison of PMARC and Analytic Results for Two-Dimensional Unsteady Airfoils", AIAA Paper 93-0636, 31st Aerospace Sciences Meeting, Reno, NV, January 1993.

14. Teng, N. H., "The Development of a Computer Code for the Numerical Solution of Unsteady, Inviscid, and Incompressible Flow over an Airfoil," Master's Thesis, Naval Postgraduate School, Monterey, CA, June 1987.

15. Platzer, M. F., Neace, K. S., and Pang, C. K., "Aerodynamic Analysis of Flapping Wing Propulsion," AIAA Paper No. 93-0484, January 1993.

16. Jones, K. D., and Platzer, M. F., "Time-Domain Aeroelastic Analysis of a Two Airfoil System with Application to Unsteady Rotary Wing Flowfields," AIAA Paper No. 95-0337, January 1995.

17. Bisplinghoff, R. L., Ashley, H., and Halfman, R. L., Aeroelasticity, Addison-Wesley Publishing Company, Cambridge, MA, 1955.

18. Katz, J. and Plotkin, A., Low-Speed Aerodynamics—From Wing Theory to Panel Methods, McGraw-Hill, NY, 1991.

19. Lomax, H., "Indicial Aerodynamics," AGARD Manual on Aeroelasticity, Volume 2, Chapter 6, 1960.

20. Glauert, H., The Elements of Aerofoil and Airscrew Theory, Cambridge at the University Press, 1936.

21. Smith, E. H., Hebbar, S. K., and Platzer, M., "Aerodynamic Characteristics of a Canard-Controlled Missile at High Angles of Attack," AIAA Paper No. 93-0763, 31st Aerospace Sciences Meeting, Reno, NV, January 1993.

22. Smith, E. H., Salazar, M. E., Hebbar, S. K., and Platzer, M., "Aerodynamic Characteristics of the MMPT ATD Vehicle at High Angles of Attack," AIAA Paper No. 93-3493, August 1993.

23. Meyer, J., "Effects of the Roll Angel on Cruciform Wing-Body Configurations at High Incidences," Journal of Spacecraft and Rockets, Vol. 31 No. 1, January-Feburary 1994, pp. 113-122.

24. Myers., J. A., "Handbook of Equations for Mass and Area Properties of Various Geometrical Shapes," NAVWEPS Report 7827, NOTS TP 2838, U. S. Naval Ordnance Test Station, China Lake, CA, April 1962.

25. Platzer, M., and Hoffman, G., "Quasi-Slender Body Theory for Slowly Oscillating Bodies of Revolution in Supersonic Flow," NASA TN D-3440, June 1966.

26. Mendenhall, M. R., Perkin, S. C., and Lesieutre, D. J., "Vortex Cloud Model for Body Vortex Shedding and Tracking," Tactical Missile Aerodynamics: Prediction Methodology, American Institute of Aeronautics and Astronautics, 1992.

27. Nielsen, J., Missile Aerodynamics, McGraw-Hill Book Company, 1960, Reprinted by Nielsen Engineering & Research, Inc., 1988.

28. Moore, F., McInville, R., and Hymer, T., "The 1995 Version of the NSWC Aeroprediction Code: Part I–Summary of New Theoretical Methodology," NSWCDD/TR-94/379, Dahlgren Division, Naval Surface Warfare Center, VI, February 1995.

INITIAL DISTRIBUTION LIST

1. Defense Technical Information Center 2
   Cameron Station
   Alexandria, VA 22304-6145

2. Library Code 52 2
   Naval Postgraduate School
   Monterey, CA 93943-5101

3. Chairman 1
   Department of Aeronautics and Astronautics, Code AA
   Naval Postgraduate School
   699 Dyer Road, Room 137
   Monterey, CA 93943-5106

4. Dr. Max F. Platzer 5
   Department of Aeronautics and Astronautics, Code AA/PL
   Naval Postgraduate School
   699 Dyer Road, Room 137
   Monterey, CA 93943-5106

5. Dr. Kevin Jones 1
   Department of Aeronautics and Astronautics, Code AA/Jo
   Naval Postgraduate School
   699 Dyer Road, Room 137
   Monterey, CA 93943-5106

6. Dr. Ismail Tuncer 1
   Department of Aeronautics and Astronautics, Code AA/Tu
   Naval Postgraduate School
   699 Dyer Road, Room 137
   Monterey, CA 93943-5106

7. Robert Vandyken 1
   Naval Air Warfare Center—Weapons Division
   Code 473110D
   China Lake, CA 93555

8. Edward L. Jeter 1
   Naval Air Warfare Center—Weapons Division
   Code 414170D
   China Lake, CA 93555

9. Dr. Craig S. Porter 1
Naval Air Warfare Center—Weapons Division
Code 473C00D
China Lake, CA 93555

10. Donald J. Christison 1
Naval Air Warfare Center—Weapons Division
Code 472110D
China Lake, CA 93555

11. Mark A. Lambert 2
Naval Air Warfare Center—Weapons Division
Code 472110D
China Lake, CA 93555

GAYLORD S

DUDLEY KNOX LIBRARY
3 2768 00315282 8